

Energy management for vehicular electric power systems

Citation for published version (APA):

Koot, M. W. T. (2006). *Energy management for vehicular electric power systems*. [Phd Thesis 1 (Research TU/e / Graduation TU/e), Mechanical Engineering]. Technische Universiteit Eindhoven.
<https://doi.org/10.6100/IR613007>

DOI:

[10.6100/IR613007](https://doi.org/10.6100/IR613007)

Document status and date:

Published: 01/01/2006

Document Version:

Publisher's PDF, also known as Version of Record (includes final page, issue and volume numbers)

Please check the document version of this publication:

- A submitted manuscript is the version of the article upon submission and before peer-review. There can be important differences between the submitted version and the official published version of record. People interested in the research are advised to contact the author for the final version of the publication, or visit the DOI to the publisher's website.
- The final author version and the galley proof are versions of the publication after peer review.
- The final published version features the final layout of the paper including the volume, issue and page numbers.

[Link to publication](#)

General rights

Copyright and moral rights for the publications made accessible in the public portal are retained by the authors and/or other copyright owners and it is a condition of accessing publications that users recognise and abide by the legal requirements associated with these rights.

- Users may download and print one copy of any publication from the public portal for the purpose of private study or research.
- You may not further distribute the material or use it for any profit-making activity or commercial gain
- You may freely distribute the URL identifying the publication in the public portal.

If the publication is distributed under the terms of Article 25fa of the Dutch Copyright Act, indicated by the "Taverne" license above, please follow below link for the End User Agreement:

www.tue.nl/taverne

Take down policy

If you believe that this document breaches copyright please contact us at:

openaccess@tue.nl

providing details and we will investigate your claim.

Energy management for vehicular electric power systems

A catalogue record is available from the Library Technische Universiteit Eindhoven.

ISBN-10: 90-386-2868-4

ISBN-13: 978-90-386-2868-4

This thesis was prepared using the L^AT_EX documentation system.

Cover design by Oranje Vormgevers, Eindhoven.

Printed by Universiteitsdrukkerij, Technische Universiteit Eindhoven.

Copyright © 2006 by M.W.Th. Koot

All rights reserved. No parts of this publication may be reproduced or utilized in any form or by any means, electronic or mechanical, including photocopying, recording or by any information storage and retrieval system, without written permission of the copyright holder.

Energy management for vehicular electric power systems

PROEFSCHRIFT

ter verkrijging van de graad van doctor
aan de Technische Universiteit Eindhoven,
op gezag van de Rector Magnificus, prof.dr.ir. C.J. van Duijn,
voor een commissie aangewezen door het College voor Promoties
in het openbaar te verdedigen op
woensdag 11 oktober 2006 om 16.00 uur

door

Michael Wilhelmus Theodorus Koot

geboren te Sittard

Dit proefschrift is goedgekeurd door de promotoren:

prof.dr.ir. M. Steinbuch

en

prof.dr.ir. P.P.J. van den Bosch

Copromotor:

dr.ir. A.G. de Jager

Preface

This thesis results from the project “The Development of an Energy and Power Management System for Conventional and Future Vehicle Power Nets”.

This project was initiated and financed by Ford Forschungszentrum Aachen, Germany. The research work was carried out by Technische Universiteit Eindhoven at two departments: the Control Systems Group at the Department of Electrical Engineering, and the Control Systems Technology Group at the Department of Mechanical Engineering. Both groups employed a PhD student. The second thesis, by John Kessels from the Department of Electrical Engineering, is expected to appear in 2007.

Contents

1	Introduction	11
1.1	Trends in automotive transportation	11
1.2	Solutions for fuel and exhaust emissions reduction	12
1.2.1	Continuously variable transmissions	12
1.2.2	Electric vehicles	12
1.2.3	Fuel cell vehicles	13
1.2.4	Hybrid electric vehicles	13
1.2.5	Advanced power net control	14
1.3	Energy management	14
1.3.1	Energy management as an optimization problem	15
1.3.2	Energy management of hybrid electric vehicles	15
1.3.3	Relation with similar problems	16
1.4	Problem definition	17
1.4.1	Open issues	17
1.4.2	Goals of this thesis	17
1.4.3	Main contributions of this thesis	17
1.5	Layout of this thesis	18
2	Vehicle Model	19
2.1	Introduction	19
2.2	Power flow in a vehicle	20
2.3	Model structure	20
2.3.1	Simulation model	21
2.3.2	Control model	21
2.4	Drive train	22
2.4.1	Driving cycle	22
2.5	Internal combustion engine	23
2.5.1	Combustion	23
2.5.2	Power-based model	24
2.5.3	Exhaust emissions	27
2.6	Alternator	27
2.7	Battery	28
2.7.1	Electric circuit	29
2.7.2	Power-based model	30
2.8	Electric loads	32
2.9	Conclusion	32
3	Energy Management Strategies	33
3.1	Introduction	33
3.2	Problem definition	33

3.2.1	Control objective	34
3.2.2	Applied control techniques	35
3.3	Dynamic Programming	36
3.3.1	Implementation DP algorithm	36
3.4	Quadratic Programming	38
3.4.1	Model approximation	39
3.4.2	Cost function	39
3.4.3	Constraints	39
3.4.4	Solution	40
3.5	Model Predictive Control	40
3.5.1	Reduction of the QP problem	40
3.5.2	Elimination of the prediction horizon	41
3.6	Simulations	42
3.6.1	Model	42
3.6.2	Strategies	43
3.6.3	Results	43
3.6.4	Evaluation	45
3.7	Conclusion	47
4	Fuel Reduction Potential	49
4.1	Introduction	49
4.2	Energy management	49
4.2.1	Efficiency improvement versus fuel reduction	50
4.2.2	Regenerative braking	51
4.2.3	Start-stop operation	52
4.2.4	Hybrid electric vehicles	52
4.3	Engineering rules	52
4.3.1	Baseline strategy	52
4.3.2	Regenerative braking strategy	54
4.3.3	Advanced energy management strategy	55
4.3.4	Start-stop operation	56
4.4	Comparison	57
4.4.1	Strategies	57
4.4.2	Simulation parameters	58
4.4.3	Results & evaluation	58
4.5	Conclusion	59
5	Dual Storage Power Net	61
5.1	Introduction	61
5.2	Dual storage power net	61
5.2.1	Power flow	62
5.2.2	Analysis	62
5.3	Control objective	63
5.3.1	Optimization method	63
5.4	Modeling	64
5.4.1	Components	64
5.4.2	Power flow	65
5.4.3	Decision variables	65

5.4.4	Cost function	66
5.4.5	Constraints	66
5.4.6	Complementarity constraint	66
5.5	Global optimization	67
5.6	Real-time control strategy	67
5.7	Simulations	68
5.7.1	Model	68
5.7.2	Strategies	68
5.7.3	Results	69
5.8	Conclusion	69
6	Parallel Hybrid Electric Vehicles	73
6.1	Introduction	73
6.2	Parallel hybrid electric vehicles	73
6.2.1	Power flow description	74
6.3	Control objective	74
6.4	Modeling	75
6.4.1	Components	75
6.4.2	Start-stop operation	76
6.5	Optimization	78
6.5.1	Cost function	78
6.5.2	Constraints	78
6.5.3	Model Predictive Control	79
6.5.4	Removing the endpoint constraint	79
6.6	Simulations	80
6.6.1	Model	80
6.6.2	Strategies	80
6.6.3	Results	80
6.6.4	Fuel consumption	83
6.6.5	Exhaust emissions	83
6.7	Conclusion	84
7	Implementation on a Hardware-in-the-Loop test setup	85
7.1	Introduction	85
7.2	Hardware-in-the-Loop test setup	85
7.2.1	Power controller	86
7.3	Control strategies	86
7.4	Results	87
7.4.1	Drive train	87
7.4.2	Single storage power net	87
7.4.3	Dual storage power net	89
7.4.4	Fuel consumption	91
7.5	Conclusion	91
8	Discussion	93
8.1	Conclusions	93
8.1.1	Methodology	93
8.1.2	Application	94

8.2	Future research	95
A	Overview of Optimization Methods	97
A.1	Introduction	97
A.2	Dynamic optimization	97
A.3	Static optimization	98
A.4	Linear Programming	99
A.4.1	Piecewise linearities	99
A.5	Quadratic Programming	99
A.5.1	Unconstrained QP	100
A.5.2	QP with equality constraints	100
A.5.3	The Quadratic Knapsack Problem	101
A.6	Mixed Integer Programming	102
A.6.1	Enumeration	102
A.6.2	Branch and Bound	102
A.6.3	Outer Approximation	102
A.6.4	Generalized Benders Decomposition	103
A.6.5	Convert to nonlinear constraint	104
A.6.6	Heuristic methods	104
A.7	Complementarity Constraints	105
A.7.1	Convert to Mixed Integer Programming problem	105
A.7.2	Substitute complementarity constraint in cost function	106
A.7.3	Nonlinear Programming	107
A.8	Dynamic Programming	107
A.9	Evaluation	108
B	Stability Analysis	109
B.1	Introduction	109
B.2	Storage Control Problem	109
B.3	Model Predictive Control	111
B.4	MPC without Endpoint Constraint	112
B.4.1	P-controller	113
B.4.2	PI-controller	113
B.5	Conclusions	114
	Bibliography	115
	Nomenclature	121
	Summary	123
	Samenvatting	125
	Dankwoord	127
	Curriculum Vitae	129

Introduction

1.1 Trends in automotive transportation

Transportation of persons and goods over land, sea, and air is increasing worldwide, as has been the case since the dawn of mankind. An overview of the total current and expected energy use in various transportation sectors is given in [56]. Looking at passenger vehicles, several trends can be noticed. The mobility of people is increasing, both the number of people and the distances covered. Today's customers have higher demands from new vehicles, such as:

- more performance, *e.g.*, a more powerful engine,
- more comfort, *e.g.*, a larger and heavier vehicle and climate control,
- more safety, *e.g.*, airbags
- more luxury, *e.g.*, navigation and entertainment systems.

Another trend is that mechanical and hydraulic components in the vehicle, are being replaced by electrical devices, which can be operated independently from the engine. An example is the drive-by-wire concept. These trends lead to more power consumption in a vehicle, and especially the electric power consumption is increasing. At the same time, customers expect a lower fuel consumption, and governments impose tight restrictions on emissions.

Over the last two decades, the electric power consumption in automobiles increased significantly, approximately 4% every year, and in the near future, even higher power demands are expected [35, 53]. At this moment, the average electric power consumption in modern vehicles ranges between 200 W and 1 kW, depending on the vehicle and its accessories [35]. Considering the fact that a belt driven 14 V alternator typically supplies 1.5 kW at full load, power limitations cannot be neglected in the next years.

To keep up with future power demands, the automobile industry has suggested new 42 V power net topologies which should extend (or replace) the traditional 14 V power net from present vehicles. These topologies make use of more efficient high-power components. The 42 V power net has been extensively discussed in literature, see, *e.g.*, [19, 21, 35, 53].

Before coming to the problem formulation of this thesis, a brief overview of recent developments in automotive engineering to reduce fuel consumption and exhaust emissions will be given.

1.2 Solutions for fuel and exhaust emissions reduction

To prevent depletion of fossil fuels and to limit air pollution, the restrictions on fuel consumption and emissions are increasing. One way to meet these requirements, is to maintain a conventional vehicle configuration, but to improve the vehicle design and the components. By making vehicles smaller, lighter, and more aerodynamic, the power necessary to propel the vehicle can be reduced, and thereby also the fuel consumption.

Fuel reduction can also be obtained by improving the drive train components, especially the engine. The working principle of internal combustion engines has been the same for over a century, but in the last 20 years, large improvements have been made. Although the improvement in fuel economy of modern engines is rather small, huge improvements have been made in lowering various exhaust emissions. This is done partly by replacing the traditional carburetor by a direct injection system in combination with a computer controlled motor management system that adjusts the amount of fuel, the air to fuel ratio, and the ignition timing, such that emissions are reduced. However, the largest improvement comes from using exhaust aftertreatment systems, especially the three-way catalytic converter, see, *e.g.*, [6].

A more radical way to lower fuel consumption and emissions, is to use alternative drive train configurations, of which the most popular will be discussed below.

1.2.1 Continuously variable transmissions

A continuously variable transmission (CVT) can obtain a continuous range of gear ratios instead of the usual 4 or 5 of a manual or automatic transmission. This has the benefit that the engine can run at the engine speed with the lowest fuel consumption. On the other hand, the CVT itself has a lower efficiency than a manual transmission.

In [11], an electromechanically actuated and slip-controlled CVT is shown to have superior efficiency over a conventional CVT.

In [66], a CVT is combined with a flywheel for energy storage, and a controller is designed that improves the drivability. In [39], a CVT is combined with a flywheel, such that the engine can be operated intermittently. This results in a reduction of fuel consumption and exhaust emissions.

In the Zero Inertia project [64, 70, 71], a CVT is combined with a flywheel and a planetary gear set. This is done to obtain a faster change in engine speed, thereby improving drivability and fuel economy.

1.2.2 Electric vehicles

Electric vehicles [12, 20] use electric motors for propulsion. The electric power is provided by a battery. The battery is recharged when the vehicle is not used, using the main electricity supply, which is a time consuming process. The electricity is produced at power plants using a variety of primary energy sources. These power plants are usually operated at their most efficient operating point and have relatively low emissions. The vehicle itself does not produce any emissions. Compared to fossil fuels, batteries have a

low energy content per weight ratio. This limits the radius of action of electric vehicles, making them mostly suitable for urban traffic and special transport applications, such as shuttle services.

1.2.3 Fuel cell vehicles

Fuel cell vehicles [20, 73] are electric vehicles that use a fuel cell instead of or next to a battery to produce electric power. A fuel cell converts hydrogen and oxygen into water. During this process, electric energy becomes available. Although a fuel cell does not produce any exhaust emissions itself, the production of hydrogen does require another energy source and does produce exhaust emissions. Because hydrogen has a higher energy content per weight ratio than a battery, a fuel cell vehicle has a much larger radius of action. Furthermore, refilling the hydrogen tank can be done much faster than recharging a battery. Currently, fuel cells are still in development and an infrastructure for supply of hydrogen is not yet available.

1.2.4 Hybrid electric vehicles

Hybrid electric vehicles (HEV) [20, 28, 51] combine a fuel combustion engine and one or more electric motors and use a battery for temporary storage of electric energy. They are charge sustaining, meaning that the battery is recharged during driving, usually at beneficial moments. HEV's come in various drive train configurations, the most common are the series and the parallel HEV.

Series hybrid electric vehicles are electric vehicles that use a combustion engine with an alternator and a battery to provide the electric power. The engine is usually operated intermittently in its most efficient operating point and turned off where possible. The topology is shown in Fig. 1.1. A drawback of this topology is that the energy is first converted from mechanical to electrical by the alternator and then back again to mechanical by the motor, both introducing losses.

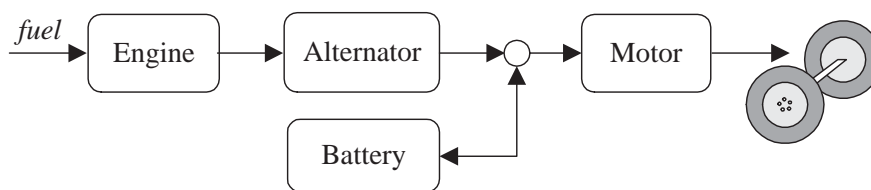


Figure 1.1: Series hybrid electric vehicle topology

Parallel hybrid electric vehicles are more like conventional vehicles. The topology is shown in Fig. 1.2. They use both the combustion engine and an integrated starter generator (ISG) for propulsion. The battery is charged when the ISG is used in generator mode, and discharged when using the ISG in motor mode. If the ISG is mounted directly on the crank shaft, it can only be operated simultaneously with the engine. If it is mounted on the drive shaft, after the clutch, the engine can be turned off during propulsion. An example currently in production is the Honda Civic with Integrated Motor Assist (IMA) [26], which has an ISG mounted directly on the crank shaft.

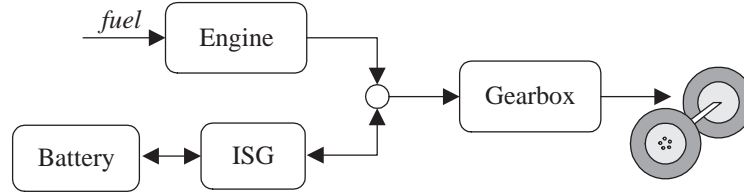


Figure 1.2: Parallel hybrid electric vehicle topology

The Toyota Prius [29], which has been on the market since 2000, has a combined series parallel drive train using a planetary gear set.

Hybrid electric vehicles require an energy management strategy to control the power split between the engine and the electric motors. Energy management can also be applied to the electric power system of a vehicle with a conventional drive train.

1.2.5 Advanced power net control

The vehicular electric power system, or simply power net, usually consists of an alternator that generates electric power, a storage device, such as a battery, and various electric consumers in the vehicle [21].

In a conventional vehicle, the alternator tries to maintain a fixed voltage level on the power net. A traditional lead-acid battery is present for supplying key-off loads and for making the power net more robust against peak-power demands. Although the battery offers freedom to the alternator in deciding when to generate power, this freedom is generally not used.

The research described in this thesis exploits this freedom as it replaces the conventional alternator with an advanced alternator that is power controlled. The alternator is directly coupled to the engine's crankshaft, so by controlling its output power, it will influence the operating point of the combustion engine, and thus the fuel use of the vehicle. An energy management strategy can be used to control the alternator such that it generates the required amount of electric energy in a more beneficial way by temporarily charging and discharging the battery.

1.3 Energy management

The energy management problem of an automotive vehicle deals with controlling the amount of power exchange and other available input variables such that desired behavior of the vehicle is obtained. Desired behavior can be expressed by demands on, *e.g.*, fuel consumption, exhaust emissions, component wear, and comfort, while satisfying restrictions on operating points of components and energy storage levels.

1.3.1 Energy management as an optimization problem

The energy management problem can be formulated as an optimization problem, where a cost function is minimized subject to constraints. Because energy is temporarily stored and later retrieved, the optimization problem is usually defined over a time horizon instead of at a single time instant.

The energy management problem can be formulated as a continuous time dynamic optimization problem, where the vehicle is represented by a dynamic system:

$$\dot{x}(t) = f(x(t), u(t), t) \quad (1.1)$$

which has to be controlled, such that the cost criterion:

$$\int_0^{t_n} \gamma(x(t), u(t), t) dt \quad (1.2)$$

is minimized, satisfying the constraints:

$$\phi(x(t), u(t), t) \leq 0 \quad \psi(x(t), u(t), t) = 0 \quad (1.3)$$

where $x(t)$ are the state variables, such as vehicle speed, engine speed, and energy storage levels and $u(t)$ are the control variables. The control variables can be continuous, for instance, the power flow, discrete, such as engine on/off, or complementary, meaning that only one of a set of variables can be nonzero at a time, like the gear position.

Demands on vehicle behavior that should be strictly met can be written as constraints. Demands that are less strict can be incorporated into the cost function.

If the energy management problem is formulated in discrete time, it can be rewritten as a static optimization problem. This is discussed in detail in Appendix A, which also presents an overview of suitable optimization algorithms.

The optimization problem can be carried out off-line for a specific driving cycle. This gives a lower bound for what can be achieved in practice. For online application of an energy management controller, computation time is limited and a prediction of the future driving cycle is usually not available, which requires modifications to the optimization problem.

If a limited prediction horizon is available, the optimization problem can be solved with a Model Predictive Control (MPC) structure, which uses a receding horizon [50]. This means that the optimization is carried out at each time step over a limited prediction horizon. The first value of the optimal control sequence is implemented. The next time step a new optimization is done using an updated prediction and new measurement data.

If no prediction is available, instantaneous optimization at each time instant can be done, but this requires modifications to the cost function, such that a trade-off is made between benefits now and expected costs later and vice versa.

1.3.2 Energy management of hybrid electric vehicles

In recent years, a lot of research is carried out in the field of hybrid electric vehicles (HEV). Especially the research activities on energy management strategies for parallel

HEV's (see, *e.g.*, [74] for an overview) address many useful concepts that are strongly related to the research presented in this thesis. Although the electric power requirements in a parallel HEV are higher than in a conventional vehicle, both configurations can use the same concepts for controlling the amount of stored electric power. Because of the relevance to the work presented in this thesis, a short literature overview will be given on energy management strategies for HEV.

Strategies that are based on heuristics can easily be implemented in a real vehicle by using a rule-based strategy [7] or by using fuzzy logic [58]. Although these strategies can offer a significant improvement in energy efficiency, they do not guarantee an optimal result in all situations. Consequently, strategies are developed that are based on optimization techniques.

To find the optimal solution, techniques as linear programming [68], optimal control [17, 60], and especially Dynamic Programming [3, 4, 31, 48, 62] have been studied. In general, these techniques do not offer an online solution, because they assume that the future driving cycle is entirely known. Nevertheless, their result can be used as a bench-mark for the performance of other strategies, or to derive rules for a rule-based strategy. If only the present state of the vehicle is considered, optimization at each time instant can be beneficial, but profits will be limited, see [32, 57].

Another possibility is to perform an instantaneous optimization over the current time step, using a cost function that makes a trade off between fuel consumption, battery use and optionally a penalty on undesired behavior, such as done, *e.g.*, in [13, 61, 75].

A different approach is taken in [40, 47]. Instead of focussing on one particular driving cycle, a certain set of driving cycles is considered, resulting in a stochastic optimization approach. A difficulty will be to cover a real-world driving situation with a set of individual driving cycles. Promising results on the prediction of the vehicle load in the near future make it possible to execute the optimization over a short horizon [3]. One step further is to incorporate the optimization into a Model Predictive Control framework, as done, *e.g.*, in [4], such that the energy management strategy will be able to anticipate on upcoming events. The benefits of such a strategy are directly related to the quality of the prediction information as well as the length of the prediction horizon.

1.3.3 Relation with similar problems

The energy management problem for automotive vehicles shows some similarities with other applications and active fields of research.

The problem is very similar to electricity production and scheduling. See, *e.g.*, [59, 76] for an overview and [33, 34] for some recent results. The method described in [69] served as an inspiration for the strategy presented in Chapter 3.

Power transmission expansion planning deals with the problem of determining the optimal number of lines that should be added to an existing power network to supply the forecasted load as economically as possible, subject to operating constraints, see, *e.g.*, [1, 2]. Because the number of lines is discrete, this is usually solved as an integer programming problem.

Other related applications include warehouse storing, stock market trading and logistics. Related problems in mathematics are the Knap-Sack problem, the shortest path problem,

and the traveling salesman problem, which are described, *e.g.*, in [14].

1.4 Problem definition

1.4.1 Open issues

Although a lot of research is recently carried out on energy management for automotive vehicles, there are still several open issues, some of which will be addressed in this thesis.

Many energy management strategies are designed for hybrid electric vehicles, but not specifically for the electric power net in a conventional vehicle. These strategies are often based on heuristics. Heuristic strategies are often tuned by hand using trial and error or fitted on the optimal solution for a known cycle, but not on the physical explanation of this solution. An analysis and explanation on where the profits come from, is usually lacking or incomplete.

1.4.2 Goals of this thesis

The goals of the research described in this thesis are the following:

- Investigate the potential fuel and exhaust emissions reduction that can be obtained by applying energy management to the electric power system of a passenger vehicle with a conventional drive train.
- Design an online implementable strategy that is derived directly from the global optimization problem.
- Implement and test the strategy on a Hardware-in-the-Loop test setup.
- Apply the approach to mild hardware extensions of the vehicle: a vehicle with a dual storage power net and a parallel hybrid electric vehicle with an integrated starter generator.

1.4.3 Main contributions of this thesis

The main contributions of this thesis are the following:

- The vehicle model is reduced drastically, such that it can be used in an optimization.
- By analyzing the typical component characteristics, it is explained why and how much fuel reduction can be obtained.
- It is explained why for this application, shifting the engine to an operating point with a higher efficiency will not necessarily lead to a lower fuel consumption.
- Several optimization methods have been studied and compared with respect to their suitability to solve the energy management problem.

- An online implementable strategy is analytically derived from the global optimization problem. This strategy does not require prediction of the future, while yielding results that are close to the global optimum.

1.5 Layout of this thesis

This thesis is built up as follows.

In Chapter 2, the vehicle configuration is described, a detailed simulation model and a simplified control model are derived and the relevant component characteristics are modeled.

In Chapter 3, energy management strategies for a conventional vehicle are presented. First, the global optimization problem is formulated and suitable solvers are discussed. Further, the problem is simplified to reduce computation time. Then, a strategy is derived that does not require a prediction of the future, such that it can be implemented online. The strategies are compared by simulations.

In Chapter 4, the potential benefits of energy management are analyzed. First, the component characteristics that give rise to fuel reduction are discussed. Subsequently, a set of engineering rules is derived that predict the amount of fuel reduction. Finally, the predicted results are compared with results obtained with global optimization.

In Chapter 5, the conventional vehicle topology is expanded with a dual storage power net, combining a battery and an ultracapacitor. Energy management strategies are derived and evaluated.

In Chapter 6, two parallel hybrid vehicle topologies are studied. A suitable energy management strategy is derived and the performance of the topologies is compared.

In Chapter 7, the energy management strategies for the conventional and the dual storage power net are tested on the detailed simulation model and on a Hardware-in-the-Loop test setup.

In Chapter 8, conclusions and an outlook for future research are given.

Appendix A gives an overview of optimization methods that are studied for this research.

Appendix B presents a more formal description and stability analysis of the strategy described in Section 3.5.

Vehicle Model

2.1 Introduction

This chapter describes the simulation environment that is used for developing and evaluating energy management strategies. Two different models are distinguished: a simulation model to analyze the energy management strategy and a control model as part of the strategy itself. Both models only cover vehicle characteristics that are relevant for energy management. The latter one requires drastic model reductions, to make it useable for an optimization algorithm. These reduced models also give a better insight in how fuel reduction can be obtained, as will be the topic of Chapter 4.

The vehicle model that is used within this thesis is based on a Ford Mondeo built in 2001, with a 2.0 liter Spark Ignition engine and a 5 gear manual transmission. A picture of the vehicle is shown in Fig. 2.1.



Figure 2.1: Ford Mondeo

For the power net, two varieties are used: a conventional 14 V, and an advanced 42 V power net.

The 14 V power net consists of a 1.5 kW alternator and a 12 V Absorption Glass Mat (AGM) lead-acid battery with a capacity of 60 Ah, which corresponds to an energy capacity of 3 MJ.

The 42 V power net consists of a 5 kW alternator and a 36 V AGM lead-acid battery with a capacity of 27.5 Ah, which corresponds to an energy capacity of 4 MJ.

Both power nets are equipped with a programmable electric load on top of the electric loads already present in the vehicle.

This chapter is built up as follows. The power flow in the vehicle is described in Section 2.2. Two model structures are discussed in Section 2.3. The drive train is modeled in Section 2.4. The engine is modeled in Section 2.5. The alternator is modeled in Section 2.6. The battery is modeled in Section 2.7. The electric loads are modeled in Section 2.8. Conclusions are given in Section 2.9.

2.2 Power flow in a vehicle

This thesis focusses on vehicles with a conventional drive train and a manual transmission. The power flow in such a vehicle is shown in Fig. 2.2.

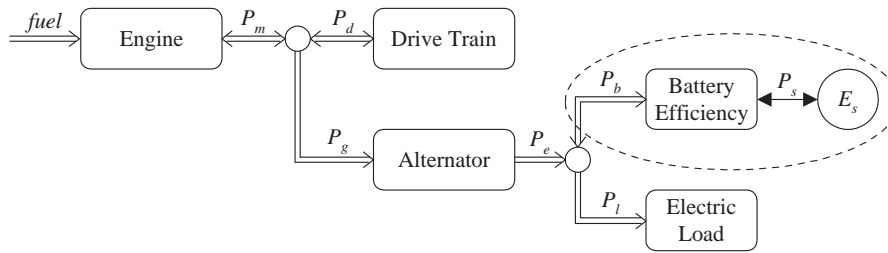


Figure 2.2: Power flow in a conventional vehicle

The power flow in the vehicle starts with fuel that is injected in the combustion engine. The resulting mechanical power P_m splits up into two directions: one part P_d goes to the drive train for vehicle propulsion, whereas the other part P_g goes to the alternator. The alternator provides electric power P_e for the electric loads P_l but also takes care of charging the battery P_b . Contrary to the other components, the power flow of the battery can be positive as well as negative. In the end, all power, except for losses, is used for vehicle propulsion and for electric devices connected to the power net.

The drive train block contains all drive train components including clutch, gears, wheels, and vehicle inertia. The alternator is connected to the engine by a belt with a fixed gear ratio.

2.3 Model structure

Depending on the purpose of the model, two model classes can be distinguished: a simulation model and a control model.

The simulation model is used to analyze and validate the control actions of an energy management strategy. This is a complex dynamic vehicle model with a flexible interface for connecting the energy management strategy, similar to the real vehicle.

The control model is incorporated in the energy management strategy itself. By evaluating this model, the strategy determines which control actions should be taken. The control model is less complex and runs at a much lower sampling frequency than the simulation model, such that real-time implementation of the energy management strategy can be realized.

Both models only cover the longitudinal dynamics, *i.e.*, the relation between engine torque and vehicle speed on a straight road. Phenomena like suspension and roadholding in curves are neglected as those are not expected to be influenced heavily by the energy management strategy.

2.3.1 Simulation model

The simulation model accurately represents all relevant characteristics of a real vehicle, and is used to evaluate energy management strategies and their influence on drivability.

The drive train is represented by a forward facing (or integrating) model, which means that the input is the engine throttle and the output is the resulting vehicle speed. The throttle is controlled by a driver model that tries to track the desired speed.

A schematic overview of the model is given in Fig. 2.3, also showing the physical connections that are present between subsystems. The simulation model is described in more detail and validated with real vehicle measurement data in [37]. This model will only be used in Chapter 7.

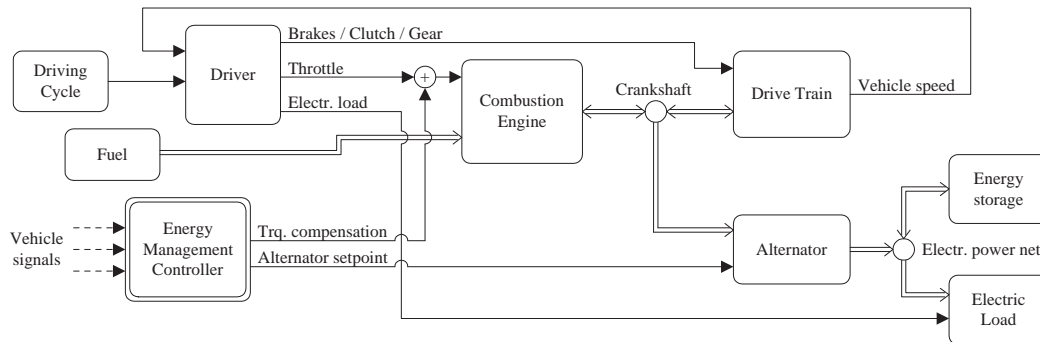


Figure 2.3: Forward facing simulation model

2.3.2 Control model

The control model is used by an optimization routine to compute the optimal control signals that minimize the fuel consumption. It is also used for evaluation of the fuel consumption.

To reduce complexity, the drive train is represented by a backward facing or differentiating model. This model assumes that the desired velocity is tracked exactly. The inputs are the desired velocity and gear position, and the outputs are the engine speed and the propulsion torque. By adding the alternator torque, the fuel consumption is computed. The alternator torque depends on the electric power delivered to the electric loads and the battery. A schematic overview of the control model is given in Fig. 2.4.

The control model uses simple power-based models for the drive train, the engine, the alternator, the battery, and the loads, which are described below.

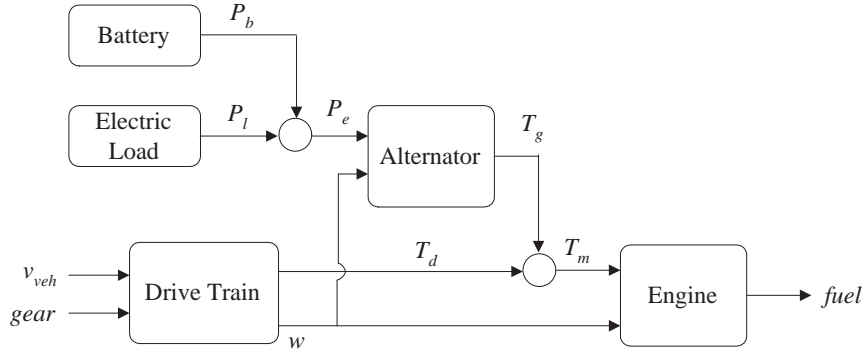


Figure 2.4: Backward facing control model

2.4 Drive train

The drive train consists of clutch, transmission, final drive, wheels, and inertia. They are not modeled in detail, as only the relation between vehicle speed, engine speed, and drive train torque is of interest. For a given vehicle speed profile $v(t)$, road slope $\alpha(t)$, and selected gear ratio $g_r(t)$, the corresponding engine speed and torque needed for propulsion can be calculated as follows.

The force $F_d(t)$ necessary to propel the vehicle consists of inertia, air drag, road slope and rolling resistance:

$$F_d(t) = M \dot{v}(t) + \frac{1}{2} \rho C_d A_d v(t)^2 + M g \sin(\alpha(t)) + C_r M g \cos(\alpha(t)) \quad (2.1)$$

By neglecting losses in the transmission, the torque at the crank shaft becomes:

$$\tau_d(t) = \frac{w_r}{f_r} \frac{1}{g_r(t)} F_d(t) \quad (2.2)$$

The engine speed is given by:

$$\omega(t) = \frac{f_r}{w_r} g_r(t) v(t) \quad (2.3)$$

The power required for propulsion is given by:

$$P_d(t) = \omega(t) \tau_d(t) \quad (2.4)$$

When the engine speed drops below idle speed, the clutch is opened, the drive train torque becomes zero, and the engine keeps running at idle speed. The engine power becomes equal to the alternator power and the drive train power becomes equal to the brake power.

In Table 2.1, the parameters are explained and their values as used in this thesis are given.

2.4.1 Driving cycle

All simulations in this thesis will be done for the New European Driving Cycle (NEDC) [22] of which the vehicle speed and gear position are shown in Fig. 2.5. It consists of 4

Table 2.1: Parameter values for the simulation model

<i>Quantity</i>	<i>Symbol</i>	<i>Value</i>	<i>Unit</i>
Mass	M	1400	kg
Frontal area	A_d	2	m ²
Air drag coefficient	C_d	0.3	-
Rolling resistance	C_r	0.015	-
Wheel radius	w_r	0.3	m
Final drive ratio	f_r	4.0	-
Gear ratio	g_r	3.4 - 2.1 - 1.4 - 1.0 - 0.77	-
Idle speed	ω_i	73.3	rad/s
Air density	ρ	1.2	kg/m ³
Gravity	g	9.8	m/s ²

identical urban cycles and one extra-urban cycle. The corresponding engine speed, torque and power are shown in Fig. 2.6. This cycle is rather conservative for this vehicle as the engine speed and torque remain far below their maximum allowed values.

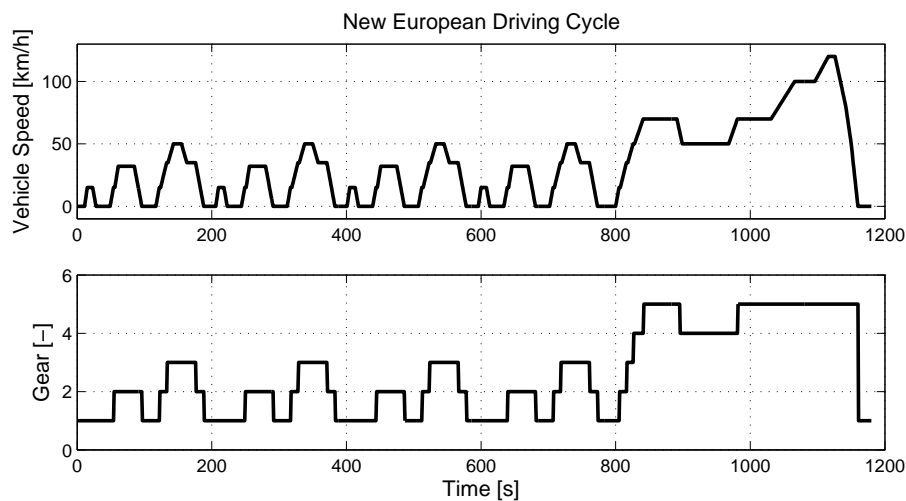


Figure 2.5: New European Driving Cycle

2.5 Internal combustion engine

The two most commonly used internal combustion engines (ICE) are spark ignition (SI) engines using gasoline and compression ignition (CI) engines using diesel [30, 67].

2.5.1 Combustion

Gasoline and diesel fuels are both complex hydro-carbons H_yC_z . Air is a mixture of mostly nitrogen (N_2) and oxygen (O_2). When fuel is combusted, ideally the hydrogen and

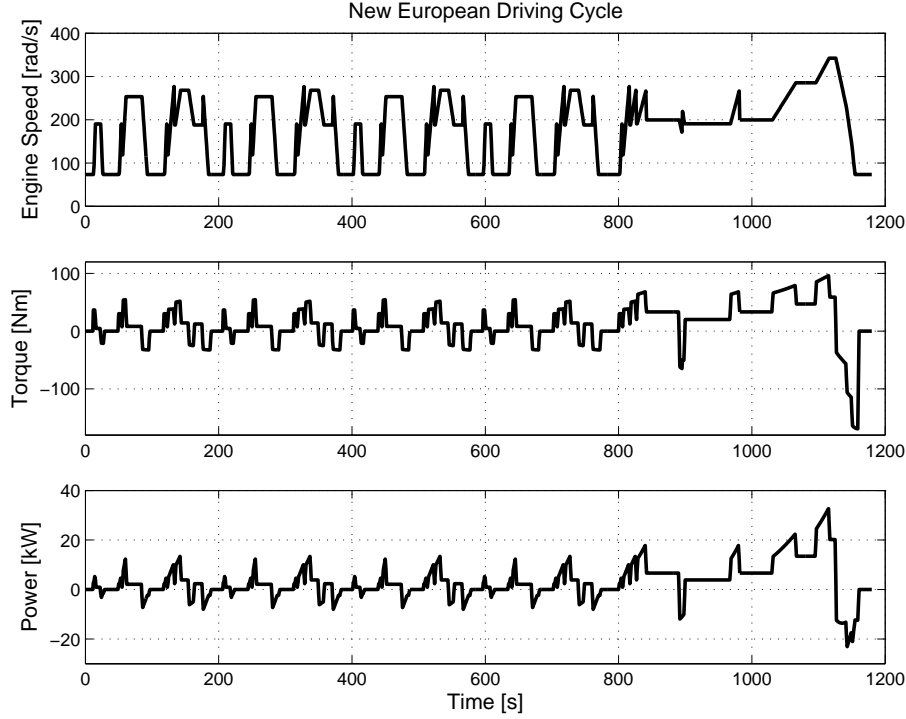


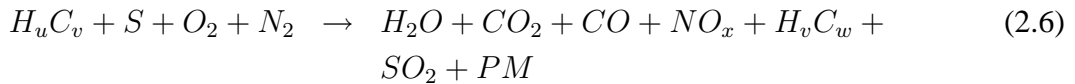
Figure 2.6: New European Driving Cycle

oxygen turn into water (H_2O) and the carbon and oxygen turn into carbon-dioxide (CO_2). However, in reality, several other reactions take place. If the air-to-fuel ratio is too low, carbon and oxygen partly turn into toxic carbon-monoxide (CO). This is especially the case for a cold engine and in the highest torque region. At high temperatures, nitrogen reacts with oxygen, becoming NO_x which is toxic and one of the causes of smog. Partly unburned fuel turns into various other hydro-carbons (HC) H_vC_w .

Neglecting the molar ratios, the chemical reaction equation for gasoline is roughly as follows:



Diesel also contains sulfur (S) and produces considerable amounts of particle matter (PM), leading to the following reaction equation:



A more detailed description of the chemical reactions and properties of the exhaust emissions can, *e.g.*, be found in [6].

2.5.2 Power-based model

For simplicity, and by lack of accurate data, the temperature dependency and the dynamic behavior of the internal combustion engine are neglected. The engine is represented by a

nonlinear static map that describes the fuel rate \dot{m} as function of the engine speed ω , and the torque delivered by the engine τ_m :

$$\dot{m} = \hat{f}(\tau_m, \omega) \quad (2.7)$$

For given engine speed, the mechanical power delivered by the engine P_m can be derived from the engine torque as follows:

$$P_m = \tau_m \omega \quad (2.8)$$

Using this relation, the fuel map can also be written as a nonlinear function of engine speed and power:

$$\dot{m} = f(P_m, \omega) \quad (2.9)$$

The fuel map of a Spark Ignition (SI) engine is displayed in Fig. 2.7. In this figure, fuel consumption curves are drawn for different engine speeds as function of mechanical power. As can be seen, the fuel map can be approximately represented by a linear relation between the mechanical power and the fuel rate for each engine speed:

$$f(P_m, \omega) \approx f_0(\omega) + \frac{k_f}{h_f} P_m \quad (2.10)$$

The fuel consumption at zero torque $f_0(\omega)$ is caused by mechanical friction and pumping losses in the engine. It increases with the engine size, the number of cylinders, and the engine speed. The dimensionless factor k_f has a typical value of 2.5, which corresponds to a combustion efficiency of 40%. Parameter h_f is the lower heating value of fuel, *i.e.*, the chemical energy content of fuel, with a typical value of 44 kJ/g for gasoline and 49 kJ/g for diesel. The chemical power of the fuel rate is given by:

$$P_f = h_f \dot{m} \quad (2.11)$$

The affine relation between fuel and engine power corresponds with the so-called Willans lines model [30], which is a scaling method used to create numerical models of IC engines of any desired size.

In automotive engineering, the fuel map of an engine is usually visualized by normalizing the fuel consumption with respect to the power delivered by the engine. This so called Brake Specific Fuel Consumption (BSFC) β_{ice} , which is usually expressed in g/kWh, is defined as:

$$\beta_{ice} = 3.6 \cdot 10^6 \frac{\dot{m}}{P_m} = 3.6 \cdot 10^6 \frac{\dot{m}}{\omega \tau_m} \quad (2.12)$$

The dimensionless efficiency of the engine η_{ice} is inverse to the BSFC:

$$\eta_{ice} = \frac{P_m}{P_f} = \frac{\omega \tau_m}{h_f \dot{m}} = \frac{3.6 \cdot 10^6}{h_f \beta_{ice}} \quad (2.13)$$

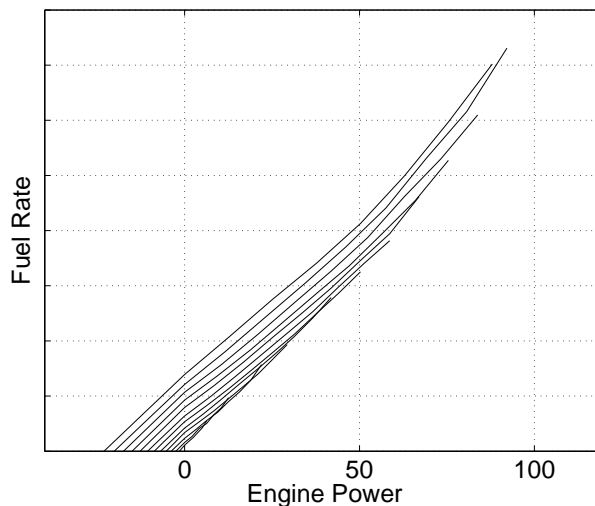


Figure 2.7: Fuel map of a SI engine for various engine speeds

The efficiency is usually visualized as a contour plot of engine speed and torque, as done in Fig. 2.8. The efficiency is zero at zero torque, because there, fuel is combusted, but no useful power is provided. For increasing torque, the efficiency increases, because the fuel use at zero torque, \dot{m}_0 becomes relatively less. For negative torques, \dot{m} is still positive, which results in a negative efficiency.

Although the efficiency varies drastically over the operating range, the absolute fuel use increases more or less linearly with the delivered power, as shown in Fig. 2.7. This is a very important observation with respect to energy management, as will be further explained in Section 4.2.1.

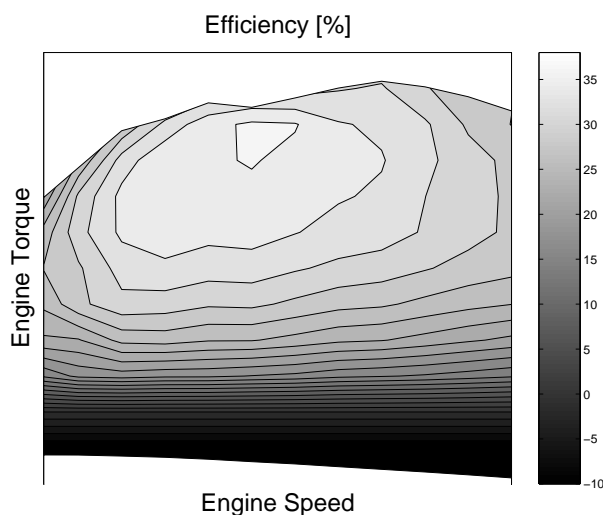


Figure 2.8: Efficiency map of an SI engine

As is illustrated in the efficiency map in Fig. 2.8, the operating range of the fuel converter is bounded by a drag torque and a maximum torque that are both speed dependent. The drag torque is defined as the engine torque when no fuel is injected. Translated to power

this becomes:

$$f_0(\omega) + \frac{k_f}{h_f} P_{m \min}(\omega) = 0 \quad \Rightarrow \quad P_{m \min}(\omega) = -\frac{h_f}{k_f} f_0(\omega) \quad (2.14)$$

The fuel map can then also be described as:

$$\dot{m} \approx \frac{k_f}{h_f} (P_m - P_{m \min}(\omega)) \quad (2.15)$$

The fuel consumption over a driving cycle can be computed by:

$$m = \int_0^{t_n} \dot{m} dt \approx \frac{k_f}{h_f} \int_0^{t_n} (P_m - P_{m \min}(\omega)) dt \quad (2.16)$$

2.5.3 Exhaust emissions

Compared to fuel, emissions are more dependent on dynamic phenomena, such as temperature, air moisture, and the dynamic change in engine torque and speed. However, static maps are the only available information on them.

The CO₂ and CO maps of an SI engine are shown in Fig. 2.9, while Fig. 2.10 shows the maps of HC and NO_x. CO₂ is more or less proportional with fuel, except for the high power area, where a lower air-to-fuel ratio is used, leading to more CO and HC, but less NO_x. NO_x shows a more nonlinear non-convex behavior.

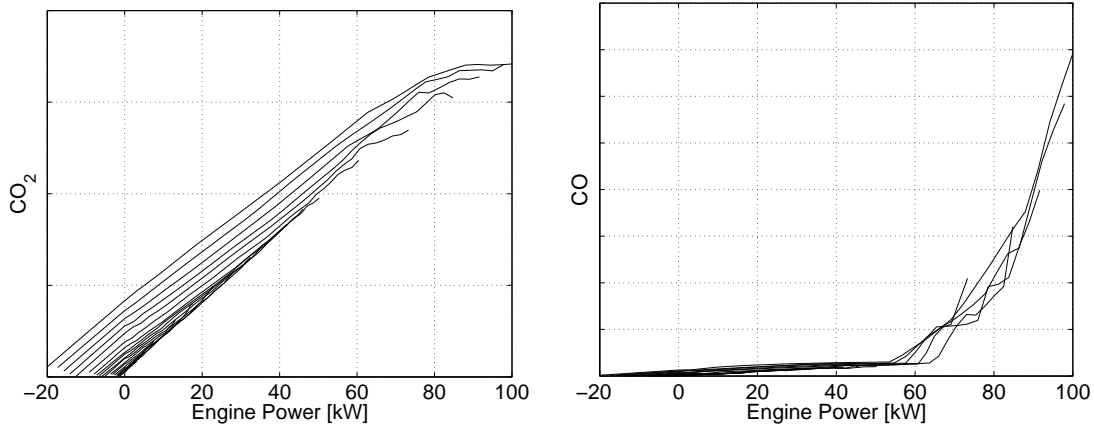
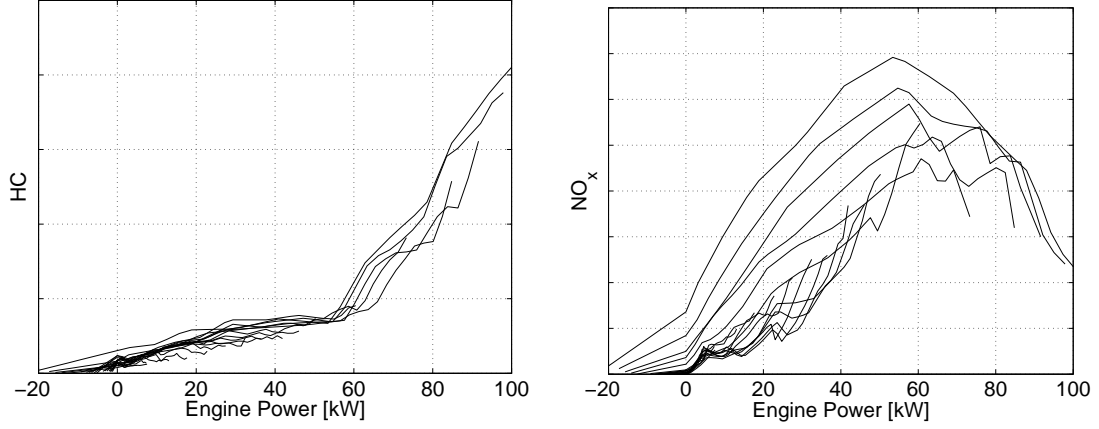


Figure 2.9: CO₂ and CO map for various engine speeds

2.6 Alternator

Alternators as used in vehicles are equipped with a voltage regulator that tries to maintain a constant power net voltage. The alternators used in this project are equipped with a voltage regulator of which the voltage set-point can be adjusted, thereby also affecting the resulting current to the battery and the loads. An outer control loop is applied that controls the delivered electric power by measuring the current and manipulating the voltage.

Figure 2.10: HC and NO_x map for various engine speeds

The remaining dynamics are sufficiently fast to represent the alternator by a static nonlinear map that describes the mechanical power as function of the electrical power and the rotational speed:

$$P_g = g(P_e, \omega) \quad (2.17)$$

The measured map of the 42 V 5 kW alternator is shown for various engine speeds in Fig. 2.11. Similar to the engine, the alternator can be approximated by a linear relation between electrical power P_e and mechanical power P_g with a constant slope k_g :

$$P_g \approx g_0(\omega) + k_g P_e(\omega) \quad (2.18)$$

The slope k_g has a typical value around 1.25, which corresponds to a conversion efficiency of 80%. The term $g_0(\omega)$ is caused by mechanical friction and increases with the speed. The operating range of the alternator is bounded between:

$$0 \leq P_e \leq P_{e \max}(\omega) \quad \Rightarrow \quad P_{g \min}(\omega) \leq P_g \leq P_{g \max}(\omega) \quad (2.19)$$

where:

$$P_{g \min}(\omega) = g_0(\omega) \quad \text{and} \quad P_{g \max}(\omega) = g_0(\omega) + k_g P_{e \max} \quad (2.20)$$

2.7 Battery

A lead-acid battery has a complex nonlinear electro-chemical behavior. First, its electric behavior will be illustrated using a simplified linear electric circuit. Subsequently, the losses during charging and discharging are approximated by a power-based model.

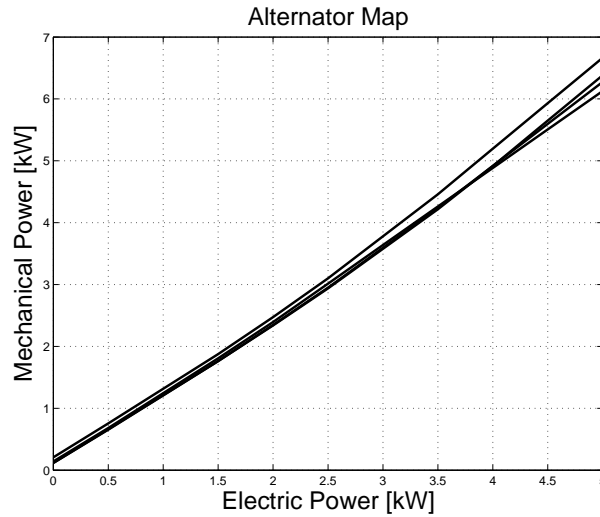


Figure 2.11: 42 V 5 kW alternator map for various engine speeds

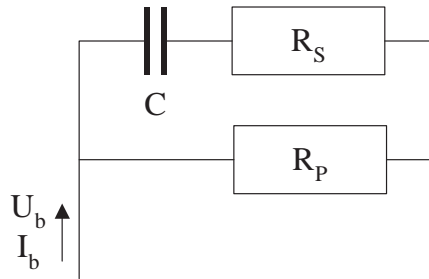


Figure 2.12: Battery modeled as an RC circuit

2.7.1 Electric circuit

A battery behaves roughly like a capacitor and a resistor in series together with a resistor in parallel, as illustrated in Fig. 2.12.

The resistor in series R_s causes a voltage drop and thus power losses during (dis)-charging, where a higher value of R_s causes higher losses. The resistor in parallel R_p causes a leak current, resulting in self-discharging of the battery, where a higher value of R_p means a lower self-discharging rate. The self-discharge of a battery becomes significant if a vehicle is not used for several weeks, but can be neglected during driving, resulting in Fig. 2.13.

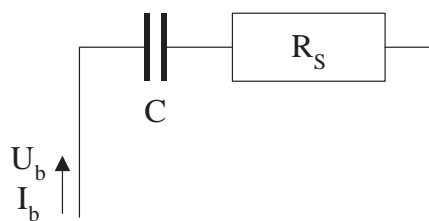


Figure 2.13: Battery modeled as a simplified RC circuit

The charge level of the battery is given by a simple integrator:

$$Q_c(t) = Q_c(0) + \int_0^t I(\tau) d\tau \quad (2.21)$$

The state of charge (*SOC*) represents the relative charge in the battery:

$$SOC = \frac{Q_c}{Q_{cmax}} \cdot 100\% \quad (2.22)$$

The relation between the open circuit voltage U_c and the state of charge of a lead-acid battery is highly nonlinear, as illustrated in Fig. 2.14. However, between 20 and 100% state of charge, the voltage is more or less linear with the state of charge, but with a large offset $U_c(0)$. It can be modeled as:

$$U_c(t) = U_c(0) + \frac{1}{C} \int_0^t I(\tau) d\tau \quad (2.23)$$

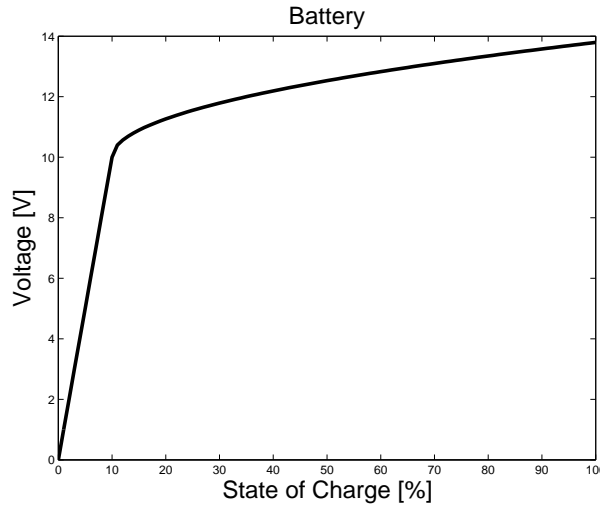


Figure 2.14: Open circuit voltage of a 6-cell lead-acid battery

Using Kirchoff's laws, the electric equation for the battery then becomes:

$$U_b(t) = U_c(t) + U_r(t) = U_c(0) + \frac{1}{C} \int_0^t I(\tau) d\tau + R I(t) \quad (2.24)$$

2.7.2 Power-based model

Although a battery has a nonlinear dynamic behavior, it's most important property for this research is that it has losses during charging and discharging that increase with the stored or retrieved power. To be able to incorporate the battery losses in the control model, the battery characteristic is modeled as a power based model:

$$P_b = P_s + P_{loss}(P_s, E_s, T) \quad (2.25)$$

P_b represents the power entering or leaving the battery terminals, and P_s represents the power actually stored in the battery. P_{loss} represents the battery losses that depend on the storage power, the energy level in the battery E_s , and the temperature T . The charging losses increase with the SOE , whereas the discharging losses decrease with SOE . Usually, they are both acceptable around 70% SOE .

Assuming the variation in energy level and temperature is small, (2.25) reduces to:

$$P_b = P_s + P_{loss}(P_s) \quad (2.26)$$

The battery voltage and current can only be measured at the terminals, which makes it difficult to identify the losses. Therefore, the losses are identified using an accurate simulation model of the 42 V battery, consisting of multiple nonlinear resistors and capacitors. A sinusoidal current with an amplitude of 50 A and a frequency of 0.01 Hz is applied and the corresponding voltage of the main capacitor and at the terminals are measured. The resulting power losses are shown in Fig. 2.15. As can be seen, the energy losses are approximately 10% for charging and 5% for discharging. There is some hysteresis due to the dynamic behavior of the battery, which becomes more obvious when higher frequencies are used.

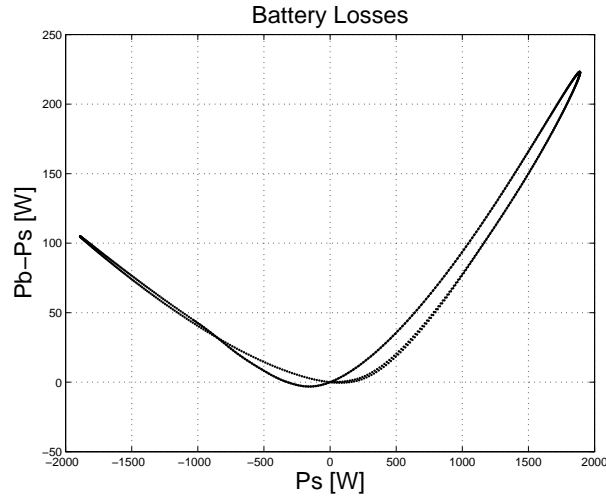


Figure 2.15: Battery losses of a detailed simulation model

The energy level of the battery is given by a simple integrator:

$$E_s(t) = E_s(0) + \int_0^t P_s(\tau) d\tau \quad (2.27)$$

The state of energy (SOE) represents the relative energy level in the battery:

$$SOE = \frac{E_s}{E_{smax}} \cdot 100\% \quad (2.28)$$

If the open circuit voltage U_c would be constant, SOE and SOC are identical. In reality, U_c varies a little, as was illustrated in Fig. 2.14. In this thesis, SOE will be used, as all models are power-based.

2.8 Electric loads

There are many electric consumers present in a vehicle. Some of them are required for running the engine, such as the motor management system, the ignition system and the fuel pump. Others are for safety, such as lighting. Others are for driver and passenger comfort, such as window heating and audio and navigation equipment.

Some loads, such as light bulbs and window heating, behave as resistors, which means that their current increases linearly with the power net voltage, and their power consumption quadratically. Other more advanced loads, such as audio equipment, have an internal voltage regulator, which means that their power consumption is independent from the power net voltage. For convenience, the electric loads are modeled as one lumped power consumer.

2.9 Conclusion

A control model of the vehicle is derived that uses severe simplifications of the components in order to come to a model that can be used by an optimization algorithm. The engine and the alternator are modeled as static lookup tables and the battery is approximated as a power-based model. The engine and the alternator roughly show a linear behavior. This property will be used in Chapter 4 to explain what potential fuel can be obtained using an energy management strategy to control the alternator.

Energy Management Strategies

3.1 Introduction

This chapter presents a practically implementable energy management strategy that is directly derived from global optimization methods. This strategy is obtained by taking the following steps.

First a formal problem definition is given, by expressing the total fuel consumption and emissions along the driving cycle as a function of the control variables. To find the optimal control sequence for the alternator, Dynamic Programming has been applied. Under the assumption that the entire driving cycle is known in advance, the method calculates the power set-points for the alternator. For the problem formulation considered here, several modifications of the algorithm are carried out, thereby reducing the amount of computations. Nevertheless, the computation time of Dynamic Programming still remains too large for a practical real-world application.

To come to a solution that is implementable in a vehicle, additional modifications are necessary. First, the vehicle model is further simplified, such that the problem formulation reduces to a simpler Quadratic Programming structure. However, this solution still depends on the assumption that information about the driving cycle in the near future is available. Second, based on the Quadratic Programming formulation, a strategy is designed that only requires present vehicle information and uses a single state to capture information of the past.

This chapter is built up as follows. Section 3.2 formulates the energy management problem as an optimization problem. The Dynamic Programming strategy is explained in Section 3.3. Section 3.4 reduces the problem to a Quadratic Programming problem. Section 3.5 presents an online implementable strategy. The performances of all individual strategies are compared by simulations in Section 3.6. Conclusions are given in Section 3.7.

The contents of this chapter are published earlier in [46], which continued on the work presented in [15, 42, 54, 55].

3.2 Problem definition

The idea of controlling the alternator power is initiated by the fact that energy losses in the internal combustion engine, alternator, and battery change according to their operat-

ing point. Minimizing these energy losses will result in an energy management strategy achieving higher fuel economy.

3.2.1 Control objective

The control objective of energy management is to lower the fuel consumption and exhaust emissions while satisfying several constraints. This control problem can be formulated as a dynamic optimization problem. Using discrete time, the system dynamics (1.1) can be described as:

$$x(k+1) = f(x(k), u(k), k) \quad (3.1)$$

The cost criterion (1.2) then becomes:

$$\sum_0^n \gamma(x(k), u(k), k) \Delta t \quad (3.2)$$

and the constraints (1.3) become:

$$\phi(x(k), u(k), k) \leq 0 \quad \psi(x(k), u(k), k) = 0 \quad (3.3)$$

In this application, the only relevant state is the energy level in the battery E_s . By using a discrete time version of (2.27), (3.1) becomes:

$$E_s(k+1) = E_s(k) + P_s(k) \Delta t \quad (3.4)$$

Assuming the signals $\omega(k)$, $P_d(k)$, and $P_l(k)$ to be known, and combining the characteristics of all components, given by:

$$P_b = P_s + P_{loss}(P_s) \quad (3.5)$$

$$P_e = P_l + P_b \quad (3.6)$$

$$P_g = g(P_e, \omega) \quad (3.7)$$

$$P_m = \max(P_d + P_g, P_{mmin}) \quad (3.8)$$

$$\dot{m} = f(P_m, \omega) \quad (3.9)$$

the fuel rate can be expressed as a function of the battery storage power:

$$\dot{m}(\omega(k), P_d(k), P_l(k), P_s(k)) = \dot{m}(P_s(k), k) \quad (3.10)$$

Instead of minimizing the fuel use only, the cost function can also be a weighted sum of the fuel use and the exhaust emissions by using:

$$\begin{aligned} \gamma(P_s, k) = & w_1 \dot{m}(P_s, k) + w_2 CO_2(P_s, k) + w_3 CO(P_s, k) + \\ & w_4 NO_x(P_s, k) + w_5 HC(P_s, k) \end{aligned} \quad (3.11)$$

where w_i are weighting factors for the respective mass flows.

The cost function expresses the fuel use and the emissions over the driving cycle in the time interval $t = \Delta t \cdot [0, \dots, n]$, so (3.2) becomes:

$$J = \sum_{k=0}^n \gamma(P_s(k), k) \quad (3.12)$$

By choosing P_s as decision variable z , the characteristics of all components are included in the cost function. The actual controlled input in the vehicle is P_e . Because the relation between P_s and P_e is known, P_e can be computed from the optimal P_s .

The operating range of the components is limited, so bounds have to be set on the engine power, electrical power, and battery power throughput. This can be done using the following constraints:

$$P_{m \min} \leq P_m \leq P_{m \max} \quad (3.13)$$

$$P_{e \min} \leq P_e \leq P_{e \max} \quad (3.14)$$

$$P_{b \min} \leq P_b \leq P_{b \max} \quad (3.15)$$

Because the relations (2.17) and (2.26) are invertible, the constraints (3.13)-(3.15) can be translated to time varying bounds on P_s . Combining them leads to one lower and upper bound for P_s at each time instant:

$$P_{s \min} \leq P_s \leq P_{s \max} \quad (3.16)$$

The bounds on the battery energy level E_s can also be translated to constraints on P_s :

$$E_{s \min} - E_s(0) \leq \sum_{i=0}^k P_s(i) \Delta t \leq E_{s \max} - E_s(0) \quad \forall \quad k \in [0, n] \quad (3.17)$$

A charge-sustaining vehicle requires some kind of endpoint penalty to guarantee that the state of charge of the battery remains in a neighborhood around a desired value. An endpoint constraint will be used here, requiring the state of energy at the end of the cycle to be the same as at the beginning:

$$E_s(t_n) = E_s(0) \quad \Rightarrow \quad \sum_{k=0}^n P_s(k) = 0 \quad (3.18)$$

3.2.2 Applied control techniques

The nonlinear optimization problem can be carried out using nonlinear problem solvers. The problem is defined such that it can be easily incorporated into an optimization technique called *Dynamic Programming* [10], as will be done in Section 3.3.

Because computation time is limited in online applications, the nonlinear optimization problem will be approximated by a *Quadratic Programming* [23] problem in Section 3.4. For practical data, the problem is convex, which makes solution easier.

In reality, only a limited prediction of the future driving cycle will be available. A possible control technique that is able to use this prediction is *Model Predictive Control* [50], which will be the topic of Section 3.5.

3.3 Dynamic Programming

After discretization, the optimization problem formulated in the previous section can be seen as a multi-step decision problem: at each time instant, one has to decide which alternator setpoint, for the next time interval, will achieve the smallest objective value over a certain trajectory, while satisfying the constraints. To find this optimal control sequence, Dynamic Programming (DP) [10] will be applied.

DP is commonly used for global optimization of the energy management problem of hybrid electric vehicles [3,4,31,48]. For the problem formulation considered here, several modifications are carried out, thereby reducing the amount of computations.

3.3.1 Implementation DP algorithm

Equations (2.9), (2.17), (2.26), and (3.4) define the fuel consumption of a dynamic system with one control input P_s and one state variable E_s . The sample moments are indicated by variable $k = [1, \dots, n]$ with n defined by the length of the driving cycle:

$$n = \left\lceil \frac{t_n}{\Delta t} \right\rceil \quad (3.19)$$

Due to the bounds (3.17), only energy levels between $E_{s \min}$ and $E_{s \max}$ will be used. This area is mapped onto a fixed grid with distance ΔE_s , such that exactly $m + 1$ energy levels are considered, with:

$$m = \left\lfloor \frac{E_{s \max} - E_{s \min}}{\Delta E_s} \right\rfloor \quad (3.20)$$

The relation between the input variable P_s and the state E_s is an integrator. As will be explained at the end of this section, it is computationally beneficial to select a grid for P_s that is directly related to ΔE_s . Therefore ΔP_s is chosen as:

$$\Delta P_s = \frac{\Delta E_s}{\Delta t} \quad (3.21)$$

The control input P_s should respect the constraint (3.16). It will be selected from a discrete set of input values, separated with grid distance ΔP_s . The set of feasible input grid points at each time instant k can be defined as:

$$\mathcal{P}_s(k) = \{u \mid P_{s \min}(k) \leq u(k)\Delta P_s \leq P_{s \max}(k), u \in \mathbb{N}\} \quad (3.22)$$

The operating range of the battery reduces further by considering only those trajectories that are possible between an initial energy level of the battery $E_s(0)$ and a desired end state $E_s(n)$. For convenience, both $E_s(0)$ and $E_s(n)$ are restricted to one of the grid points for E_s . Consequently, both energy levels can be represented by an integer $e \in [0, \dots, m]$:

$$\text{Initial energy level } e_0 : E_s(0) = E_{s \min} + e_0 \Delta E_s$$

$$\text{Final energy level } e_n : E_s(n) = E_{s \min} + e_n \Delta E_s$$

Due to the endpoint constraint (3.18), $e_n = e_0$ holds.

The feasible area for E_s along the driving cycle is restricted by six individual constraints, *i.e.*, the upper and lower bound on P_s , the upper and lower bound on E_s , the initial state $E_s(0)$, and the end state $E_s(n)$. Together, they define stricter boundaries on E_s , given by:

$$E_{smin}^* = \max(E_{smin}, E_{smin}^1, E_{smin}^2) \quad (3.23)$$

$$E_{smax}^* = \min(E_{smax}, E_{smax}^1, E_{smax}^2) \quad (3.24)$$

where:

$$E_{smin}^1(k) = E_s(0) + \sum_{i=1}^k P_{smin}(i)\Delta t \quad (3.25)$$

$$E_{smin}^2(k) = E_s(n) - \sum_{i=k+1}^n P_{smax}(i)\Delta t \quad (3.26)$$

$$E_{smax}^1(k) = E_s(0) + \sum_{i=1}^k P_{smax}(i)\Delta t \quad (3.27)$$

$$E_{smax}^2(k) = E_s(n) - \sum_{i=k+1}^n P_{smin}(i)\Delta t \quad (3.28)$$

These boundaries are illustrated in Fig. 3.1. Typically, the feasible area has a diamond-shape. Starting from an initial state $E_s(0)$, it is possible to charge or discharge the battery until one of the boundaries E_{smax} or E_{smin} becomes active. It is allowed to stay between those boundaries, as long as the end of the driving cycle is sufficiently far away. In the end, it is necessary to return to $E_s(n)$, so the feasible area of E_s converges according to the limitations on P_s .

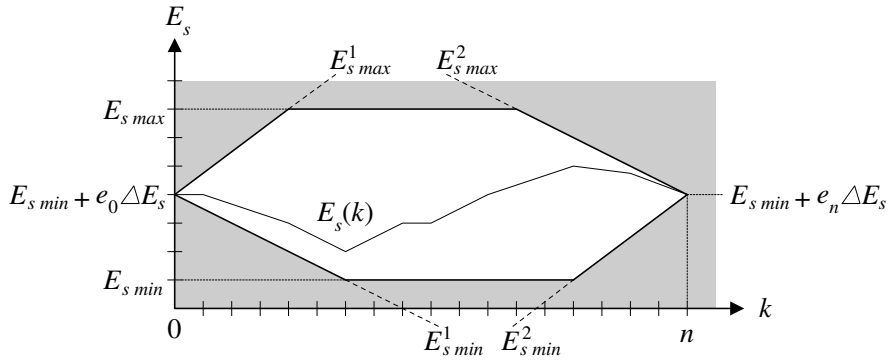


Figure 3.1: Feasible energy window for battery along driving cycle

The energy levels e that are feasible are different at each time instant. Given the boundaries (3.23) and (3.24), it is possible to define a set \mathcal{R} that represents all feasible combinations (e, k) for a given driving cycle:

$$\mathcal{R} = \left\{ (e, k) \left| \begin{array}{l} E_{smin}^*(k) \leq E_{smin} + e\Delta E_s \leq E_{smax}^*(k) \\ 1 \leq k \leq n, 0 \leq e \leq m \end{array} \right. \right\} \quad (3.29)$$

The DP algorithm creates a cost matrix $\mathbf{R} \in \mathbb{R}^{(m+1) \times n}$ and fills this matrix recursively from $k = n$ down to $k = 1$. In literature, \mathbf{R} is often called the cost-to-go matrix. Here, it represents the amount of fuel and emissions necessary to reach the end of the driving cycle:

$\mathbf{R}_{e,k}$ = the minimum cumulative cost for driving the remainder of the driving cycle, starting at $t = k\Delta t$ with an initial state $E_s(k) = E_{smin} + e\Delta E_s$

Using (3.22) and (3.29), it is possible to formulate a recursive definition for matrix \mathbf{R} . The DP algorithm uses the expressions (3.30) and (3.31) to calculate the contents of \mathbf{R} :

$$\mathbf{R}_{e_n,n} = 0 \quad (3.30)$$

$$\mathbf{R}_{e,k} = \min_{\substack{u \in \mathcal{P}_s(k) \\ (e,k) \in \mathcal{R} \\ (e+u,k+1) \in \mathcal{R}}} (\mathbf{R}_{e+u,k+1} + \gamma(u \Delta P_s, k) \Delta t) \quad \text{for } k = [n-1, \dots, 1] \quad (3.31)$$

From (3.31) it should become clear why it is beneficial to select ΔE_s and ΔP_s according to (3.21). Consider the dynamics of the battery as described in (3.4). If the present state $E_s(k)$ is selected such that it corresponds exactly to one of the $m+1$ grid points, then the next state $E_s(k+1)$ will also be an energy level that matches exactly to a grid point, so there is no interpolation needed. This explains why the first term in (3.31) can be taken directly from cost matrix \mathbf{R} , without further calculations. Consequently, the calculation time of the DP-algorithm reduces significantly.

The sequence of P_s that achieves minimum fuel consumption is not stored in \mathbf{R} . The optimal values are calculated afterwards, by starting at $E_s(0)$ and then following the path of minimal cost, as it has been stored in \mathbf{R} . Given this sequence for $P_s(k)$, the requested set-points for the alternator are found using (2.17) and (2.26).

All calculations required for DP can be done in an acceptable amount of time due to the simple dynamics (only the energy level in the battery) and all the restrictions on E_s and P_s . However, the number of computations increases rapidly with the driving cycle length and the grid density.

3.4 Quadratic Programming

Although the computation time of the Dynamic Programming routine has been reduced significantly, as discussed in Section 3.3, it is still very time consuming for long driving cycles, so for real-time implementation other modifications need to be considered. In this section, simplifications will be introduced to achieve a Quadratic Programming structure (QP) [23], which has the advantage that a global minimum is guaranteed and short computation times can be achieved, provided that the problem is convex. Limiting the prediction length of the driving cycle in the optimization is the subject of Section 3.5.

A QP problem is given by a quadratic cost criterion subject to linear constraints:

$$\min_z J(z) = \frac{1}{2} z^T H z + \underline{h}^T z + h_0 \quad \text{subject to} \quad A z \leq \underline{b} \quad (3.32)$$

3.4.1 Model approximation

To obtain a quadratic cost function, the nonlinear relation for $\gamma(P_s)$ in (3.11) is approximated as a convex quadratic relation:

$$\gamma(P_s) \approx \varphi_2 P_s^2 + \varphi_1 P_s + \varphi_0 \quad , \quad \varphi_2 > 0 \quad (3.33)$$

where parameters φ_i are time varying, as they depend on ω , P_d , and P_l . The approximation is done at each time instant, for the valid range of P_s , given by (3.16).

3.4.2 Cost function

The cost function is the weighted sum of fuel use and emissions over the driving cycle. By discretization one may obtain:

$$J = \sum_{k=1}^n \gamma(P_s(k)) \Delta t \quad (3.34)$$

The sample time Δt may be omitted, since it is constant.

Returning to (3.32), this means that H is diagonal with:

$$H(k, k) = 2 \varphi_2(k) \quad (3.35)$$

The other terms become:

$$\underline{h}(k) = \varphi_1(k) \quad \text{and} \quad h_0 = \sum_{k=1}^n \varphi_0(k) \quad (3.36)$$

The decision variables are:

$$z = [P_s(1) \cdots P_s(n)]^T \quad (3.37)$$

3.4.3 Constraints

The bounds on P_s (3.16), that include the bounds on P_m , P_e , and P_b are still present. The bounds on E_s can be written as linear constraints on P_s , by using the following discretization:

$$E_s(k) = E_s(0) + \sum_{i=1}^k P_s(i) \Delta t \quad (3.38)$$

The equality constraint (3.18) becomes:

$$E_s(n) = E_s(0) \Rightarrow \sum_{k=1}^n P_s(k) = 0 \quad (3.39)$$

From (3.16), (3.38), and (3.39) it is easy to construct A and \underline{b} in (3.32).

3.4.4 Solution

When only the upper and lower bounds on P_s (3.16) and the equality constraint (3.39) are taken into account, the exact solution of the problem can be solved efficiently with a routine described in [69]. If the upper and lower bound on E_s or other constraints are taken into account, a general QP solver must be used.

3.5 Model Predictive Control

When the complete driving cycle is known a priori, the optimization problem has to be solved only once. However, if only a limited prediction horizon is available, both the DP and QP problem can be used within a Model Predictive Control (MPC) structure using a receding horizon [50]. This means that the optimization is carried out at each time step over a limited prediction horizon. The first value of the optimal control sequence is implemented. The next time step a new optimization is done using an updated prediction and new measurement data.

In [4], DP optimization is used within an MPC framework for an HEV. As shown in [54], for short prediction horizons, the variation in P_s and thus the performance is limited by the endpoint constraint on E_s . Inspired by [69], a new approach based on QP that does not require a prediction has been developed and will be presented below.

3.5.1 Reduction of the QP problem

If only the cost function (3.34) and the equality constraint (3.39) are considered, the QP problem can be solved analytically by introducing the Lagrange function:

$$L(z, \lambda) = \sum_{k=1}^n \{ \varphi_2(k) P_s(k)^2 + \varphi_1(k) P_s(k) + \varphi_0(k) \} - \lambda \sum_{k=1}^n P_s(k) \quad (3.40)$$

The optimal solution can be calculated by solving:

$$\frac{\partial L(z, \lambda)}{\partial z} = 0 \quad \text{and} \quad \frac{\partial L(z, \lambda)}{\partial \lambda} = 0 \quad (3.41)$$

The solution is given by:

$$P_s^o(k) = \frac{\lambda - \varphi_1(k)}{2 \varphi_2(k)} \quad (3.42)$$

where:

$$\lambda = \sum_{k=1}^n \frac{\varphi_1(k)}{2\varphi_2(k)} / \sum_{k=1}^n \frac{1}{2\varphi_2(k)} \quad (3.43)$$

The incremental costs are given by:

$$\frac{\partial \gamma(P_s)}{\partial P_s} = 2\varphi_2(k) P_s(k) + \varphi_1(k) \quad (3.44)$$

Substituting (3.42) in (3.44) yields:

$$\left. \frac{\partial \gamma(P_s)}{\partial P_s} \right|_{P_s^o} = 2\varphi_2(k) \frac{\lambda - \varphi_1(k)}{2\varphi_2(k)} + \varphi_1(k) = \lambda \quad (3.45)$$

which means that the optimal solution is characterized by equal incremental cost λ at each time instant.

3.5.2 Elimination of the prediction horizon

Although for the computation of $P_s^o(k)$ only current values $\varphi_1(k)$ and $\varphi_2(k)$ are needed, computation of the value of λ requires knowledge of φ_1 and φ_2 over the entire driving cycle. When a prediction of the complete cycle is not available, an estimate of λ can be used. However, if this value is too low, E_s will increase on the long run, whereas it will decrease if the estimate is chosen too low.

Long term drift of E_s can be prevented by adapting λ online, based on the measured E_s . This can for instance be done using the following PI-type controller:

$$\lambda(k+1) = \lambda_0 + K_P(E_s(0) - E_s(k)) + K_I \sum_{i=1}^k (E_s(0) - E_s(i))\Delta t \quad (3.46)$$

where λ_0 is an initial guess and $K_P, K_I > 0$.

Because P_s is proportional with λ , and E_s is the integral of P_s , the closed loop system becomes a discrete time version of a time varying second order dynamic system:

$$\begin{aligned} E_s(k+1) = E_s(k) + \frac{\Delta t}{2\varphi_2(k)} \{ & \lambda_0 - \varphi_1(k) + K_P(E_s(0) - E_s(k)) \\ & + K_I \sum_{i=1}^k (E_s(0) - E_s(i))\Delta t \} \end{aligned} \quad (3.47)$$

If the initial value λ_0 is chosen too high, E_s will increase, which will lead to a lower value of λ . If λ_0 is chosen too low, E_s will decrease, which will lead to a higher value of λ .

The feedback of E_s is meant to avoid draining or overcharging the battery in the long run, but short term fluctuations of E_s should still be possible, so the bandwidth of the

PI-controller should be chosen rather low. The stability of this control strategy and a conventional MPC strategy is analyzed in Appendix B.

As an alternative to the PI-controller (3.46), it is also possible to use MPC with zone control, which means that λ is only adapted if E_s exceeds some boundary, see, *e.g.*, [72].

For given λ , computing $P_s^o(k)$ using (3.42) is equivalent to solving at each time instant k :

$$P_s^o(k) = \arg \min_{P_s(k)} \{ \varphi_2(k) P_s(k)^2 + \varphi_1(k) P_s(k) + \varphi_0(k) - \lambda(k) P_s(k) \} \quad (3.48)$$

Instead of the quadratic approximation, the original nonlinear cost function can also be used:

$$P_s^o(k) = \arg \min_{P_s(k)} \{ \gamma(P_s(k), k) - \lambda(k) P_s(k) \} \quad (3.49)$$

This can be solved using DP with a horizon length of 1 on a dense grid.

Equation (3.49) provides a nice physical interpretation of the control strategy. At each time instant the actual incremental cost for storing energy is compared with $\lambda(k)$, which can be seen as the average incremental cost of the past. Energy is stored when generating now is more beneficial than average, whereas it is retrieved when it is less beneficial.

The bounds on P_s can be respected by saturation:

$$P'_s(k) = \min(\max(P_{smin}(k), P_s^o(k)), P_{smax}(k)) \quad (3.50)$$

This is a suboptimal solution, which doesn't guarantee stability.

3.6 Simulations

3.6.1 Model

Simulations are done for the Ford Mondeo, as described in Section 2.1, equipped with the 42 V power net. Simulations are done for the New European Driving Cycle (NEDC). For the electric power request, constant loads of 500, 1000, and 2000 W are used.

The battery has an energy capacity of $E_{cap} = 4 \cdot 10^6$ J and is operated around 70% *SOE*, because the efficiencies for both charging and discharging in this range are acceptable. The battery losses are approximated as quadratic with the stored power, such that (2.26) reduces to:

$$P_b = P_s + b P_s^2 \quad (3.51)$$

Parameter b has a value of $5 \cdot 10^{-5} \text{ W}^{-1}$, which gives an energy efficiency of 95% at 1000 W and 90% at 2000 W.

When the drive train power is negative and the clutch is closed, the drive train power is partly delivered by the internal combustion engine (which has a negative drag power), by the alternator, and by the brakes. Because regenerative braking delivers electrical power without extra fuel use, it is expected that it will be used as much as possible. The brakes are only used when the desired deceleration power is larger than the maximum negative power that can be taken up by the engine and the alternator.

3.6.2 Strategies

The following strategies are implemented and their results will be compared:

- BL* Baseline strategy where the alternator power is equal to the requested load.
- DP* This strategy solves the DP problem once for the complete driving cycle.
- QP* This strategy solves the QP problem once for the complete driving cycle.
- QP1* QP at each time step with adapted λ using (3.42), (3.50), and (3.46).
- DP1* DP at each time step with adapted λ using (3.49) and (3.46).

The DP and QP strategies require knowledge of the entire driving cycle. The QP1 and DP1 strategies are causal as they do not need any prediction. They do require knowledge of the current $\omega(k)$, $P_d(k)$, $P_l(k)$, and $E_s(k)$.

To limit the computation time, the DP strategy is used with an input grid of 100 W and a state grid of 100 J. The DP1 strategy is used with an input grid of 10 W and does not need a state grid.

The PI-controller (3.46) is designed as follows. For λ_0 the value of the Lagrange multiplier resulting from the global QP optimization is used. The value depends on the electric load, a typical value is $\lambda_0 = 2.7$.

K_P and K_I are designed such that for average values of $\varphi_1(t)$ and $\varphi_2(t)$, (3.47) becomes a critically damped second order system with a bandwidth of 10^{-3} rad/s. The average values of $\varphi_1(t)$ and $\varphi_2(t)$ are:

$$\tilde{\varphi}_1 = 2.5 \quad \text{and} \quad \tilde{\varphi}_2 = 2 \cdot 10^{-4} \quad (3.52)$$

The corresponding values of K_P and K_I then become:

$$K_P = 6.7 \cdot 10^{-7} \quad \text{and} \quad K_I = 3.3 \cdot 10^{-4} \quad (3.53)$$

The QP1 and DP1 strategy do not guarantee that the endpoint constraint is exactly satisfied. The difference in SOE is accounted for in the fuel consumption using the initial value of λ :

$$m_c = \sum_{k=1}^n \dot{m}(k) - \lambda_0 (E_s(n) - E_s(0)) \quad (3.54)$$

3.6.3 Results

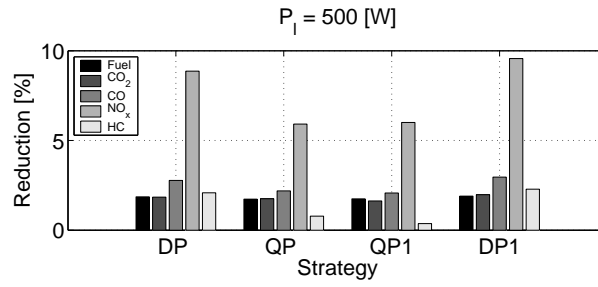
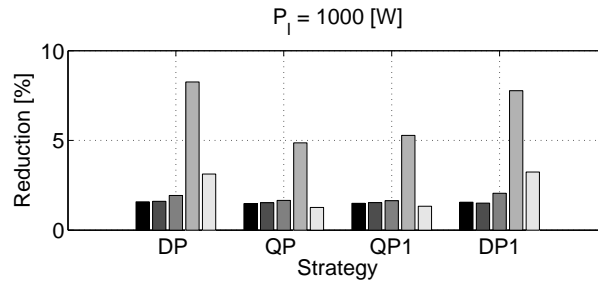
The fuel consumption and emissions are evaluated with the control model described in Section 2.3.2 using the nonlinear fuel and alternator map and the quadratic battery losses.

When the cost function represents only the fuel consumption, it turns out that for this case the CO_2 , CO , and NO_x emissions are also reduced significantly. However, the emission of H_C increases. Therefore, a weighted sum of fuel and H_C emission is used as cost function. The weighting factors in (3.11) are $w_1 = w_5 = 1$ and $w_2 = w_3 = w_4 = 0$. This

time, all emissions are reduced, at the cost of a slight decrease in fuel reduction. The fuel consumption is given in Table 3.1. The savings with respect to the baseline strategy for the various loads are presented in Fig. 3.2, Fig. 3.3, and Fig. 3.4.

Table 3.1: Fuel Consumption

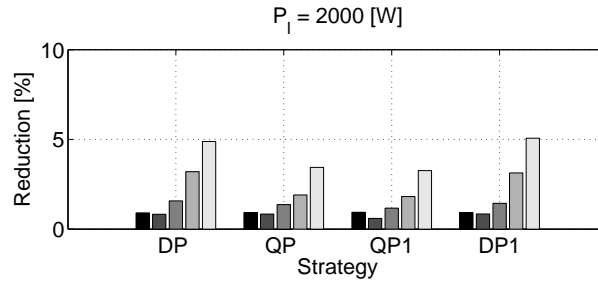
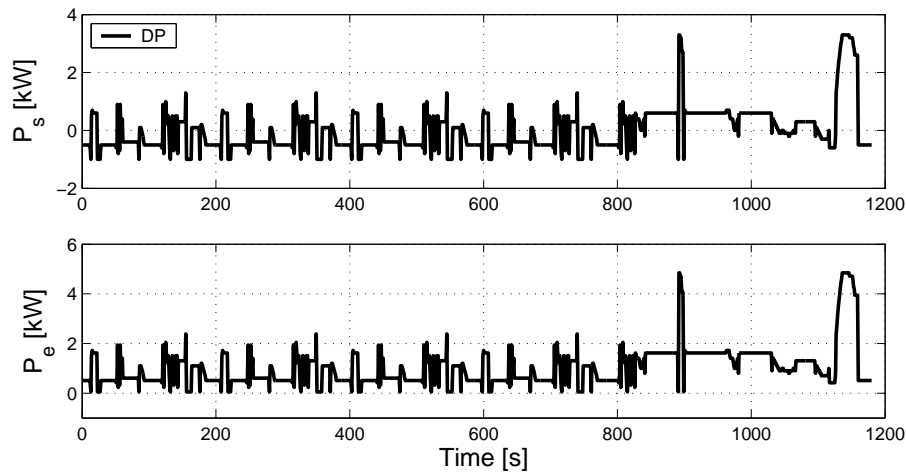
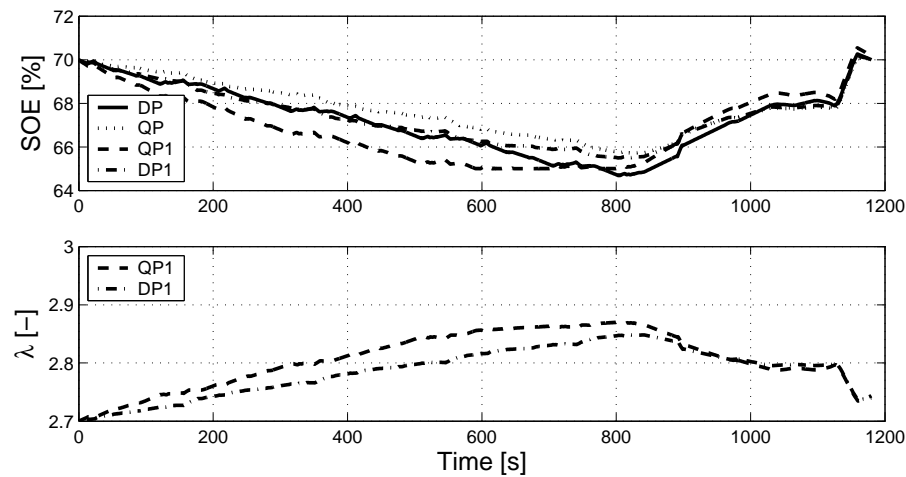
P_l	500 W	1000 W	2000 W
Strategy	Fuel Use [g]	Fuel Use [g]	Fuel Use [g]
BL	556.157	589.862	661.464
DP	545.806	580.549	655.460
QP	546.524	581.140	655.374
QP1	546.456	581.057	655.259
DP1	545.613	580.693	655.434

Figure 3.2: Fuel and emissions reduction for $P_l = 500$ WFigure 3.3: Fuel and emissions reduction for $P_l = 1000$ W

The resulting trajectories of P_s and P_e for the DP strategy with $P_l = 1000$ W are shown in Fig. 3.5. As can be seen, the optimization anticipates on regenerative braking phases and generates less in between.

Figure 3.6 shows the SOE for all strategies. All trajectories of SOE show a similar behavior. The variation in SOE is small, because of the large capacity of the battery. This justifies that for this simulation, the battery efficiency is chosen independently of E_s .

The trajectories of the adaptive λ for the DP1 and QP1 strategies are also shown in Fig. 3.6. The value of λ varies slightly around its initial value.

Figure 3.4: Fuel and emissions reduction for $P_l = 2000 \text{ W}$ Figure 3.5: Battery storage power and electrical alternator power for $P_l = 1000 \text{ W}$ Figure 3.6: Battery state of energy and adapted λ for $P_l = 1000 \text{ W}$

3.6.4 Evaluation

The simulations show that the strategies are effective, as they all succeed in lowering the fuel consumption and the exhaust emissions. The results might be improved by fine tuning the weighting factors of the cost function.

Most of the profit comes from regenerative braking, which delivers a certain amount of

energy for free. As will be explained in Section 4.3.2, the baseline already exploits a part of the free energy from regenerative braking and that part increases with increasing load. Therefore the relative fuel savings of a strategy exploiting the full regenerative braking potential compared to the baseline are higher at low electric powers.

Both Dynamic Programming and Quadratic Programming do not find the global optimum of the original nonlinear optimization problem. The DP algorithm uses the original nonlinear cost criterion, but restricts itself to a grid, whereas the QP algorithm finds the global optimum of a quadratic approximation of the original problem. The small difference between DP and QP for fuel use and CO_2 indicates that these terms in the nonlinear cost function are approximated adequately by a QP problem, and that the chosen grid is not too restrictive for the DP problem. For the other emissions, that show more non-smooth behavior, the differences between DP and QP are larger, because the QP based methods use smooth convex approximations.

The adaptive strategies QP1 and DP1, that do not use future knowledge, perform equally well. For some loads, the DP1 strategy outscores the DP strategy, because of its finer input grid.

The DP1 strategy is the one to choose for, because of its good results and because it is easy implementable online. However, realtime implementation in a vehicle of the DP1 strategy still has some requirements.

Accurate measurements of the current values of $\omega(k)$, $P_d(k)$, $P_l(k)$, and $E_s(k)$ are required. A measurement of ω is usually available in a vehicle. P_d cannot be measured directly, but it is possible to measure τ_d or to estimate it based on the throttle position. P_l can be measured simply using a voltage and a current sensor. E_s can not be measured directly, but can be estimated using measurements of U_b and I_b .

Furthermore, the alternator must be equipped with a power control loop that manipulates the alternator voltage such that the desired P_e is realized. This will be addressed in Chapter 7, where the DP1 strategy will be implemented on the simulation model and a hardware-in-the-loop test setup.

The performance is limited by the losses that occur during charging and discharging of the battery. As an alternative, or in addition, an ultracapacitor can be used, which has a much higher efficiency, but also a lower capacity. This will be addressed in Chapter 5.

The strategies presented here are based on optimization using the component characteristics of a specific vehicle. They are easy to adapt for a different vehicle by replacing these component characteristics.

Because the realtime strategies do not use information of the entire driving cycle, it is expected that they will also perform well for different driving cycles or real world driving. Furthermore, the few controller parameters are not fine-tuned for a specific driving cycle or vehicle configuration, so this method is likely more robust with regard to performance than existing heuristic strategies, although this has not been verified yet.

3.7 Conclusion

Several energy management strategies for the electrical power net are presented, that use either a prediction of the future or information about the current state of the vehicle, to reduce the fuel consumption and exhaust emissions over a driving cycle.

Simulations show that applying energy management on the vehicle power net is effective. With the degree of freedom considered here and the component characteristics used, a fuel reduction of 2% can be obtained, while at the same time reducing the emissions even more. The largest part of the fuel reduction is obtained with regenerative braking.

Application of energy management on the vehicle power net does not require changes to the drive train and is therefore cheap to implement. The DP1 strategy is the most suitable for online implementation, as it exploits the non-convexity of the cost function and does not require a prediction of the future. It does require measurement of the actual engine speed and torque and the electric load.

The strategies can also be applied to a mild hybrid electric vehicle with an integrated starter generator. The only difference is that the lower bound on the alternator power is negative instead of zero. The approach can be extended to vehicle topologies with more degrees of freedom, as will be done in Chapter 5 and Chapter 6.

Fuel Reduction Potential

4.1 Introduction

In the previous chapter, energy management strategies have been developed and tested. To explain the results, this chapter investigates the potential fuel reduction that can be obtained with regenerative braking and more advanced energy management. This is done by analyzing the typical characteristics of components that are directly related to the power flow in the vehicle. It is explained why for this application, shifting the engine to an operating point with a higher efficiency will not necessarily lead to a lower fuel consumption.

Subsequently, engineering rules are presented to estimate the amount of fuel reduction that can be expected for each strategy. The characteristics of components are included as input parameters to make the method general applicable. This makes it easy to predict the influence of component sizing when designing a vehicle.

To show the value of the engineering rules, the potential fuel reduction is computed for a specific vehicle configuration and driving cycle and compared with simulation results.

This chapter is built up as follows: The concept of energy management including regenerative braking will be handled in Section 4.2. The engineering rules to predict the performance of an energy management strategy are presented in Section 4.3. In Section 4.4, the expected performance is compared with simulation results. Finally, conclusions are given in Section 4.5.

The contents of this chapter will be published in [44], of which a preliminary version was presented as [43].

4.2 Energy management

Energy management strategies shift the operating points of energy converting components, such that the losses are reduced. In the situation considered in this thesis, only the alternator power is controlled, thereby shifting the engine torque, which should lead to a lower fuel consumption. This section takes a closer look at the fuel consumption characteristics of an engine and explains how fuel savings can be obtained.

4.2.1 Efficiency improvement versus fuel reduction

As can be seen in Fig. 2.8, the efficiency of the combustion engine varies drastically over the operating range. This may give the impression that a large fuel reduction can be obtained by a small shift in engine torque, by manipulating the alternator power. It will be shown here, that this is not the case.

It is easy to assume that increasing the efficiency will result in a lower fuel consumption. In some situations this is true, *e.g.*, the gear shifting problem where the requested engine power is predefined and freedom exists in the engine speed by selecting the optimal gear shifting pattern. Because the engine power is fixed at each time instant, a higher efficiency corresponds to a lower fuel rate and results in a lower fuel consumption for a driving cycle.

However, the energy management problem considered in this thesis is not solved by simply bringing the engine to an area with a higher efficiency, as will be explained below.

In a vehicle with a conventional drive train and manual transmission, the engine speed is controlled by the driver, so only the engine torque can be altered. Fig. 4.1 shows the fuel rate vs. mechanical power for a particular engine speed. The power required for propulsion, is indicated by P_d . Depending on the requested alternator power P_e , the engine moves to the operating point $P_m = P_d + P_g$. The corresponding change in fuel consumption $\Delta \dot{m}$ depends directly on the slope of the fuel map and the alternator map, leading to the definition of the incremental cost λ :

$$\lambda = \frac{\partial P_f}{\partial P_e} = h_f \frac{\partial \dot{m}}{\partial P_m} \frac{\partial P_g}{\partial P_e} \quad (4.1)$$

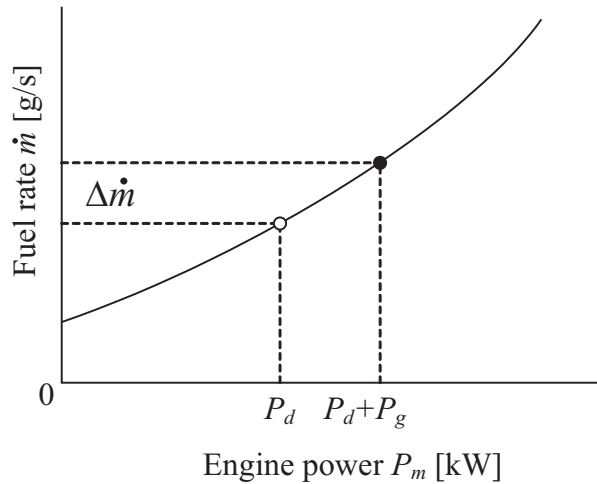


Figure 4.1: Explanation of the incremental cost

Additional electric energy can be produced cheaply at moments when λ is low. Therefore, an effective strategy should compare the incremental cost at each time instant and store electric energy when λ is low and retrieve it when it is high. This does not necessarily correspond to shifting the engine to the high efficiency area. This can be seen from Fig. 4.2, where a linear, a convex and a concave fuel curve and their corresponding efficiency curves are drawn. For all three cases, the efficiency increases for increasing power, because the fuel consumption at zero power $f_0(\omega)$ becomes relatively less.

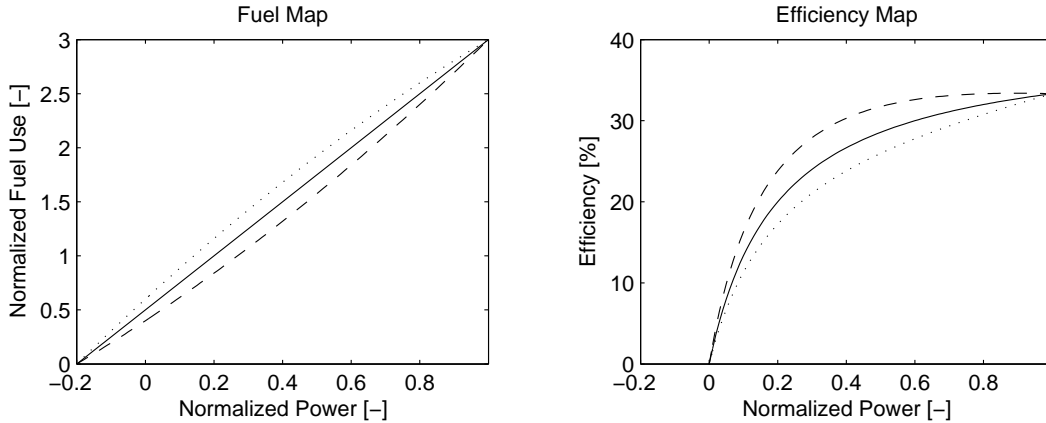


Figure 4.2: Fuel and efficiency curves

By looking at the slope of the fuel map it turns out that for the convex fuel curve, it is cheaper to generate in the low torque area, whereas for the concave fuel curve, it is cheaper to generate in the high torque area. For the linear curve, it does not matter where electricity is generated.

For most engines, the changes in λ are rather small over a large range of operating conditions. This enables the use of the approximation (2.10), but limits the fuel reduction that can be obtained with an electric energy management system. When battery losses are taken into account, the differences of the fuel map must be larger than the additional losses of storing and retrieving energy, which further reduces the potential.

4.2.2 Regenerative braking

When a vehicle is decelerating, kinetic energy becomes available, causing a negative drive train torque. As long as the clutch is closed, a part of this energy is absorbed by the engine (which has a negative drag torque). The remaining part can be absorbed by the brakes that convert it into useless heat and wear, but it can also be used by the alternator to convert it into useful electric energy. When the clutch is engaged, the kinetic energy can no longer be used by the engine or the alternator, so it will all be absorbed by the brakes.

Because regenerative braking delivers electrical power with no extra fuel consumption, it should be used as much as possible. When the clutch is closed, the brakes should only be used if the desired deceleration torque exceeds the maximum negative torque that can be delivered by the engine and the alternator.

The potential of regenerative braking can be increased by altering the drive train configuration such that the alternator is connected to the drive train instead of to the engine. In this case, generating can be continued when the clutch is open and the vehicle is still decelerating. A drawback is that no electric power can be generated when the vehicle is standing still, so electricity is drawn from the battery. This configuration is further investigated in Chapter 6.

4.2.3 Start-stop operation

When the vehicle is standing still, the engine runs at idle speed and provides the torque requested by the alternator to supply the electric loads. The engine can also be turned off, which saves fuel. The electric loads that are still active are supplied by the battery, which should be recharged when the engine is running again. Furthermore, restarting the engine requires electric energy and leads to additional wear of the engine, starter, and battery.

4.2.4 Hybrid electric vehicles

The analysis presented in this chapter also applies to mild hybrid electric vehicles with an integrated starter generator (ISG) that is mounted directly on the crank shaft of the engine, such as the Honda Insight [26] and the Honda Civic IMA (Integrated Motor Assist). The only difference is that $P_{e\min}$ is negative. There, the engine and the ISG are always operating simultaneously and there is no freedom in the engine speed. Fuel reduction is obtained mostly by the fact that a smaller engine can be used, because the ISG can be used for boosting to obtain a similar performance as a larger engine. A smaller engine has smaller friction and pumping losses, and thus a smaller drag torque. This results in less fuel consumption during propulsion, and also leaves more energy available for regenerative braking. Furthermore, the engine is turned off during standstill.

Full hybrid electric vehicles, such as the Toyota Prius [29], have both freedom in the engine speed and torque, and the engine and the electric motor can be operated independently. This makes the energy management problem more complex and lies beyond the scope of this thesis.

4.3 Engineering rules

This section presents a set of engineering rules to predict the amount of fuel reduction that can be obtained with regenerative braking and with a more advanced energy management strategy compared to a baseline strategy for a given vehicle configuration and driving cycle. This is done using the linear approximations of the fuel map (2.10) and the alternator map (2.18). The battery is assumed to be ideal, such that (2.26) reduces to:

$$P_b = P_s \quad (4.2)$$

4.3.1 Baseline strategy

The baseline strategy is defined such that the alternator always generates exactly what is requested, so the battery is not used:

$$P_e = P_l \quad \Rightarrow \quad P_g = g_0(\omega) + k_g P_l \quad (4.3)$$

For a given speed and gear profile, the corresponding engine speed ω and propulsion power P_d can be computed as shown in Section 2.4. By adding the alternator power, the

total mechanical power becomes:

$$P_p = P_d + P_g \quad (4.4)$$

The power delivered by the engine is then given by:

$$P_m = \max(P_p, P_{m \min}) \quad (4.5)$$

Using the linear approximation of the fuel map (2.10), the fuel consumption can be estimated by the following simple equation:

$$m_{bl} = \frac{k_f}{h_f} \int_0^{t_n} (P_m - P_{m \min}) dt \quad (4.6)$$

It turns out that the baseline strategy already uses some of the regenerative braking potential. During deceleration periods where $P_d < P_{m \min}$, some or all of the electrical power for the load is generated without using fuel. This is illustrated for the last 400 s of the NEDC in Fig. 4.3, where the mechanical energy that can be obtained for free and used for generating electric power is indicated by the solid areas. This amount of free mechanical energy can be calculated as follows:

$$P_{g \text{ regen } bl} = -\min(\max(P_{m \min} - P_g, P_d), P_{m \min} - P_{g \min}) + P_{m \min} - P_{g \min} \quad (4.7)$$

The corresponding electric power is then given by:

$$P_{e \text{ regen } bl} = \frac{1}{k_g} P_{g \text{ regen } bl} \quad (4.8)$$

If the baseline strategy would not exploit the regenerative braking potential at all, the fuel consumption is given by:

$$m_{bl}^* = \frac{k_f}{h_f} \int_0^{t_n} (P_m^* - P_{m \min}) dt \quad (4.9)$$

where P_m^* is defined as:

$$P_m^* = \max(P_d, P_{m \min}) + P_g \quad (4.10)$$

The amount of fuel that is saved by exploiting the regenerative braking potential is given by:

$$\Delta m_{\text{regen } bl} = \frac{k_f}{h_f} \int_0^{t_n} P_{g \text{ regen } bl} dt \quad (4.11)$$

The amount of electric energy that is obtained for free increases with P_g and thus with the requested load.

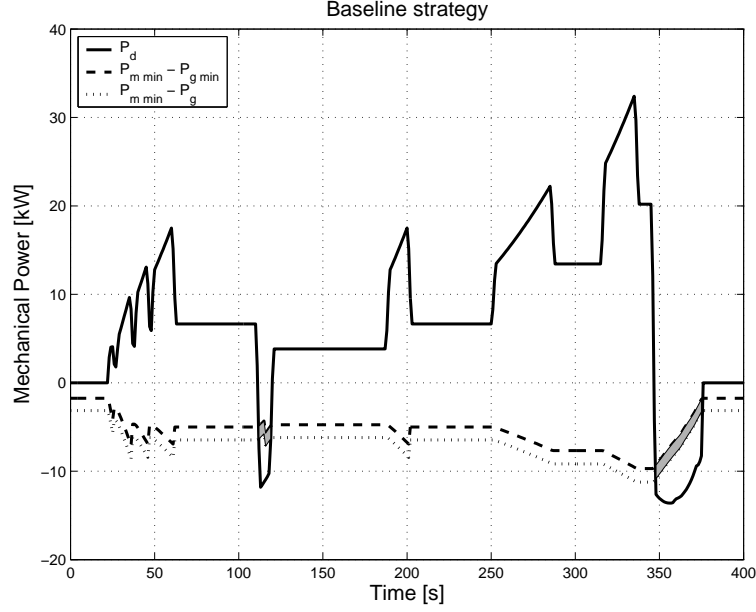


Figure 4.3: Regenerative braking potential of the baseline strategy

4.3.2 Regenerative braking strategy

The regenerative braking strategy as will be considered in this chapter is defined as follows. During normal operation, the alternator generates exactly what is requested. During deceleration phases, it generates the maximum amount of electrical power that does not cost fuel. If this is more than what is requested at that moment, the surplus of electrical energy is stored in the battery. After the braking period, the electric load is supplied by the battery, till it reaches the original *SOE* level. From that point on, the load is provided by the alternator again.

During normal operation, the additional fuel consumption is more or less proportional with the electric energy provided, so the fuel saving that can be obtained with regenerative braking depends on the amount of electric energy that can be generated for free during deceleration periods.

The mechanical power that can be used for free during braking is the part between the engine drag power minus the alternator drag power, and the engine drag power minus the maximum alternator power. This is illustrated by the solid areas in Fig. 4.4. The amount of power can be calculated as follows:

$$P_{g\,regen} = -\min(\max(P_{m\,min} - P_{g\,max}, P_d), P_{m\,min} - P_{g\,min}) + P_{m\,min} - P_{g\,min} \quad (4.12)$$

The corresponding electric power is then given by:

$$P_{e\,regen} = \frac{1}{k_g} P_{g\,regen} \quad (4.13)$$

The corresponding fuel consumption that can be saved is given by:

$$\Delta m_{regen} = \frac{k_f}{h_f} \int_0^{t_n} P_{g_{regen}} dt \quad (4.14)$$

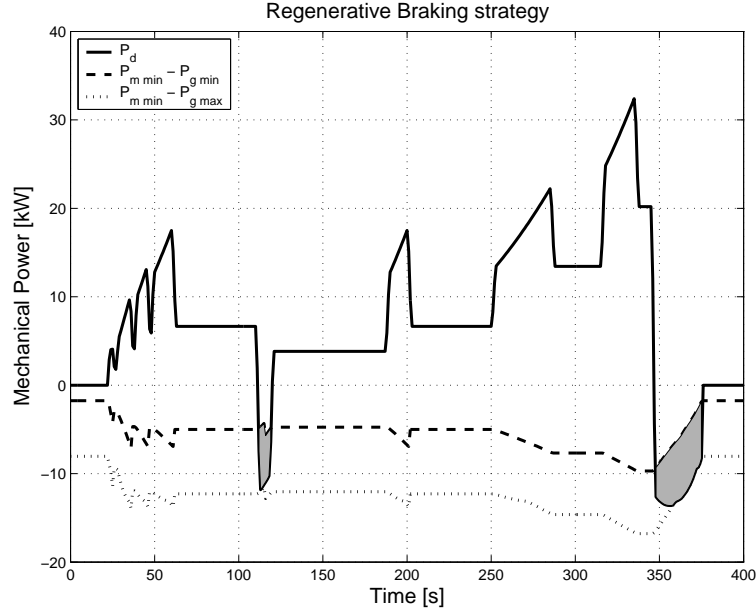


Figure 4.4: Regenerative braking potential of a regenerative braking strategy

The amount of electrical energy that can be obtained for free with regenerative braking does not depend on the requested electric load, but only on the power needed for propulsion and the alternator capacity $P_{e_{max}}$. How much of the electric energy is stored for later usage, does depend on the load.

The amount of electrical energy that is already obtained for free by the baseline strategy increases with the requested load. This means that for higher electric loads, the additional improvement of a real regenerative braking strategy will decrease.

4.3.3 Advanced energy management strategy

On top of regenerative braking, an additional fuel reduction can be obtained by using a more advanced energy management strategy, that exploits differences in the incremental cost and only generates electric power when these costs are low, as explained in Section 4.2.1. Its potential depends on the differences between the nonlinear fuel and alternator map and their linear approximations, in other words, the deviation of $\lambda(P_m, \omega)$ from the linear approximation $\lambda_0 = k_f k_g$.

The fuel reduction also depends on the amount of the requested electric load and the maximum alternator power. When the amount of the electric load is small compared to the maximum alternator power, most of the electricity can be generated in the cheapest area. Since the load is small, the fuel consumption needed for it is also small and the fuel reduction will also be small. When the load is higher, it causes more fuel consumption,

so the fuel that can be saved by generating only at cheap moments also increases. When the requested load is close to the maximum alternator power, there is not much freedom anymore when to generate, so the fuel reduction will decrease again.

Suppose that the driving cycle is such that the corresponding value of λ is uniformly distributed between:

$$1 - \sigma_f < \frac{\lambda}{\lambda_0} < 1 + \sigma_f \quad (4.15)$$

If the requested electrical load equals the maximum alternator power, it is generated within the entire interval $[1 - \sigma_f, 1 + \sigma_f]$, with an average of 1. If the requested load is half of the maximum alternator power, it can be generated cheapest within the interval $[1 - \sigma_f, 1]$, so with an average of $1 - \frac{1}{2} \sigma_f$. If the requested load is a quarter of the maximum alternator power, it can be generated cheapest within the interval $[1 - \sigma_f, 1 - \frac{1}{2} \sigma_f]$, so with an average of $1 - \frac{3}{4} \sigma_f$.

More general, the load can be generated cheapest within the interval $[1 - \sigma_f, 1 - (1 - 2\alpha)\sigma_f]$, with an average of $1 - (1 - \alpha)\sigma_f$, where α is the ratio between the average requested load over a driving cycle and the maximum electric alternator power:

$$\alpha = \frac{\tilde{P}_l}{P_{emax}} \quad (4.16)$$

The fuel that can be saved on top of regenerative braking is then given by:

$$\Delta m_{em} = (1 - \alpha) \sigma_f \frac{\lambda_0}{h_f} \int_0^{t_n} (P_l - P_{e\,regen}) dt \quad (4.17)$$

4.3.4 Start-stop operation

The fuel that can be saved by start-stop operation, is the fuel that is required for engine idling during the stand still periods. It can be computed as follows:

$$\Delta m_{ss} = \int_0^{t_n} i_{ss}(t) f_0(\omega(t)) dt \quad (4.18)$$

where:

$$i_{ss}(t) = \begin{cases} 1 & \text{if } v(t) = 0 \\ 0 & \text{if } v(t) \neq 0 \end{cases} \quad (4.19)$$

Hereby, it is assumed that the engine can be turned on and off immediately. Furthermore, the costs for restarting the engine, both the required electric energy and component wear, are neglected.

4.4 Comparison

In this section, the fuel reduction that can be obtained with regenerative braking and advanced electric energy management for a specific vehicle and driving cycle will be estimated with the rules presented in the previous section, and will be compared with simulation results.

4.4.1 Strategies

The fuel consumption is estimated using the engineering rules for the following 4 strategies:

1. The fictive baseline strategy that does not use regenerative braking according to (4.9)
2. The realistic baseline strategy according to (4.11)
3. The regenerative braking strategy according to (4.14)
4. The advanced energy management strategy according to (4.14) and (4.17)

The results are compared with simulation results for the following 4 strategies:

1. The fictive baseline strategy that does not use regenerative braking, as described in Section 4.3.1
2. The realistic baseline strategy, as described in Section 4.3.1
3. The heuristic regenerative braking strategy, as described in Section 4.3.2
4. Dynamic Programming, as described in Section 3.3

The simulation results are obtained with the control model described in Section 2.3.2 using the original nonlinear fuel and alternator map

When using the fictive baseline strategy, fuel is injected during deceleration periods to supply the load, whereas the realistic baseline strategy recuperates part of the kinetic energy from the vehicle. The heuristic regenerative braking strategy operates as described in the beginning of Section 4.3.2.

The Dynamic Programming [10] strategy used for the simulations minimizes the fuel consumption over the entire driving cycle with the constraint that the energy level of the battery at the end is the same as at the beginning. This method assumes that the entire driving cycle is known and acts as a benchmark for other strategies. The implementation of this method is described in more detail in Section 3.3.

4.4.2 Simulation parameters

Simulations are done for the Ford Mondeo driving the New European Driving Cycle. The variation of the incremental cost λ at each time instant of this cycle at $P_e = 2000$ W is shown as a histogram in Fig. 4.5. It varies roughly between 2.4 and 3.2, although not uniformly, leading to a value for σ_f of 0.1.

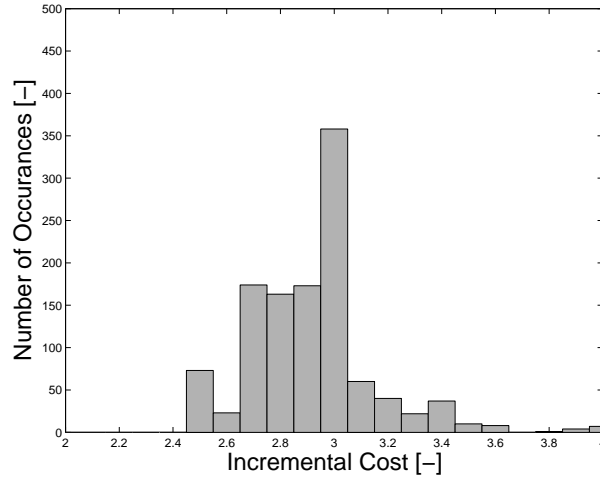


Figure 4.5: Distribution of λ

For the power net, both the 14 V and the 42 V version are used. As electric power request, constant loads between 0 and 1500 W are used with the 1.5 kW alternator and loads between 0 and 5000 W with the 5 kW alternator.

4.4.3 Results & evaluation

The results for the 5 kW alternator are presented in Fig. 4.6. The total fuel consumption, the absolute fuel reduction with respect to the fictive baseline and the percentile reduction with respect to the realistic baseline are displayed. As could be expected, the total fuel consumption increases almost proportionally with the requested electric load.

The fuel reduction of regenerative braking is predicted rather well. The benefits of regenerative braking over a normal baseline strategy are large for low electric loads and decrease for higher loads. A load of 200 W can be provided solely by regenerative braking. For smaller loads, the regenerative braking potential is not completely used, because the *SOE* at the end must equal its initial value. This explains the rapid increase in fuel reduction between 0 and 200 W.

The additional fuel reduction of advanced energy management shows larger differences between analysis and simulation. According to the analysis, the highest additional fuel reduction is obtained with a load that is half of the maximum alternator power. In the simulations, the fuel reduction is smaller for loads between 1000 and 4000 W. This can be explained, because the distribution of the slope of the real fuel map, as shown in Fig. 4.5, is not uniform, but more gaussian, leading to a lower fuel reduction than predicted.

The results for the 1.5 kW alternator are presented in Fig. 4.7. The fuel savings by regenerative braking are smaller, because of the smaller alternator capacity. The additional fuel

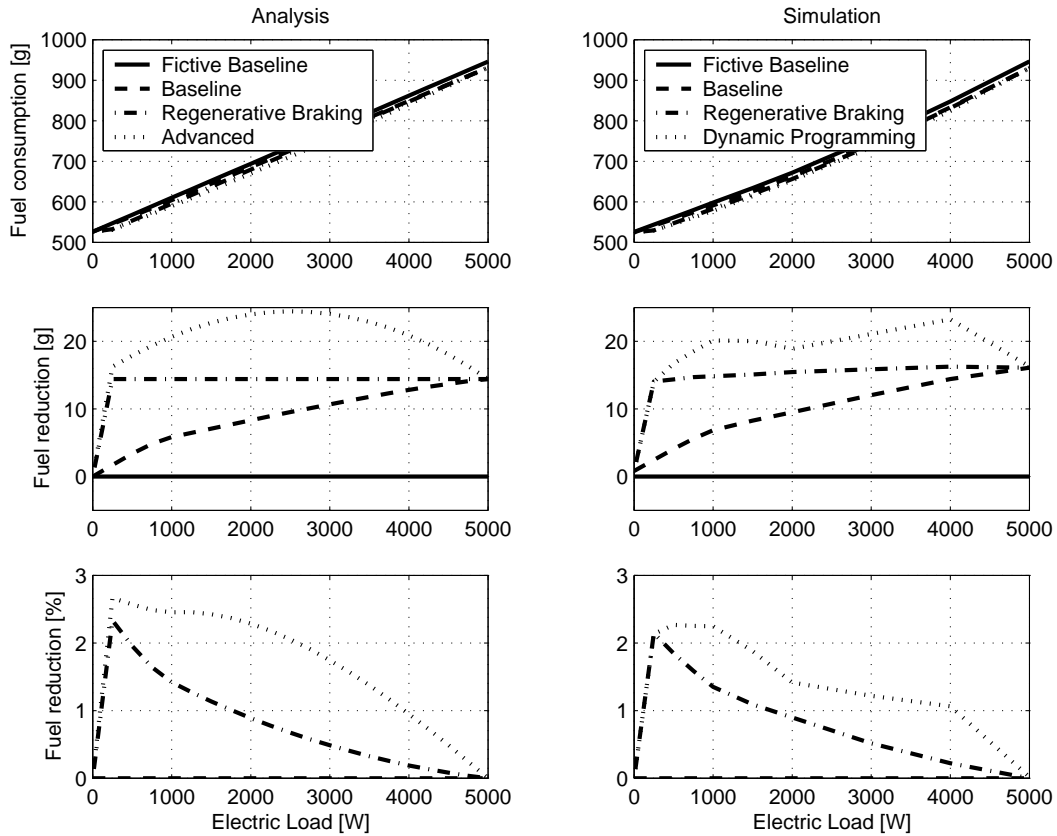


Figure 4.6: Results for the 5 kW alternator

saving by advanced energy management is smaller because the electric load is smaller compared to the mechanical load. Besides from that, the results look similar to the 5 kW configuration. A load of only 100 W can be provided solely by regenerative braking.

The additional fuel reduction that can be obtained with start-stop is about 30 gram. This amount does not vary much with the electric load or the strategy.

When battery losses are taken into account, the profits of regenerative braking and advanced energy management will be smaller, because the baseline strategy does not use the battery.

4.5 Conclusion

A set of engineering rules are presented to estimate the fuel reduction that can be obtained with regenerative braking and with more advanced electric energy management strategies in conventional vehicles.

For a specific vehicle configuration and driving cycle, the estimated fuel consumption is compared with simulations, with reasonable results, showing the value of this method.

With regenerative braking a fixed amount of electrical energy can be obtained for free. This amount does not depend on the requested load. The baseline strategy already does some regenerative braking, where the amount increases with the requested load. This

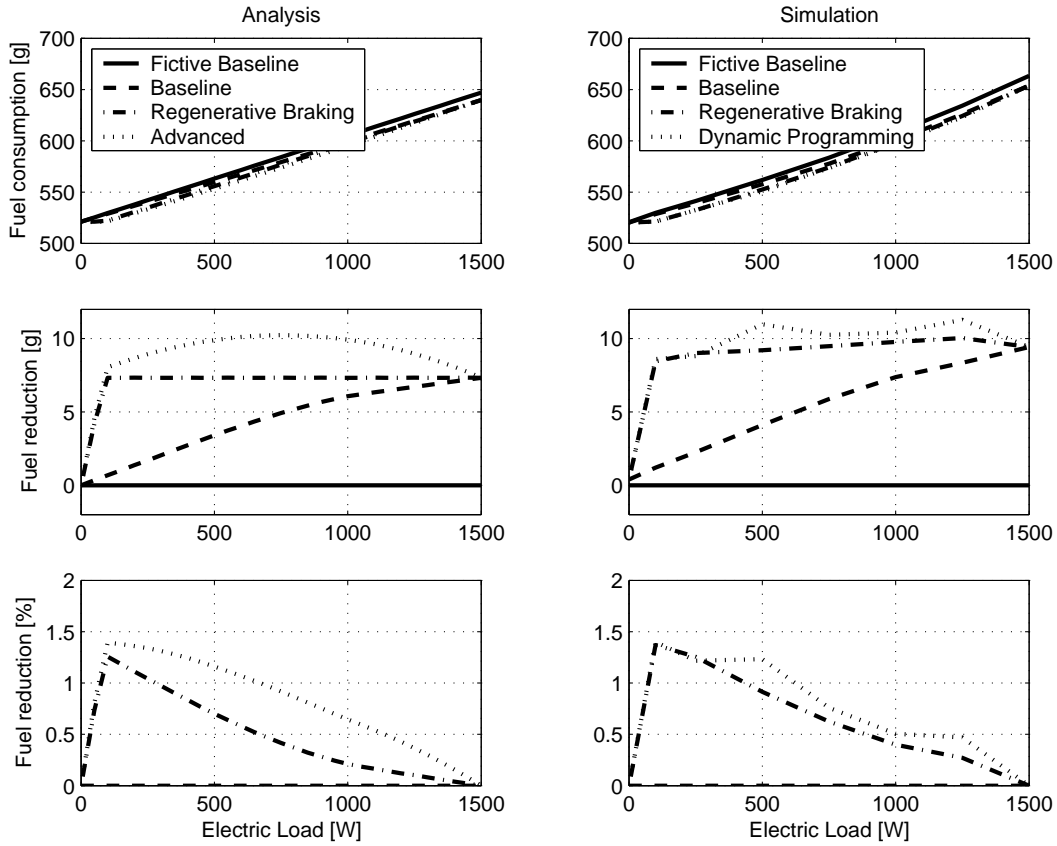


Figure 4.7: Results for the 1.5 kW alternator

means that for higher electric loads, the additional fuel reduction of a real regenerative braking strategy becomes smaller.

It is explained why for this application, shifting the operating point of the engine to a higher efficiency area will not necessarily lead to a lower fuel consumption.

The fuel consumption of an internal combustion engine increases more or less proportionally to the delivered mechanical power. The additional fuel reduction that can be obtained with an advanced electric energy management system depends on nonlinearities and speed dependencies in the fuel map. For the engine used in this analysis, these deviations are rather small, which limits the additional fuel reduction.

Dual Storage Power Net

5.1 Introduction

The fuel reduction that can be obtained with energy management applied to a conventional vehicle is to some extent limited by the losses in the battery. A possible solution is to use an advanced dual storage power net topology, as proposed in [63], which combines a lead acid battery and an ultracapacitor. This chapter studies this power net topology and presents both a global optimization method and a real-time implementable strategy to control it.

This chapter is built up as follows. The dual storage power net topology is described in Section 5.2. The control objective is formulated in Section 5.3. The reduced vehicle model is derived in Section 5.4. The global optimization strategy is presented in Section 5.5. Section 5.6 presents an online implementable strategy. The performances of the strategies are compared by simulations in Section 5.7. Conclusions are given in Section 5.8.

A preliminary version of this chapter is published earlier in [41].

5.2 Dual storage power net

The dual storage power net consists of an alternator, a switch, a lead acid battery, an ultracapacitor and a DC-DC converter. The reason for using two storage devices is to combine their advantageous properties, see also [5] for a comparison.

A lead acid battery has a large capacity and small energy leakage over time. However, the losses during charging and discharging and battery wear are large, especially when using high powers.

The open cell voltage of the battery is linear with the energy level but with a large offset. Because of this offset, the battery can be operated between 20% and 100% state of charge while maintaining an acceptable power net voltage.

An ultracapacitor, or ultracap, has a smaller capacity, but the charge and discharge losses are also much smaller. This makes the ultracap advantageous to use for high peak powers. An ultracap has considerable energy leakage, so it is not suitable for long term storage.

The open cell voltage of the ultracap is linear with the energy level. If the ultracap is connected directly to the power net, it can only be operated within a small *SOE* window

while maintaining an acceptable board net voltage. By connecting it to the board net using a DC-DC converter, it can be used in its full range.

Two methods to control such a power net are presented: global optimization using knowledge of the complete driving cycle and an online implementable strategy doing without future knowledge. The alternator and the DC-DC converter are power controlled.

5.2.1 Power flow

The power flow in the vehicle is shown in Fig. 5.1. It starts with fuel that goes into the internal combustion engine (ICE) which converts it into mechanical power. One part goes to the drive train (DT) for vehicle propulsion, whereas the other part goes to the alternator (GEN) which converts it into electric power.

The alternator is connected to a switching device (S) that divides the electric alternator power between the ultracap (C) and the battery (B). The switch can be a discrete switch or a continuous power divider. The battery and the ultracap are connected to a DC-DC converter (DC). The loads are connected to the battery.

There are three control variables: the electric alternator power P_e , the power through the DC-DC converter P_{dc} and the position of the switch S .

Independently from the position of the switch, the electric power provided by the alternator is equal to the sum of the powers to the load, the battery, and the ultracap, and the power losses of the DC-DC converter.

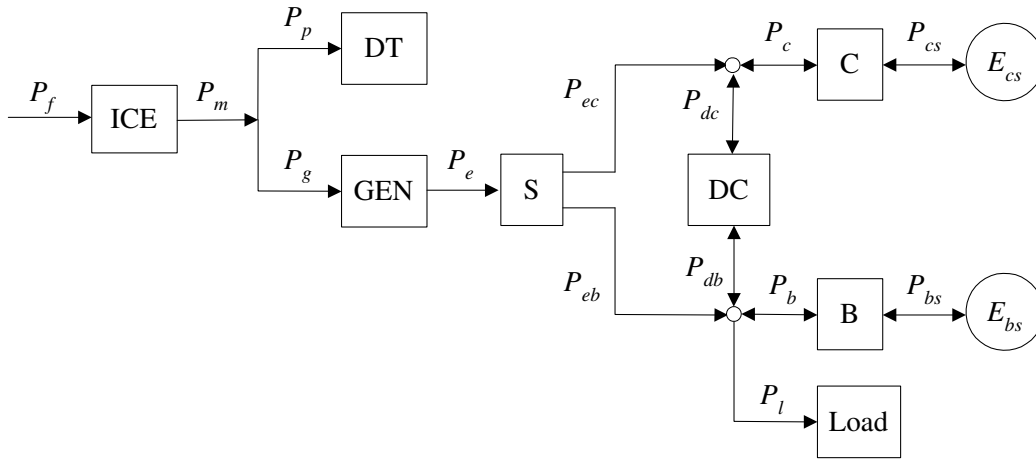


Figure 5.1: Power flow in a dual storage power net

5.2.2 Analysis

The possible benefits of a dual storage net will be analyzed for the two positions of the switch.

Case $S = 0$

The alternator is connected to the battery and the loads. This is the baseline situation.

Additionally, the ultracap can be charged and discharged through the DC-DC converter. Doing so is only beneficial if the losses of the ultracap and the DC-DC converter together are smaller than the battery losses.

Case $S = 1$

The alternator is connected to the ultracap, so the ultracap can be charged directly. The loads can be provided by the battery or by the combination of alternator, ultracap, and DC-DC converter. It is only beneficial to use the switch in this position if the power that is stored in the ultracap is larger than the power requested by the loads, because then, the losses of the DC-DC converter are smaller in this direction.

5.3 Control objective

The control objective is to minimize the fuel consumption while satisfying several constraints. For a predefined driving cycle, this can be described as a dynamic optimization problem. The cost function J expresses the fuel use over a driving cycle as function of the decision variables z . Depending on the selected optimization method and the model structure, it might be beneficial to choose the decision variables different from the control variables and to compute the corresponding values of the control variables afterwards, such that the characteristics of all components can be combined into a single cost function over a time interval $[0, n \Delta t]$:

$$J(z) = \sum_{k=0}^n \dot{m}(z(k), k) \Delta t \quad (5.1)$$

The operating range of the components is limited, so bounds have to be set on their power and energy levels. To prevent the storage devices from being drained, endpoint constraints on the state of energy must be used.

5.3.1 Optimization method

To solve the optimization problem, various optimization algorithms have been studied, that all have their requirements on the way the system is modeled.

Because there are two storage devices, there are two state variables. With Dynamic Programming, this means that the solution space becomes three dimensional (E_{bs} , E_{cs} and t), which is too large to solve in a limited amount of time.

As a solution, the component characteristics are modeled as piecewise linear. This way, the problem can be written as a Linear Programming (LP) problem:

$$\min_z J(z) = h^T z \quad \text{subject to} \quad A z \leq b \quad (5.2)$$

which can be solved efficiently [52]. In Section A.4 it is explained how piecewise linearities are incorporated in an LP. A similar approach has been applied to a series hybrid vehicle in [68].

5.4 Modeling

The dual storage power net control problem has been described as an optimization problem. Here, the relation between the decision variables and the cost function is described which is needed to compute the solution.

5.4.1 Components

The (dis)-charging of the battery is modeled using a piecewise linear function:

$$P_b = \begin{cases} b^- P_{bs} & \text{if } P_{bs} < 0 \\ b^+ P_{bs} & \text{if } P_{bs} \geq 0 \end{cases} \quad (5.3)$$

which can also be described as follows:

$$P_b = \max(b^- P_{bs}, b^+ P_{bs}) \quad (5.4)$$

where P_b represents the power entering or leaving the battery terminals, and P_{bs} represents the power actually stored in the battery. The losses are positive both during charging and discharging, so $b^+ > 1$ and $0 < b^- < 1$. A typical curve is shown in Fig. 5.2.

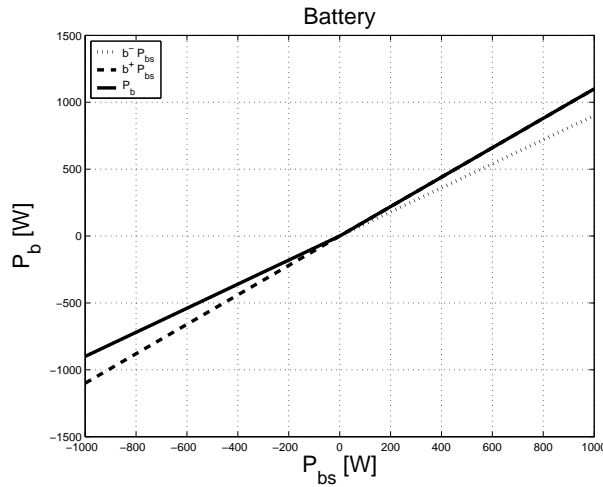


Figure 5.2: Battery characteristics

The model for the ultracap is similar:

$$P_c = \max(c^- P_{cs}, c^+ P_{cs}) \quad (5.5)$$

The DC-DC converter is modeled likewise:

$$P_{db} = \max(d^- P_{dc}, d^+ P_{dc}) \quad (5.6)$$

where $P_{db} > 0$ means power is going from the battery to the ultracap.

The characteristic of the alternator is linearly approximated for given engine speed ω :

$$P_g = g_0(\omega) + g_1 P_e \quad (5.7)$$

g_0 is caused by friction and g_1 is the inverse of the conversion efficiency, so $g_0 > 0$ and $g_1 > 1$.

The characteristics of the fuel converter is linearly approximated:

$$P_f = f_0(\omega) + f_1(t) P_m \quad (5.8)$$

The approximation is made at each time step for the range $P_m \in [P_d + P_{g \min}, P_d + P_{g \max}]$. Because this range is small compared to the entire operating range of the engine, a linear fit is sufficient.

5.4.2 Power flow

The mechanical power P_m is given by:

$$P_m = P_d + P_g + P_{br} \quad (5.9)$$

where P_{br} is the power of the friction brakes.

$P_{m \min}(\omega)$ is the friction in the engine at zero fuel use. At moments where:

$$P_d < P_{m \min} - g_0 \quad (5.10)$$

electric power can be generated without fuel use, which is called regenerative braking. It is expected that the friction brakes are only used when:

$$P_d < P_{m \min} - P_{g \max} \quad (5.11)$$

The equation for the electric power flow becomes:

$$P_e = P_{eb} + P_{ec} = P_l + P_b + P_c + P_{db} - P_{dc} \quad (5.12)$$

As stated before, independently from the position of the switch, the electric power provided by the alternator is equal to the sum of the powers to the load, the battery, and the ultracap, and the power losses of the DC-DC converter.

5.4.3 Decision variables

Suppose the primary decision variables are chosen to be:

$$z_1 = [P_{bs} \ P_{cs} \ P_{dc}]^T \quad (5.13)$$

The piecewise linear component models and the linear power flow equations can be incorporated by introducing the following secondary decision variables:

$$z_2 = [P_b \ P_c \ P_{db} \ P_{eb} \ P_{ec} \ P_e \ P_g \ P_m \ P_{br} \ P_f]^T \quad (5.14)$$

If optimization is carried out over a horizon of n time steps, the variables are vectors with length n , so the total number of decision variables is $13n$.

5.4.4 Cost function

The cost function is the fuel consumption over a driving cycle with length $t_n = n \Delta t$:

$$J(z) = \sum_{i=1}^n P_f(i) \Delta t \quad (5.15)$$

5.4.5 Constraints

The power flow equations and the alternator and engine model are incorporated as linear equality constraints:

$$P_{eb} = P_l + P_b + P_{db} \quad (5.16)$$

$$P_{ec} = P_c - P_{dc} \quad (5.17)$$

$$P_e = P_{eb} + P_{ec} \quad (5.18)$$

$$P_m = P_d + P_g + P_{br} \quad (5.19)$$

$$P_g = g_0 + g_1 P_e \quad (5.20)$$

$$P_f = f_0 + f_1 P_m \quad (5.21)$$

The piecewise linear component models are incorporated using the following linear inequality constraints:

$$P_b \geq b^\pm P_{bs} \quad (5.22)$$

$$P_c \geq c^\pm P_{cs} \quad (5.23)$$

$$P_{db} \geq d^\pm P_{dc} \quad (5.24)$$

The physical limitations of the components are incorporated using upper and lower bounds on the decision variables:

$$z_{min} \leq z \leq z_{max} \quad (5.25)$$

The endpoint constraints on the energy storage levels become:

$$E_{*s}(n) = E_{*s}(0) \Rightarrow \sum_{i=1}^n P_{*s}(i) = 0 \quad * \in \{b, c\} \quad (5.26)$$

5.4.6 Complementarity constraint

If the switch is considered to be a continuous power divider, P_{eb} and P_{ec} can both be positive at the same time. In the case of a discrete switch, either $P_{eb} = 0$ and/or $P_{ec} = 0$ at each time instant. This can be modeled by adding a complementarity constraint:

$$P_{eb} \cdot P_{ec} = 0 \quad (5.27)$$

As shown in Appendix A.7.1, the LP problem with complementarity constraint for the discrete switch can be translated to a mixed integer LP problem by introducing a binary variable $S \in \{0, 1\}$ and adding the following linear constraints:

$$0 \leq P_{eb} \leq (1 - S) P_{ebmax} \quad (5.28)$$

$$0 \leq P_{ec} \leq S P_{ecmax} \quad (5.29)$$

Note that $S = 0$ yields that $P_{ec} = 0$ and $S = 1$ yields that $P_{eb} = 0$, which corresponds to the two positions of the switch.

5.5 Global optimization

If the switch is considered to be a continuous power divider, the binary variable $S \in \{0, 1\}$ can be relaxed to a continuous variable $S \in [0, 1]$. In this case, the optimization problem can be solved with a standard LP solver. The problem is very sparse, so despite the large number of decision variables, the computation time remains short.

For the discrete switch, a mixed integer LP solver can be used, *e.g.*, a branch and bound algorithm. The computation time of mixed integer solvers increases drastically with the number of discrete variables, because the algorithms evaluate many combinations of these variables. This makes mixed integer optimization not suitable for optimization over a long horizon, despite the sparseness of the problem.

A suboptimal mixed integer solution can be obtained as follows. First the problem is solved for the continuous switch. Then the position of the switch is rounded off to boolean values. The continuous optimization is repeated, but with the upper bounds modified according to (5.28) and (5.29).

The solution for the continuous switch provides a lower bound for the mixed integer minimum, whereas the suboptimal mixed integer solution is an upper bound. If the difference between this upper and lower bound is small, not much improvement can be obtained by searching for the global minimum of the mixed integer problem.

5.6 Real-time control strategy

A control strategy is derived that can be used in real-time. It is similar to the method for a single storage system as presented in Section 3.5.

Optimization is done at each time instant with a horizon length of 1 time step. Instead of using endpoint constraints on the storage levels, the change in *SOE* is accounted for in the cost function:

$$\gamma(u, x, k) = P_f(k) - \lambda_b(k) P_{bs}(k) - \lambda_c(k) P_{cs}(k) \quad (5.30)$$

At each time instant, a trade off is made between the increase in fuel and the increase in *SOE*. All other constraints still apply.

The factors λ_b and λ_c represent the average fuel costs to store energy in the battery and the ultracap. They are online adapted using proportional state feedback:

$$\lambda_*(k) = \lambda_{*0} + K_p (E_{*s}(0) - E_{*s}(k)) \quad (5.31)$$

The state feedback ensures that the *SOE* remains bounded, although the *SOE* at the end will differ from the beginning. The changes in *SOE* are accounted for in the fuel consumption using the initial values of λ_b and λ_c .

Because of the switch, the optimization has to be carried out twice at each time instant, once with $P_{eb} = 0$ and once with $P_{ec} = 0$. The solution with the lowest cost function value is then selected.

5.7 Simulations

5.7.1 Model

Simulations are done for the Ford Mondeo driving the NEDC cycle. The vehicle is equipped with the 42 V power net. The specifications of the electric components are shown in Table 5.1. The electric load is kept constant at 1000 W.

Table 5.1: Power net components

	Energy Capacity	Power limits	Efficiency
Battery	1000 kJ	5 kW	90%
Ultracap	100 kJ	5 kW	99%
DC-DC	-	1 kW	95%
Alternator	-	5 kW	90%

5.7.2 Strategies

The following strategies are implemented:

- BL1 A baseline strategy that does not use the storage devices, so the alternator power is equal to the load
- BL2 Continuous LP optimization of the complete cycle, using only the battery
- LP1 Continuous LP optimization of the complete cycle
- LP2 Sub-optimal mixed integer LP optimization of the complete cycle
- RT The real-time strategy

The RT strategy is used with $K_p = 1 \cdot 10^{-6}$, and $\lambda_{b0} = \lambda_{c0} = 2.5$, as these values turned out to yield good results.

5.7.3 Results

The resulting trajectories of P_e , P_{dc} , S , SOE_{bat} , and SOE_{cap} are shown in Fig. 5.3 for the LP2 strategy and in Fig. 5.4 for the RT strategy. During deceleration, when much electric power is generated, the alternator is connected to the ultracap. The battery is mainly used during the braking period at the end, when the SOE of the ultracap hits its boundary.

The power levels change rapidly. This is typical for LP since the optimal solution will always lie at a constraint. Smoother behavior can be obtained by adding rate limiting constraints, or by using quadratic terms for the losses, resulting in a QP.

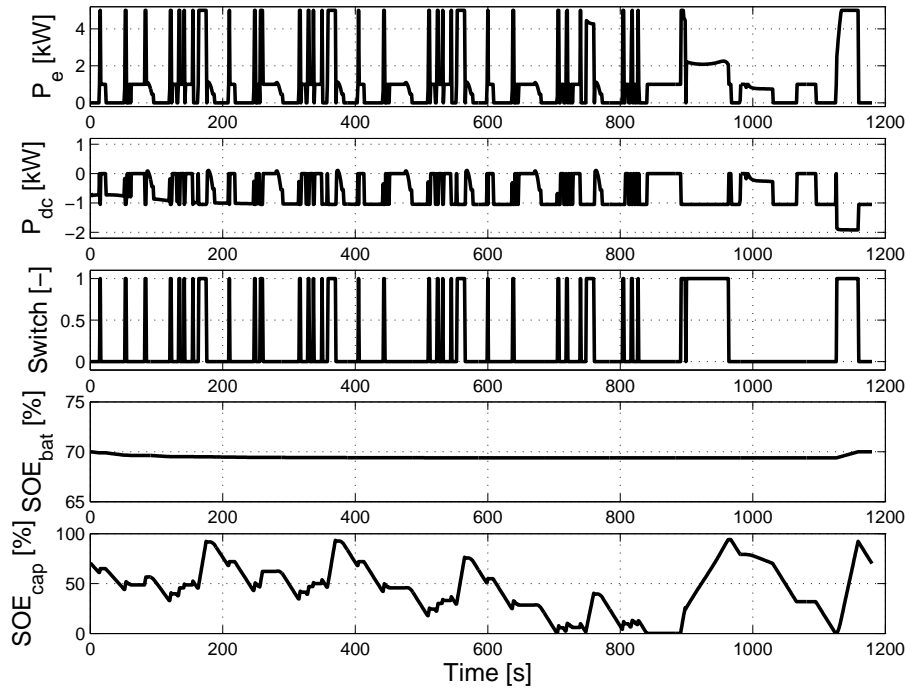


Figure 5.3: Results for the LP2 strategy

The fuel consumption of all strategies is shown in Table 5.2. It is computed both using the original nonlinear lookup table and the local linear fit as used in the optimization. The differences are very small, which justifies the approximation.

The difference in fuel consumption between the LP1 and LP2 is small, so searching for the global minimum of the mixed integer problem will not give much improvement.

Besides the fuel consumption, the exhaust emissions are also evaluated using the original lookup tables. The percentile savings in fuel with respect to the BL1 strategy are given in Fig. 5.5. All emissions show an improvement except for HC. It is possible to obtain a reduction in all emissions, by incorporating them in the cost function, at the cost of a smaller fuel reduction.

5.8 Conclusion

Simulations show that the control strategies are effective and that the performance of the real-time strategy is close to the optimal one. For the chosen parameter values, the

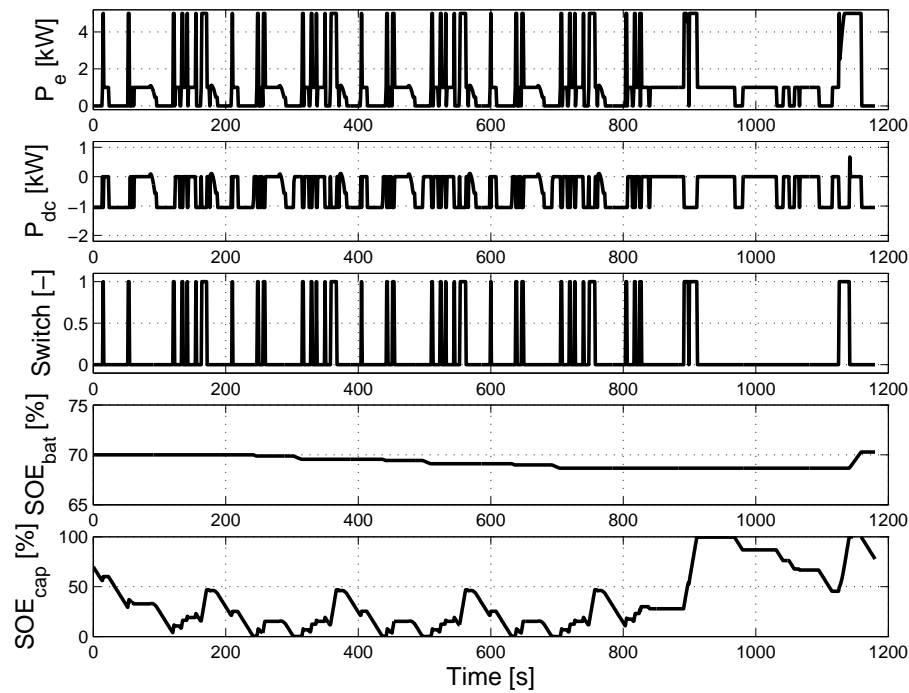


Figure 5.4: Results for the RT strategy

Table 5.2: Fuel Consumption

Strategy	Nonlinear map	Linear fit
	Fuel Use [g]	Fuel Use [g]
BL1	589.486	588.938
BL2	579.749	579.344
LP1	576.736	577.024
LP2	577.606	577.373
RT	577.970	577.452

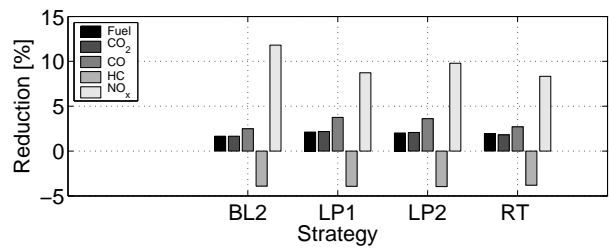


Figure 5.5: Reduction of fuel and exhaust emissions

dual storage power net only gives a limited improvement in fuel reduction over the single storage net, at the cost of additional hardware investments. This power net topology may be worthwhile for hybrid vehicles using start-stop operation, or if tight limits on the battery voltage are present.

Full optimization of the mixed integer problem can not be carried out for a reasonable driving cycle length, due to the rapidly increasing computation time. However, the difference between the suboptimal integer solution and the continuous optimum is very small.

The energy management problem considered here is easy and straight forward to formulate as a Linear Programming problem using piecewise linear component models. Because of its simple structure, the method is easy to apply on other topologies, such as a hybrid electric vehicle, as will be done in Chapter 6.

Parallel Hybrid Electric Vehicles

6.1 Introduction

The drive train of a conventional vehicle can easily be modified to look like a parallel hybrid electric vehicle (HEV) by replacing the alternator with an integrated starter generator (ISG). The possibility to change the operating point of the engine and to turn it off, gives rise to a reduction of fuel consumption and exhaust emissions.

This chapter analyzes the benefits of two parallel drive train configurations: one with the ISG connected directly to the engine, before the clutch, and one with the ISG connected directly to the drive train, after the clutch. The first configuration can only turn off the engine during standstill and deceleration. The second configuration offers the opportunity to turn off the engine during propulsion.

The effect on fuel economy is analyzed by using optimization over a given driving cycle. The optimization problem is formulated as a Linear Programming (LP) problem [52]. Adding start-stop functionality makes it a Mixed Integer LP (MILP) problem. A similar approach without start-stop is applied to a series HEV in [68]. Another formulation is a Dynamic Program [10] as done, *e.g.*, in [18, 48]. Here, LP is chosen because of its easy implementation and fast computation.

This chapter is built up as follows. The vehicle topology will be described and analyzed in Section 6.2. The objective is presented in Section 6.3. Section 6.4 presents the vehicle model. In Section 6.5, the energy management control problem is formulated and solved as an optimization problem. The performance will be evaluated by simulations in Section 6.6. Conclusions are given in Section 6.7.

A preliminary version of this chapter is published earlier in [45].

6.2 Parallel hybrid electric vehicles

The drive train of a parallel HEV is based on a conventional vehicle, where the alternator is replaced by an integrated starter generator that can also be used for propulsion. The clutch can be located before or after the power split for the ISG. If the clutch is closed, the configurations are similar.

For this case study, it is assumed that the vehicle speed is defined by the driver and that the gear ratio is selected by either the driver or by the automatic transmission. This way,

the engine speed is also predefined.

6.2.1 Power flow description

The power flows in the vehicle with configuration 1 and 2 are shown in Fig. 6.1 and Fig. 6.2 respectively. The power required for the drive train is delivered by the engine, the ISG, and the brakes. The internal combustion engine converts fuel into mechanical power. The ISG converts mechanical power into electric power or vice versa. The electric side of the ISG is connected to the battery and the auxiliary electric load. The battery can be separated in the (dis)-charging losses and the net energy storage.

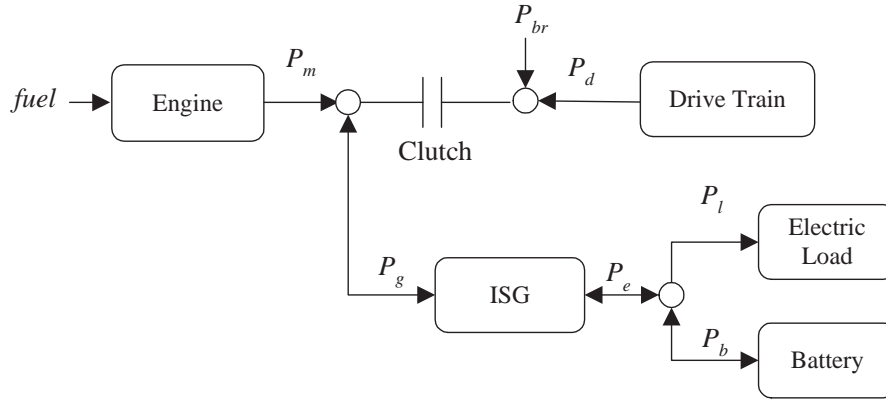


Figure 6.1: Configuration 1

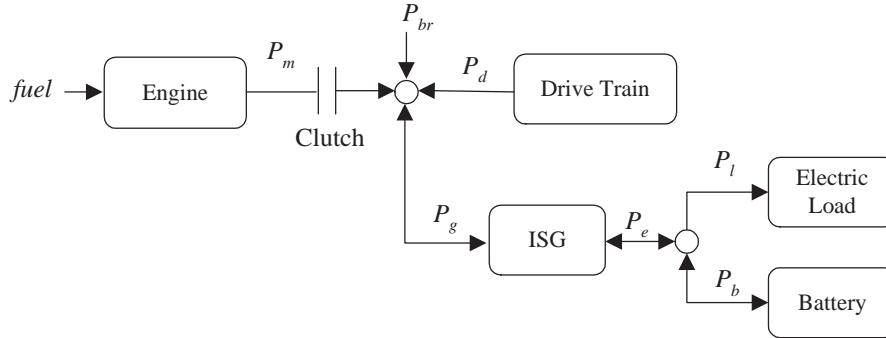


Figure 6.2: Configuration 2

6.3 Control objective

Hybrid electric vehicles require an energy management strategy to control the power flow in an optimal way, meaning that fuel consumption and emissions are reduced while maintaining requirements on performance and comfort.

In this chapter, the difference in fuel reduction depending on the location of the clutch is being evaluated. To do so, the control objective is to minimize the fuel consumption for a

given driving cycle. This can be described as an optimization problem. The cost function J expresses the fuel use over a driving cycle as function of the decision variables z . This way, the characteristics of all components can be combined into a single cost function over a time interval $[0, n \Delta t]$:

$$J(z) = \sum_{k=0}^n \dot{m}(z(k), k) \Delta t \quad (6.1)$$

The operating range of the components is limited, so bounds have to be set on their power and energy levels. To prevent the storage device from being drained, an endpoint constraint on the state of energy can be used.

The dynamics are modeled in discrete time and the component losses are modeled using piecewise linearities, such that the nonlinear optimization problem reduces to a linear programming problem, as also done in Chapter 5.

6.4 Modeling

The control problem has been described as an optimization problem. Here, the relation between the decision variables and the cost function is described which is needed to compute the solution.

6.4.1 Components

The (dis)-charging of the battery is modeled as in Section 5.4:

$$P_b = \max(b^- P_s, b^+ P_s) \quad (6.2)$$

The electric power flow equation is given by:

$$P_e = P_l + P_b \quad (6.3)$$

The characteristic of the ISG is approximated as a piecewise linear function:

$$P_g = g_0(w) + \max\left(\frac{1}{\eta_g} P_e, \eta_m P_e\right) \quad (6.4)$$

where g_0 is the friction loss, η_g is the conversion efficiency in generator mode ($P_e > 0$), and η_m the conversion efficiency in motor mode ($P_e < 0$). A typical curve is shown in Fig. 6.3.

The mechanical power flow equation is given by:

$$P_m = P_d + P_g + P_{br} \quad (6.5)$$

where $P_{br} \geq 0$ is the power dissipated by the friction brakes.

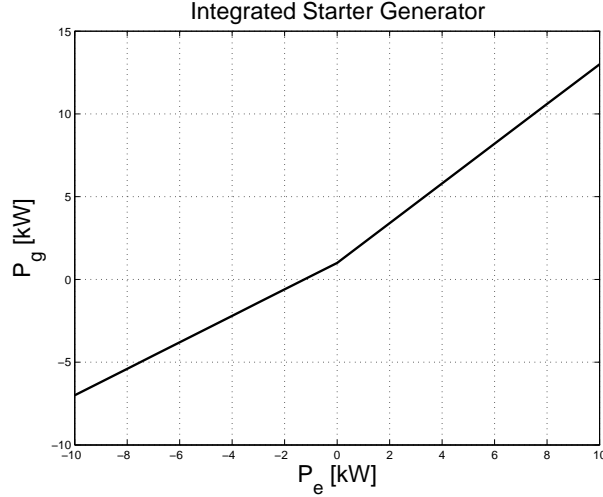


Figure 6.3: ISG map

The characteristics of the fuel converter is linearly approximated:

$$P_f = f_0(\omega) + f_1(t) P_m \quad (6.6)$$

The approximation is done at each time step for the range $P_m \in [P_{mmin}, P_d + P_{gmax}]$. The actual fuel map is more or less linear, except for the highest torque area, which is not reached very often. Therefore, a linear fit is probably sufficient.

The fuel use is positive for zero power, due to friction. This can be avoided by turning off the engine during idle, which is called start-stop.

6.4.2 Start-stop operation

For both configurations, start-stop functionality can be added using a binary variable.

Configuration I

First the case where the ISG is connected directly to the engine is considered. If the engine is turned off, this means that:

$$P_e = 0 \quad P_g = 0 \quad P_m = 0 \quad P_f = 0 \quad (6.7)$$

which results in:

$$P_b = -P_l \quad (6.8)$$

$$P_d = -P_{br} \quad (6.9)$$

Because $P_{br} \geq 0$, the engine can only be turned off when $P_d \leq 0$ and if the electric load can be delivered by the battery. It is only advantageous to do so, if the additional fuel for restarting the engine and for recharging the battery during propulsion is smaller than the fuel saved during stand still.

Start-stop can be included by introducing a binary variable S , where $S = 1$ means the engine is running, and $S = 0$ means the engine is turned off. This can be achieved with the following constraints:

$$S P_{e \min} \leq P_e \leq S P_{e \max} \quad (6.10)$$

$$S P_{m \min} \leq P_m \leq S P_{m \max} \quad (6.11)$$

Normally, the engine characteristics are such that $P_m = 0$ corresponds to $P_f > 0$ and $P_f = 0$ to $P_m < 0$, but if the engine is turned off, the operating point becomes $P_m = 0$ and $P_f = 0$. Therefore, the engine model is changed into:

$$P_f \geq f_0(\omega) S + f_1(t) P_m \quad (6.12)$$

such that $S = 0$ yields that $P_f = 0$ for $P_m = 0$.

Equivalently, the alternator model is changed into:

$$P_g = g_0(\omega) S + \max\left(\frac{1}{\eta_g} P_e, \eta_m P_e\right) \quad (6.13)$$

These constraints are still linear in the decision variables.

Configuration II

If the ISG is connected directly to the drive train, or after the clutch, the ISG can still be operated when the clutch is opened and the engine is turned off, which means that:

$$P_m = 0 \quad P_f = 0 \quad (6.14)$$

which results in:

$$P_d = -P_g - P_{br} \quad (6.15)$$

Because P_g can be both positive and negative, the engine can be turned off whenever the maximum ISG power in motor mode is sufficient to propel the vehicle. This can be achieved with the following constraints:

$$S P_{m \min} \leq P_m \leq S P_{m \max} \quad (6.16)$$

$$P_f \geq f_0(\omega) S + f_1(t) P_m \quad (6.17)$$

Penalty

To prevent frequent switching of the engine, both configurations require a penalty cost for every time the engine is restarted. This is implemented using an additional variable R as follows:

$$R(k) = \max(S(k) - S(k-1), 0) \quad (6.18)$$

This yields that $R = 1$ at times where S changes from 0 to 1, and $R = 0$ otherwise. The cost criterion is modified to:

$$J(z) = \sum_{k=1}^n (P_f(x(k)) \Delta t + C R(k)) \quad (6.19)$$

such that, for every time the engine is started, a cost C is added to the fuel consumption.

6.5 Optimization

The energy management problem is formulated as a Linear Programming problem. Adding start-stop functionality makes it a Mixed Integer LP because S is a binary variable.

6.5.1 Cost function

The complete set of decision variables becomes:

$$z = [P_s P_b P_e P_g P_{br} P_m P_f S R]^T \quad (6.20)$$

The cost function consists of the fuel use and the cost for starting the engine, so:

$$h = [0 \ 0 \ 0 \ 0 \ 0 \ 0 \ 1 \ 0 \ C]^T \quad (6.21)$$

If optimization is done over a horizon of n time steps, the variables are vectors with length n , so the total number of decision variables is $9n$.

6.5.2 Constraints

The power flow equations are incorporated as linear equality constraints:

$$P_e = P_l + P_b \quad (6.22)$$

$$P_m = P_d + P_g + P_{br} \quad (6.23)$$

The piecewise linear component models are incorporated using the following linear inequality constraints:

$$P_b \geq b^\pm P_{bs} \quad (6.24)$$

$$P_c \geq c^\pm P_{cs} \quad (6.25)$$

$$P_{db} \geq d^\pm P_{dc} \quad (6.26)$$

$$P_g \geq g_0 S + 1/\eta_g P_e \quad (6.27)$$

$$P_g \geq g_0 S + \eta_m P_e \quad (6.28)$$

$$P_f \geq f_0 S + f_1 P_m \quad (6.29)$$

The physical limitations of the components are incorporated using upper and lower bounds on the decision variables:

$$z_{min} \leq z \leq z_{max} \quad (6.30)$$

The constraints on the energy storage levels are incorporated using a discrete linear integrator model:

$$E_s(k) = E_s(0) + \sum_{i=1}^k P_s(i) \Delta t \quad (6.31)$$

The endpoint constraint then becomes:

$$E_s(n) = E_s(0) \Rightarrow \sum_{i=1}^n P_s(i) = 0 \quad (6.32)$$

All constraints are linear in the decision variables.

6.5.3 Model Predictive Control

Because the computation time of mixed integer programming increases rapidly with the number of integer variables, it is not possible to do global optimization over a long driving cycle within a reasonable time. Furthermore, obtaining a suboptimal solution as done in Section 5.5, will not give usable results. The continuous relaxation will yield a value of S , such that at every time instant:

$$P_m = S P_{mmax} \quad (6.33)$$

Because $S \in \{0, 1\}$ corresponds with $f_0(\omega)$, which is either present or not, values of $0 < S < 1$ are not realistic.

As a solution, the mixed integer optimization problem is solved using a receding horizon, as in Model Predictive Control (MPC) [50]. This means that the optimization is carried out at each time step over a limited prediction horizon. The first value of the optimal control sequence is implemented. The next time step a new optimization is done using updated prediction and state information.

6.5.4 Removing the endpoint constraint

For short horizons, the performance of the MPC strategy is limited by the endpoint constraint on the SOE . Therefore, the endpoint constraint is removed and the cost function is modified such that a trade off is made between fuel use and SOE , as presented in Section 3.5.

The cost function becomes:

$$J(z, k) = \sum_{i=k+1}^{k+N_p} [(P_f(i) - \lambda P_s(i)) \Delta t + C R(i)] \quad (6.34)$$

N_p is the length of the prediction horizon. The factor λ represents the average fuel cost to store energy in the battery. Its value is online adapted using proportional feedback of the *SOE*:

$$\lambda(k) = \lambda_0 + K_p (E_s(0) - E_s(k)) \quad (6.35)$$

The feedback ensures that the *SOE* remains bounded, although the *SOE* at the end may differ from that at the beginning. The difference in *SOE* can be accounted for in the fuel consumption using the average value of λ .

6.6 Simulations

6.6.1 Model

Simulations are done for the Ford Mondeo driving the NEDC cycle. The vehicle contains a 10 kW (electrical) ISG and a battery with a capacity of $1 \cdot 10^6$ J. The electric load is kept constant at 1000 W.

6.6.2 Strategies

Simulations are done for the following strategies:

- BL Configuration 1 using a baseline strategy where the ISG only provides the electric load, like in a conventional vehicle
- S1 Global optimization using configuration 1 without start-stop functionality
- S2 MPC strategy using configuration 1 without start-stop functionality
- S3 MPC strategy using configuration 1 including start-stop functionality
- S4 MPC strategy using configuration 2 including start-stop functionality

Strategy S1 does a single optimization over the entire driving cycle, whereas Strategies S2, S3, and S4 use a receding horizon length of 10 s. The strategies are used with $K_p = 1 \cdot 10^{-6}$, and $\lambda_0 = 2.8$, as these values turned out to yield reasonable results. All strategies run faster than real-time on an Intel Pentium IV 2.4 GHz computer.

6.6.3 Results

The trajectories of P_m , P_g , P_{br} , S , and *SOE* are shown for Strategies S1, S2, S3, and S4 in Fig. 6.4, Fig. 6.5, Fig. 6.6, and Fig. 6.7 respectively.

Strategies S1, S2, and S3 use the ISG mainly for regenerative braking and supplying the electric load. Apparently it is not beneficial to use the ISG for propulsion if the engine is already running, but this depends on the selected vehicle and driving cycle. With Strategy S3, the engine is turned off during braking and idle periods. With Strategy S4, the engine is turned off during low velocity periods and during braking, such that more energy is available for regenerative braking. The engine cannot be turned off when the required propulsion power exceeds the maximum ISG power. Because the ISG is more

intensively used, both for generation and propulsion, the *SOE* of the battery varies much more.

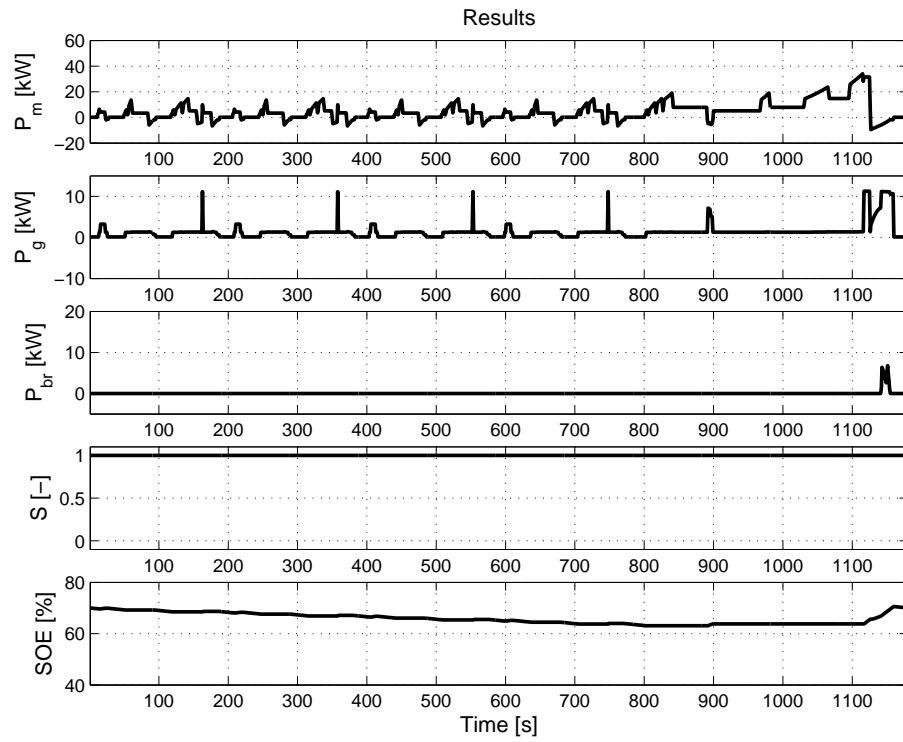


Figure 6.4: Results for Strategy S1

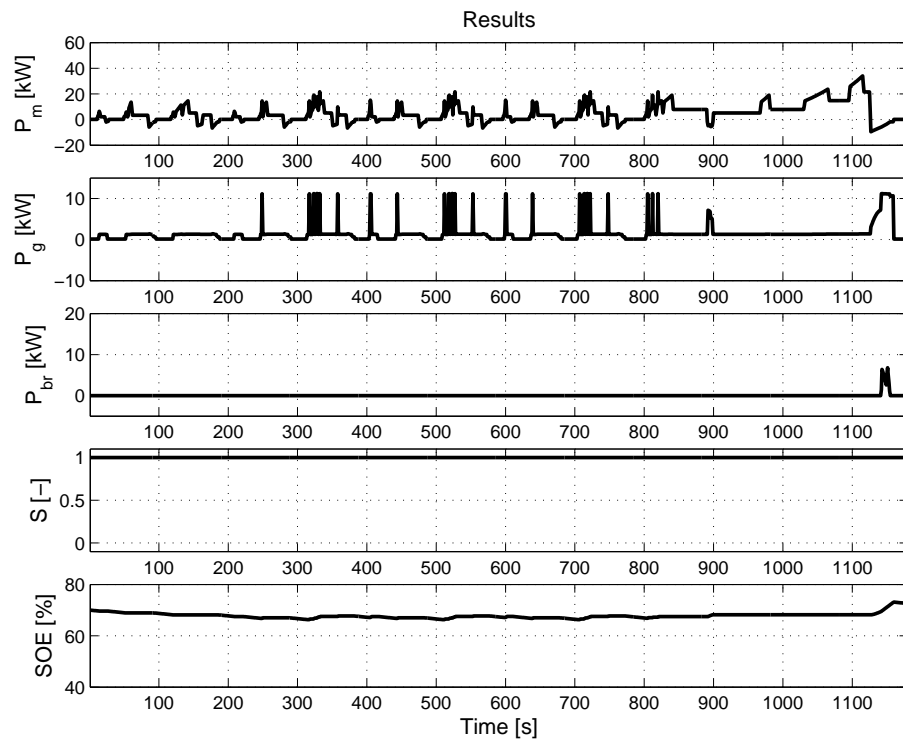


Figure 6.5: Results for Strategy S2

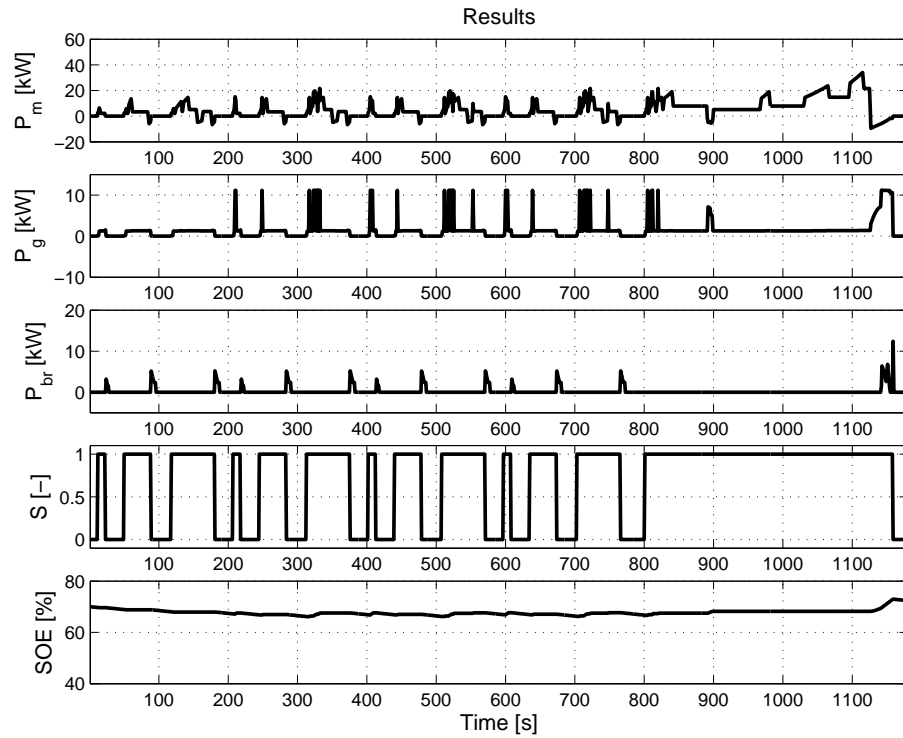


Figure 6.6: Results for Strategy S3

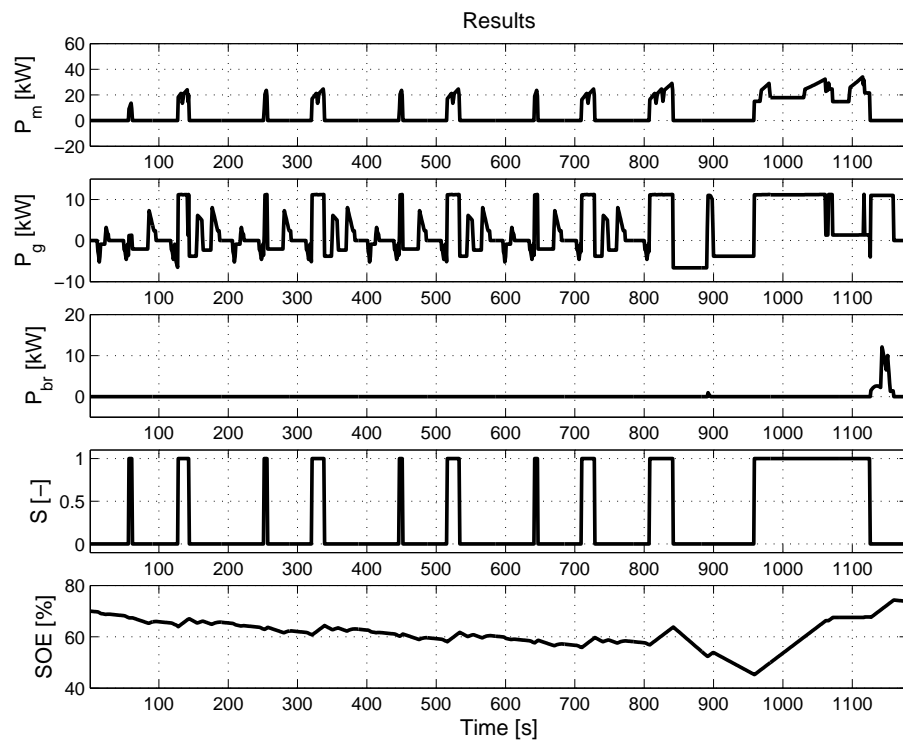


Figure 6.7: Results for Strategy S4

The engine operating points of Strategy S4 and the baseline are compared in Fig. 6.8. As can be seen, Strategy S4 switches between “engine off” and the high torque area, where the efficiency is high, whereas the baseline strategy remains in the low torque area.

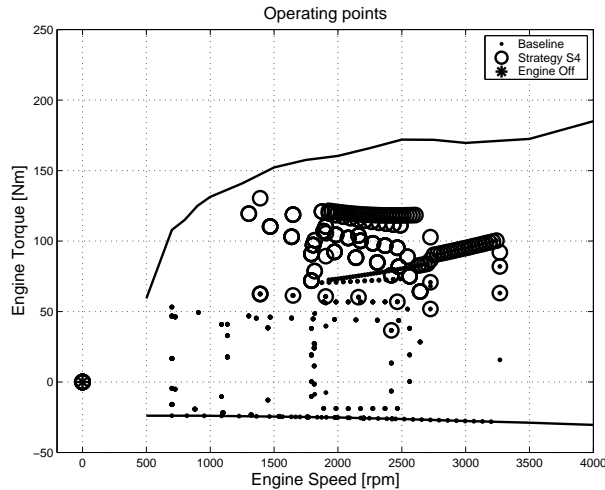


Figure 6.8: Operating points

6.6.4 Fuel consumption

The fuel consumption is given in Table 6.1. Differences in SOE are accounted for using λ_0 . Strategies S1 and S2 show a small decrease in fuel consumption because the engine is always running. Profits come mainly from regenerative braking. The difference between S1, which does optimization over the entire driving cycle, and S2, which uses a short receding horizon, is small, thereby justifying this approach. Strategy S3 shows a larger fuel reduction, because the engine is turned off during idle periods. Strategy S4 shows a much higher fuel reduction because it allows turning the engine off during propulsion phases.

Table 6.1: Fuel Consumption

Strategy	Nonlinear map	Linear fit
	Fuel Use [g]	Fuel Use [g]
BL	589.486	592.613
S1	575.948	576.665
S2	575.789	576.952
S3	544.463	541.701
S4	418.947	420.039

6.6.5 Exhaust emissions

The exhaust emissions CO_2 , CO , HC , and NO_x are also evaluated, although they are not accounted for in the cost function. CO_2 is roughly proportional to fuel consumption, whereas the other emissions are highly non-convex, which makes it harder to incorporate them into a convex LP. As can be seen in Fig. 6.9, the exhaust emissions are also reduced

significantly. This is mainly because of start-stop operation, as no emissions are produced when the engine is not running.

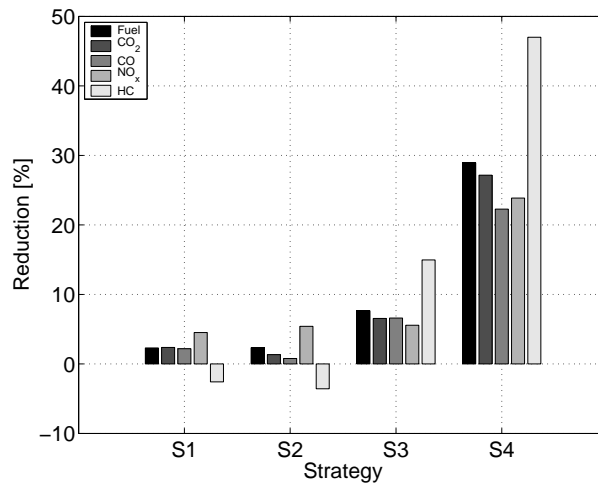


Figure 6.9: Reduction of fuel and exhaust emissions

6.7 Conclusion

The fuel consumption and exhaust emissions of two parallel hybrid drive train configurations are compared: one with the ISG connected directly to the engine, and one with the ISG connected to the drive train, after the clutch.

The simulations show a large improvement in fuel and emissions reduction if start-stop is included, especially if the ISG is placed after the clutch.

The results depend on the component sizing and the driving cycle. More improvement can possibly be obtained by including freedom in the engine speed.

The optimization is done using a short receding horizon, so the method allows easy real-time implementation. Due to the choice of cost function (6.34), including the Lagrangian term for the endpoint constraint, the results are expected to be close to the global optimum.

Implementation on a Hardware-in-the-Loop test setup

7.1 Introduction

This chapter presents the implementation of previously developed energy management strategies on a Hardware-in-the-Loop (HIL) test setup. The main purpose is to show that the power net can be power controlled in practice, thereby justifying the use of power-based models. Experiments are done both with the single storage and the advanced dual storage power net topology.

This chapter is built up as follows. The Hardware-in-the-Loop test setup is described in Section 7.2. Section 7.3 discusses the implementation of the control strategies. The results are presented in Section 7.4. Conclusions are given in Section 7.5.

7.2 Hardware-in-the-Loop test setup

A Hardware-in-the-Loop test setup is a test environment in which some components of the vehicle are actually present, some are emulated, and the remaining parts are simulated.

In this case, a lead-acid battery, an ultracapacitor, a DC-DC converter, and a controllable switch are actually present. The electrical side of the alternator is emulated by a power supply and the electric consumers are emulated by a programmable load. The driver, the drivetrain, the mechanical side of the alternator, and the engine are simulated using the forward facing simulation model as mentioned in Section 2.3.1.

The battery is a 14 V AGM lead acid battery with a capacity of 60 Ah which corresponds to an energy capacity of 3 MJ.

The ultracapacitor is a Maxwell Technologies Boostcap module. This module consists of 9 capacitor cells connected in series. Each cell has a capacitance of 2600 F and a maximum voltage of 2.5 V. The module's indicated nominal capacitance is 290 F and the nominal voltage is 22.5 V. The energy capacity is 73.4 kJ.

The DC-DC converter is bidirectional and has a maximum power throughput of 700 W. At the side of the ultracap, the voltage should be higher than 15 V. Because the voltage of the ultracap is linear with its state of energy, this limits the usable capacity of the ultracap to 67-100% *SOE*.

To emulate the alternator, a programmable electric power supply made by Delta Power Supplies is used that can provide 30 V and 200 A. The electric power is limited to 1.5 kW. The voltage is limited to 16 V when the supply is connected to the battery and to 24 V when it is connected to the ultracap. The corresponding mechanical alternator power is computed using the 14 V 1.5 kW map. Although this alternator cannot provide 24 V in reality, the map calculates the alternator torque as function of the electric power instead of using the current and voltage.

To emulate the electric power consumers, a programmable electric load made by Höcherl & Hackl GmbH is used that can withdraw up to 10 kW.

The programmable power supply, the programmable load, and the DC-DC converter return voltage and current measurements, from which the electric power can be obtained. Furthermore a current sensor is available on the wire of the battery. No *SOC* or *SOE* measurement is available for the battery or the ultracap, so the *SOE* is estimated by integrating the power.

7.2.1 Power controller

The alternator and the DC-DC converter are controlled by lower level power controllers, that manipulate the voltage and current such that the desired power is realized.

The power controller for the alternator is illustrated in Fig. 7.1. The output is the desired alternator voltage $U_{e,sp}$ and the inputs are the desired electrical alternator power $P_{e,sp}$ and the measured electrical load power P_l and battery power P_b . The controller is an integral controller with an anti-windup, to keep the alternator voltage within its allowed region.

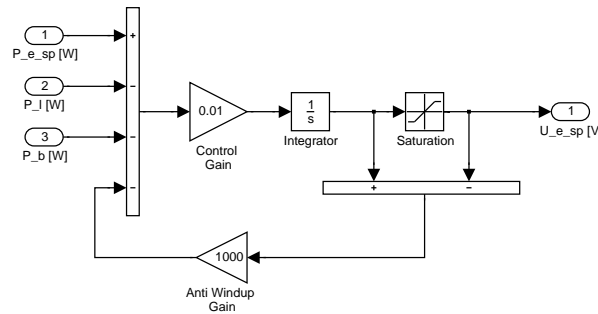


Figure 7.1: Power net controller

The power controller for the DC-DC converter is similar. It turned out that this power controller does not work well if the DC-DC converter is used in both directions. Therefore the DC-DC converter is only used to provide power from the ultracap to the battery and the load. This implies that the ultracap can only be charged at moments when the position of the switch is such that the alternator is connected to the ultracap.

7.3 Control strategies

Three strategies are implemented: a baseline strategy, an optimal strategy for the single storage power net and an optimal strategy for the dual storage power net. The baseline

strategy provides a constant alternator voltage, such that the battery is hardly used and the loads are supplied directly.

The optimal strategy that is used for the single storage power net is the DP1 strategy, as described in Section 3.6. The strategy provides one set-point: the alternator power. For a given electric load power, this uniquely defines the resulting power to the battery. The alternator is controlled by a lower level power controller, that manipulates the alternator voltage such that the desired power is realized.

The strategy that is used for the dual storage power net differs from the strategies described in Chapter 5. The strategy controls the position of the switch a priori such that during propulsion the alternator is connected to the battery and the load and during braking to the ultracap. The power set-points for P_{bs} and P_{cs} are computed by solving the following optimization problem at each time step:

$$\min_{P_{bs}, P_{cs}} P_f(P_{bs}, P_{cs}) - \lambda_b P_{bs} - \lambda_c P_{cs} \quad (7.1)$$

The corresponding set-points for P_e and P_{dc} are computed from P_{bs} and P_{cs} using the power net model. The cost function is approximated as a quadratic function, resulting in a QP. The factors λ_b and λ_c are adapted online using proportional feedback of the state of energy:

$$\lambda_* = \lambda_{*0} + K_p (E_{*s}(0) - E_{*s}) \quad (7.2)$$

7.4 Results

7.4.1 Drive train

To compare the engine speed and drive train torque of the simulation model and the control model, an experiment is done using a baseline strategy, which means that the alternator provides a constant voltage, equal to the battery voltage, such that the battery is hardly charged or discharged.

The resulting engine speed ω and drive train torque τ_d are compared with the ones calculated using the backward facing model described in Section 2.4. Both are shown in Fig. 7.2. The engine speeds are very close. The drive train torque from the forward facing model is mostly higher, because it also incorporates inertia and friction of the drive train itself. This will result in a higher overall fuel consumption.

Because the friction brakes are operated independently in the forward facing model, the drive train torque signal is already saturated at the drag torque of the engine. Besides from that, both signals are mostly alike.

7.4.2 Single storage power net

The experiment on the HIL with the single storage power net using the DP1 strategy is done with a constant load of 500 W.

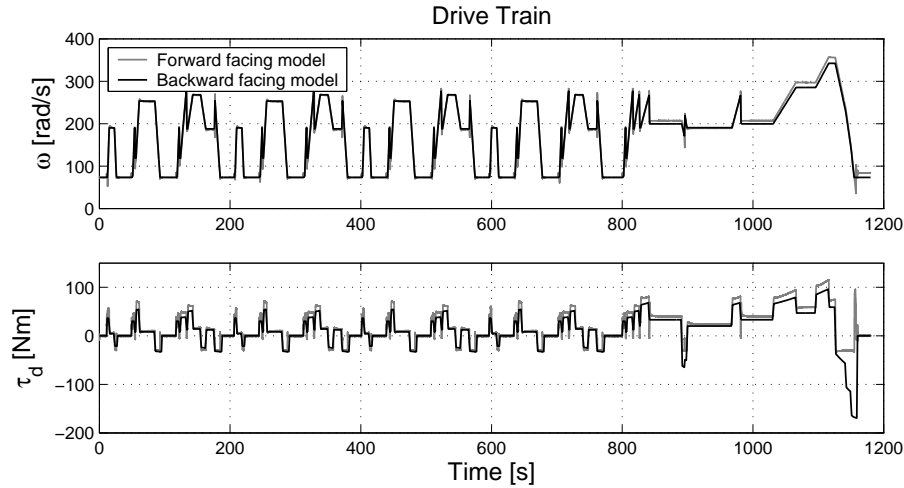
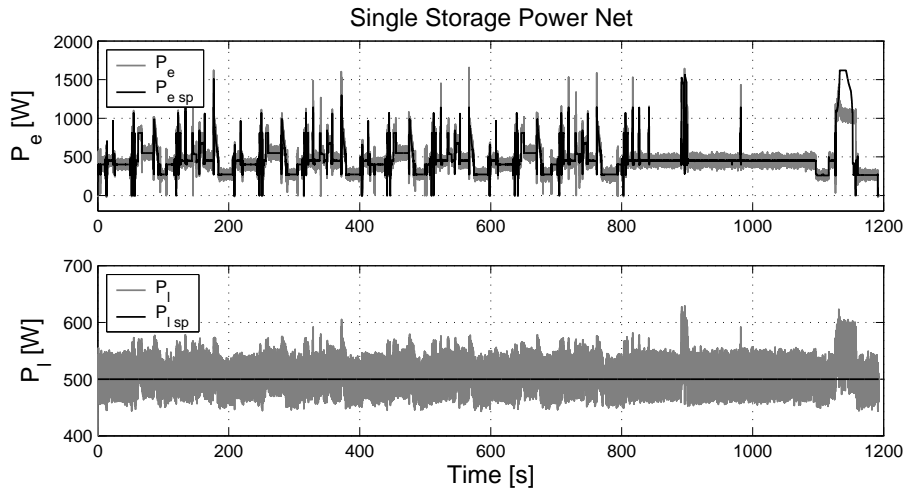


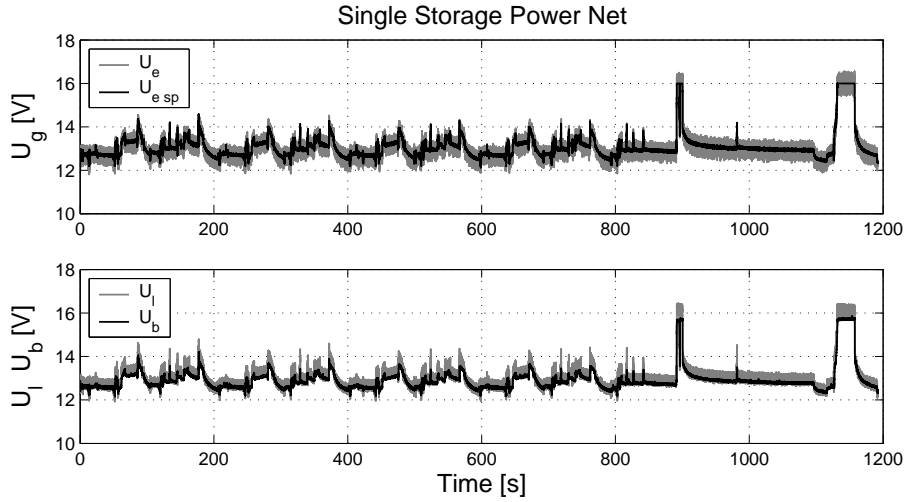
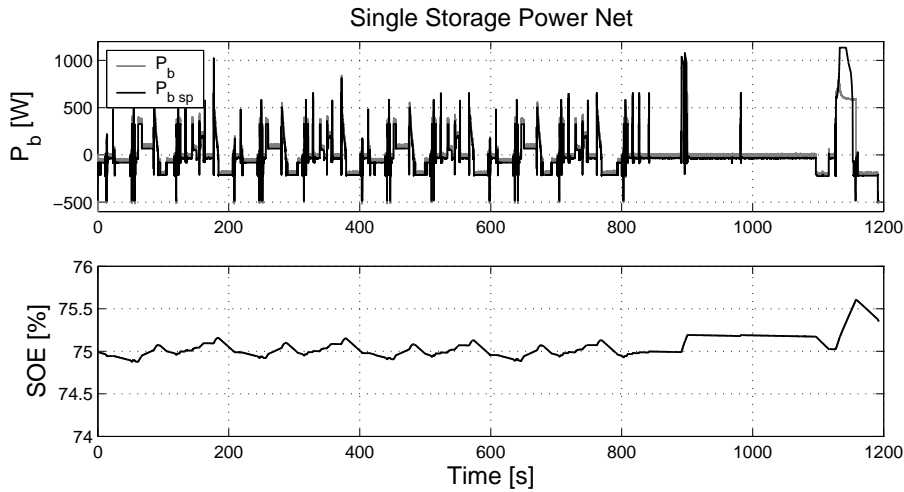
Figure 7.2: Engine speed and drive train torque

Fig. 7.3 shows the desired and realized power of the power supply (representing the alternator) and the load. The realized load power has an average value of 508 W and shows high frequent noise with a standard deviation of 19 W. It is not known to what extent this noise is caused by the power controller, the programmable supply, the programmable load, or the sensors.

Figure 7.3: Single storage results on the HIL: a) P_e b) P_l

The power delivered by the supply shows the same high frequent noise. Low frequent, the realized value corresponds with the reference values, except during the last regenerative braking period and at 900 s, where the realized alternator power is too low, because the voltage saturates at 16 V. This can be seen in Fig. 7.4, which shows the desired and realized alternator voltage, and the measured voltage of the battery and the load.

Fig. 7.5 shows the desired and realized power of the battery and the *SOE*. Like the alternator power, the desired battery power is tracked accurately, except for the last part. The *SOE* shows only a small variation, due to the high capacity of the battery.

Figure 7.4: Single storage results on the HIL: a) U_e b) U_l and U_b Figure 7.5: Single storage results on the HIL: a) P_b b) SOE

7.4.3 Dual storage power net

The experiment on the HIL with the dual storage power net using the DS strategy is also done with a constant electric load of 500 W.

Fig. 7.6 shows the desired and realized power of the alternator and the DC-DC converter. The measured powers show high frequent noise, but besides from that, the reference values are tracked accurately. Only at the end, the alternator power becomes unstable, because the ultracap reaches its maximum SOE .

Fig. 7.7 shows the desired and realized power of the battery and the ultracap. Although they are not directly controlled but result from the alternator, DC-DC converter and load power, the reference values are tracked accurately.

Fig. 7.8 shows the SOE of the battery and the ultracap. The battery SOE shows only a small variation, due to its high capacity. The ultracap is used more intensively and has a much smaller capacity. Therefore, the bounds are easily reached.

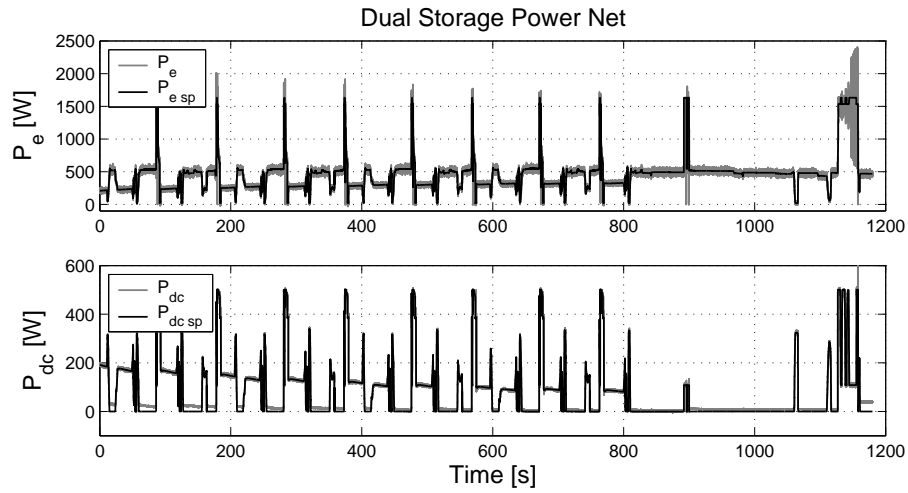


Figure 7.6: Dual storage results on the HIL: a) P_e b) P_{dc}

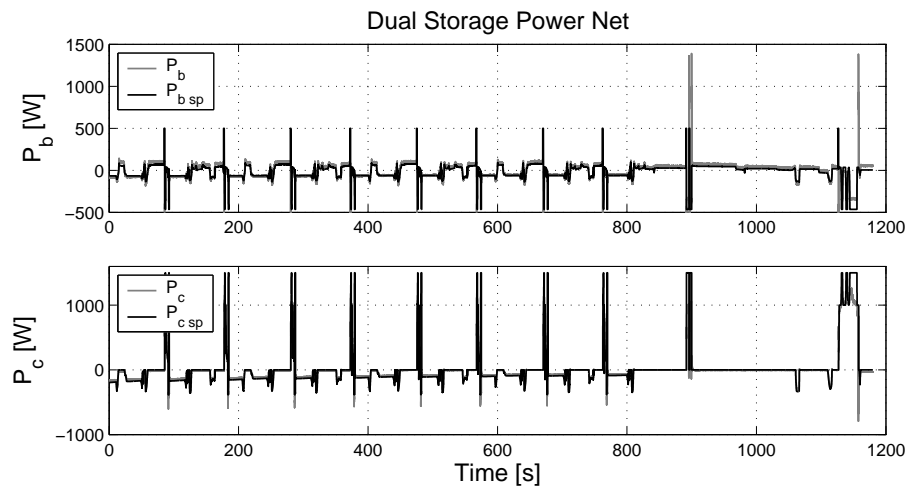


Figure 7.7: Dual storage results on the HIL: a) P_b b) P_c

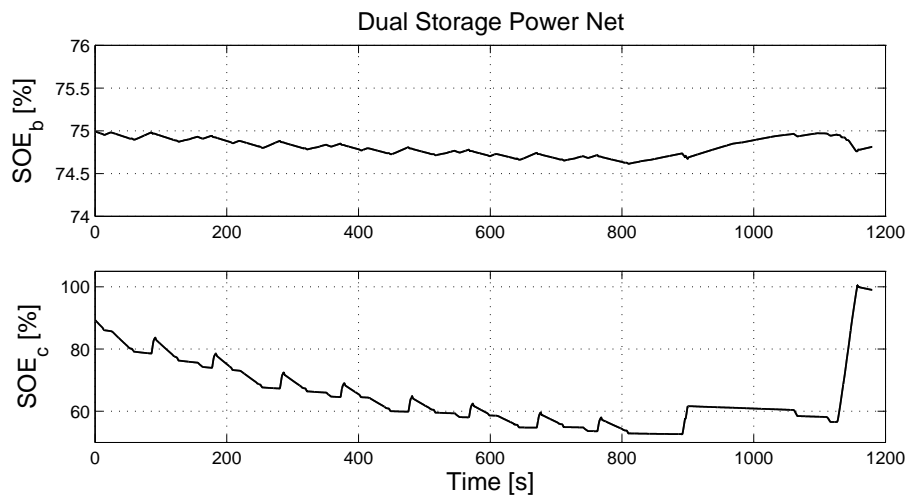


Figure 7.8: Dual storage results on the HIL: a) SOE_b b) SOE_c

7.4.4 Fuel consumption

A summary of the fuel consumption is shown in Table 7.1, together with the realized average electric load power and the difference in SOE . The fuel consumption is higher than in the previous chapters, because the drive train torque of the forward facing model is generally higher, as was shown in Section 7.4.1. No hard conclusions on the fuel reduction obtained on the HIL can be made, because the realized electric load differs for each experiment and the SOE estimation of the battery is not accurate. Furthermore, the most interesting component of the engine, the combustion engine, is still modeled by a static lookup table.

Table 7.1: Fuel Consumption

Strategy	P_{load} [W]	ΔSOE_b [%]	ΔSOE_c [%]	Fuel Use [g]
Baseline	496	0	0	633.98
DP1	508	0.46	0	632.82
DS	482	-0.18	9.6	630.08

7.5 Conclusion

A Hardware-in-the-Loop test setup is used to test whether the desired electric power set-points prescribed by an energy management strategy can be realized on an existing power net. The realized power trajectories show high frequent noise. It is not known in what extend this noise is caused by the power controller, the programmable supply, the programmable load, or the sensors.

The power controller of the alternator is working properly except for high peak powers during regenerative braking, where the power is limited by the voltage levels. The power controller of the DC-DC converter is working properly in one direction only.

The energy management strategies are power-based. The operating range of the ultracap and DC-DC converter is largely limited by the voltage levels. Although the voltage is related to the power, it would be better to design a strategy that can handle constraints on the voltage levels directly.

Some open issues are the following. The actual losses in the DC-DC converter have not been identified yet, as the measurements of in and outgoing voltage and current are too noisy and have an offset. Furthermore, a reliable SOE estimation of the battery and the ultracap is not yet available.

Discussion

Inspired by the research on energy management for hybrid electric vehicles, this thesis presents an extensive study on controlling the vehicular electric power system to reduce the fuel use and emissions, by generating and storing electrical energy only at the most suitable moments. For this purpose, both off-line optimization methods using knowledge of the driving pattern and online implementable ones are developed. The approach is extended to handle vehicles with a dual storage power net and parallel hybrid electric vehicles with an integrated starter generator.

This chapter will summarize the main conclusions, address some open issues and point directions for further research. A distinction is made between the methodology and this specific application.

8.1 Conclusions

8.1.1 Methodology

The energy management problem is formulated as an optimization problem, where a cost function is to be minimized subject to constraints, given a set of decision variables.

To solve the optimization problem, numerous solvers have been studied and several have been tested in simulations. Each optimization routine requires different model approximations and the most suitable optimization method differs for various problems.

Dynamic Programming is a suitable and often used method, as it is able to handle a non-convex cost function, and integer constraints. A disadvantage is the relatively large computation time, especially if there are multiple states.

By approximating the cost function as convex quadratic, and the constraints as linear, the problem can be casted as a Quadratic Programming problem, which requires much less computation time.

Using linear or piecewise linear component models, the energy management problem is easy and straightforward to model and solve as a Linear Programming problem. However, this is a very rough approximation and results in non-smooth trajectories, as the solution jumps from one constraint to the other.

If the optimization problem is carried out off-line for a known driving cycle, computation time is not a strong issue. This gives a lower bound on what can be achieved. For online

application of an energy management controller, computation time is limited and a prediction of the future driving cycle is usually not available, which requires modifications to the optimization problem. As computers are getting faster exponentially, computation time will not be the strongest limitation.

If a prediction of the future driving cycle is not available, an online strategy can be used that compares the current cost for generating electric power with the average incremental costs. Because the average incremental cost corresponds to the Lagrangian of the endpoint constraint of the global optimization, the results are close to the global optimum.

The average incremental costs are adapted using feedback of the state of energy, such that closed loop stability of the battery state of energy is obtained. The state of energy only contains information of the past. Thereby, it is assumed that on the long run, the average of the future will be more or less equal to the average of the past. This seems to be a reasonable assumption for this type of problem, as the driving behavior of a person is not likely to change drastically over hours or days.

8.1.2 Application

By controlling the alternator in a conventional vehicle, the engine torque can be influenced. The fuel characteristics of an internal combustion engine are usually visualized as an efficiency map, which varies roughly between 0 and 40%. Although this might give the impression that a large fuel reduction is possible by manipulating the engine torque, this is not the case, because the fuel use is more or less linear with the delivered power. This means that the additional, or incremental cost for generating electric energy does not vary very much for different operating points. Most of the profits that are obtained come from regenerative braking and engine shut-off, thereby eliminating the engine drag torque temporarily.

Simulations show a reduction in fuel use up till 2% on the NEDC cycle. Simultaneously, larger reductions of the exhaust emissions are obtained. With the online strategy doing without prediction of the future driving cycle, equally good results are obtained. The performance loss of the online strategy compared to the off-line optimization is less than 0.1% fuel consumption.

The developed method is extended to handle a vehicle with a dual storage power net and a hybrid electric vehicle with an integrated starter generator. The approach can be applied to other types of hybrid electric vehicles with slight changes in the formulation, but no change in the basic methodology.

The dual storage power net combines a battery and an ultracapacitor. For the studied configuration, only a small improvement in fuel and emission reduction is obtained, because of the limited capacity of the ultracap and the losses in the DC-DC converter. This power net topology may be worthwhile for hybrid vehicles using start-stop operation, or if tight limits on the battery voltage are present.

With a parallel hybrid electric vehicle using an integrated starter generator, fuel and emissions are reduced much more, mainly because of start-stop operation of the engine. By mounting the ISG after the clutch, the engine can be turned off more often, resulting in a tremendous fuel and emission reduction.

However, all results are obtained on simplified simulation models, so they still have to be validated on a real vehicle, where unmodeled dynamics and the influence on drivability may become important. This is especially the case for hybrid vehicles, where a frequent switching between the engine and ISG takes place.

The developed strategies for the conventional vehicle with single and dual storage power net are tested on a Hardware-in-the-Loop test setup using existing electric components and a more detailed simulation model for the drive train. It is shown, that power set-points provided by the energy management system can be realized reasonably accurate.

8.2 Future research

Some open issues and other suggestions for future research are the following.

An optimal energy management strategy for the conventional vehicle is implemented in real-time on a Hardware-in-the-Loop environment. However, the most interesting component in the vehicle, the internal combustion engine, is simulated using a simple static model. To validate the effectiveness of the strategy, implementation in a real vehicle on a test bench is necessary. These measurements have already been made and will be treated in [36], but the results are still unclear.

The fuel consumption and exhaust emissions of the internal combustion engine are modeled using static maps. Although the fuel consumption and CO₂ emission of a hot engine are modeled rather accurately by static maps, this may not hold for the other emissions, or if engine heating up is taken into consideration. Therefore, dynamic models are needed, or the fuel and emission characteristics should be identified online. A start has been made in [65], and will be treated further in [36].

The energy management strategies presented in this thesis use simple power-based models. These models and thus the developed strategies will not be sufficient if drive train topologies are used with freedom in both engine speed and torque, or if constraints on the current and voltage become dominant. A possible solution is to online adjust the bounds on the power based on the actual torque and speed or voltage and current.

So far, it is assumed that the drive train torque is defined exactly by the driver. By allowing small variations in torque that are imperceptible by the driver, an additional fuel reduction may be obtained.

The electric loads are modeled as predefined. Some loads, such as electric heating have a large time constant, so it is possible to vary their power demand without reducing driver comfort. Doing so, variations in alternator torque can be obtained without using the battery, thereby reducing (dis)-charging losses and battery wear. This is called power distribution management and is studied in [38].

Overview of Optimization Methods

A.1 Introduction

This chapter presents an overview and comparison of optimization methods that seem suitable for solving energy management problems with continuous, discrete, and/or complementary variables.

This chapter is built up as follows: The dynamic optimization problem is formulated in Section A.2. In Section A.3, it is rewritten as a static optimization problem. Linear programming is handled in Section A.4, while Section A.5 treats Quadratic Programming. Some methods for mixed integer programming are discussed in Section A.6. Section A.7 handles optimizations problems with complementarity constraints. Dynamic Programming is discussed in Section A.8. The methods are evaluated in Section A.9.

A.2 Dynamic optimization

The energy management problem can be formulated as a continuous time dynamic optimization problem, where the vehicle is represented by a dynamic system:

$$\dot{x}(t) = f(x(t), u(t), t) \quad (\text{A.1})$$

which has to be controlled, such that the cost criterion:

$$\int_0^{t_n} \gamma(x(t), u(t), t) dt \quad (\text{A.2})$$

is minimized, satisfying the constraints:

$$\phi(x(t), u(t), t) \leq 0 \quad \psi(x(t), u(t), t) = 0 \quad (\text{A.3})$$

where $x(t)$ are the state variables and $u(t)$ are the control variables. The control variables can be continuous, discrete, or complementary, meaning that only one of a set of variables can be nonzero at a time.

In discrete time, the system can be described as:

$$x(k+1) = f(x(k), u(k), k) \quad (\text{A.4})$$

The cost criterion then becomes:

$$\sum_0^n \gamma(x(k), u(k), k) \Delta t \quad (\text{A.5})$$

and the constraints become:

$$\phi(x(k), u(k), k) \leq 0 \quad \psi(x(k), u(k), k) = 0 \quad (\text{A.6})$$

A.3 Static optimization

For a given time span, the discrete time dynamic optimization problem can be formulated as a static optimization problem, of which a general formulation is the following:

$$\min_z J(z) \quad \text{subject to} \quad G(z) \leq 0 \quad G_{eq}(z) = 0 \quad z \in \mathbb{R}^n \quad (\text{A.7})$$

where $J(z)$ is the cost function to be minimized, $G(z)$ are the inequality constraints, $G_{eq}(z)$ are the equality constraints, and z are the decision variables. The decision variables include the control variables u , the state variables x and possible other slack variables s :

$$z = [u(0) \cdots u(n) \quad x(0) \cdots x(n) \quad s(0) \cdots s(n)]^T \quad (\text{A.8})$$

The cost criterion becomes:

$$J(z) = \sum_0^n \gamma(x(k), u(k), k) \Delta t \quad (\text{A.9})$$

The equality constraints $G(z)$ become:

$$G(z) = \begin{bmatrix} \phi(x(0), u(0), 0) \\ \vdots \\ \phi(x(n), u(n), n) \end{bmatrix} \leq 0 \quad (\text{A.10})$$

The equality constraints $G_{eq}(z)$ also include the system dynamics (A.4) :

$$G_{eq}(z) = \begin{bmatrix} \psi(x(0), u(0), 0) \\ \vdots \\ \psi(x(n), u(n), n) \\ x(1) - f(x(0), u(0), 0) \\ \vdots \\ x(n) - f(x(n-1), u(n-1), n-1) \end{bmatrix} = 0 \quad (\text{A.11})$$

In general, $J(z)$ and $G(z)$ are nonlinear functions, making this a Nonlinear Programming Problem (NLP). If $J(z)$ and $G(z)$ are convex, the global optimum can be found in limited

time. If they are non-convex, most algorithms will only find a local optimum. If no set of decision variables exists that satisfies all constraints, the problem is infeasible.

In the remainder of this chapter, x will be used to denote the decision variables, whereas y and z will be used as additional variables.

A.4 Linear Programming

A Linear Programming problem (LP) [52] is given by a linear cost function subject to linear constraints:

$$\min_x J(x) = f^T x \quad \text{subject to} \quad Ax \leq b \quad (\text{A.12})$$

The solution of an unconstrained LP is unbounded. The solution of a constrained LP is solved numerically, for which many fast algorithms and software implementations are available.

A.4.1 Piecewise linearities

A convex nonlinear function can be approximated as a piecewise linear function, which consists of linear approximations in various points. This piecewise linear function can be used within an LP framework by adding secondary variables z together with linear inequality constraints [52].

A piecewise linear function of the form:

$$z = \max_i (a_i x + b_i) \quad i = 1, \dots, m \quad (\text{A.13})$$

can be incorporated in an LP as follows:

$$\min_z z \quad \text{subject to} \quad z \geq a_i x + b_i \quad i = 1, \dots, m \quad (\text{A.14})$$

Because z is minimized, it will always hit one of the m constraints. If the original cost function is already monotonically increasing in z , including z in the function explicitly is not necessary.

A.5 Quadratic Programming

A Quadratic Programming problem (QP) [23] is given by a quadratic cost function subject to linear constraints:

$$\min_x J(x) = \frac{1}{2} x^T H x + f^T x \quad \text{subject to} \quad Ax \leq b \quad (\text{A.15})$$

If H is positive definite, the problem is convex, so it has one unique optimum.

A.5.1 Unconstrained QP

An unconstrained convex QP can be solved analytically as follows:

$$\frac{\partial J(x)}{\partial x} = x^T H + f^T = 0 \quad (\text{A.16})$$

so:

$$x = -H^{-1} f \quad (\text{A.17})$$

A.5.2 QP with equality constraints

A QP with only equality constraints can also be solved analytically.

Consider the following optimization problem:

$$\min_x J(x) = \frac{1}{2} x^T H x + f^T x \quad \text{subject to} \quad A_{eq} x = b_{eq} \quad (\text{A.18})$$

The equality constraints can be included in the function by introducing the Lagrange function:

$$L(x, \lambda) = \frac{1}{2} x^T H x + f^T x + \lambda^T (A_{eq} x - b_{eq}) \quad (\text{A.19})$$

where λ is a vector with the Lagrange multipliers.

The optimal solution is given by:

$$\frac{\partial L(x, \lambda)}{\partial x} = x^T H + f^T + \lambda^T A_{eq} = 0 \quad (\text{A.20})$$

and:

$$\frac{\partial L(x, \lambda)}{\partial \lambda} = A_{eq} x - b_{eq} = 0 \quad (\text{A.21})$$

so:

$$x = -H^{-1} (f + A_{eq}^T \lambda) \quad (\text{A.22})$$

Demanding that:

$$A_{eq} x = b_{eq} \quad (\text{A.23})$$

yields:

$$-A_{eq} H^{-1} f - A_{eq} H^{-1} A_{eq}^T \lambda = b_{eq} \quad (\text{A.24})$$

which results in:

$$\lambda = -(A_{eq} H^{-1} A_{eq}^T)^{-1} (A_{eq} H^{-1} f + b_{eq}) \quad (\text{A.25})$$

A.5.3 The Quadratic Knapsack Problem

Suppose the Hessian is diagonal, with $H(i, i) = h_i$, and the equality constraint applies on the sum of the decision variables. Then the problem reduces to:

$$\min_x J(x) = \sum_{i=1}^n \frac{1}{2} h_i x_i^2 + f_i x_i \quad \text{subject to} \quad \sum_{i=1}^n x_i = c \quad (\text{A.26})$$

This is called the continuous quadratic knapsack problem.

The Lagrange function becomes:

$$L(x, \lambda) = \sum_{i=1}^n \left(\frac{1}{2} h_i x_i^2 + f_i x_i + \lambda x_i \right) + \lambda c \quad (\text{A.27})$$

The optimal solution is given by:

$$\frac{\partial L(x, \lambda)}{\partial x_i} = h_i x_i + f_i - \lambda = 0 \quad (\text{A.28})$$

and:

$$\frac{\partial L(x, \lambda)}{\partial \lambda} = \sum_{i=1}^n x_i - c = 0 \quad (\text{A.29})$$

This results in:

$$x_i = -\frac{f_i + \lambda}{h_i} \quad (\text{A.30})$$

Demanding that:

$$\sum_{i=1}^n x_i = c \quad (\text{A.31})$$

yields:

$$\sum_{i=1}^n \frac{f_i + \lambda}{h_i} = c \quad (\text{A.32})$$

which results in:

$$\lambda = -\left(c + \sum_{i=1}^n \frac{f_i}{h_i} \right) / \sum_{i=1}^n \frac{1}{h_i} \quad (\text{A.33})$$

When upper and lower bounds on x are present, the problem can still be solved efficiently with a routine described in [69]. If other constraints are added, a general QP solver must be used.

A.6 Mixed Integer Programming

If some of the decision variables are required to take integer values, the optimization problem becomes a Mixed Integer Programming problem (MIP):

$$\min_{x,y} J(x,y) \quad \text{subject to} \quad G(x,y) \leq 0 \quad \text{and} \quad y \in N \quad (\text{A.34})$$

Good overviews of MIP algorithms are presented in [25, 27]. The most important algorithms for mixed integer optimization are Enumeration, Branch and Bound, Outer Approximation, and Generalized Benders Decomposition.

All routines have the disadvantage that the computation time increases exponentially with the number of discrete variables, because mixed integer problems are NP-hard [25].

A.6.1 Enumeration

Enumeration is a brute force method, where for all possible combinations of integer values, the corresponding continuous subproblem is solved. The one with the lowest objective function is a global optimum. Note that even if the continuous relaxation of the problem is strictly convex, the MIP can have multiple optimums with the same cost function value.

A.6.2 Branch and Bound

In Branch and Bound (BB) [27], a tree search is performed in the space of the integer variables. At each node of the tree some integer variables are fixed to a certain integer value, whereas the remaining integer variables are relaxed to continuous variables. The resulting continuous problem is solved, which yields a lower bound for the subproblems of the specific node.

A node is fathomed when the lower bound exceeds the current upper bound to the original problem, when the subproblem is infeasible, or when all integer variables take on discrete values. The latter yields an upper bound to the original problem.

BB is the most commonly used method for MILP, and can also be used for Mixed Integer NLP problems. The number of required continuous optimizations is always less or equal to the enumeration method. It is usually much less, but that depends heavily on the specific problem, the initial condition, and the search order of the tree search.

A.6.3 Outer Approximation

The Outer Approximation method (OA) [27] is a dedicated method for MINLP's.

NLP subproblems and MILP master problems are solved successively in a cycle of iterations. For the NLP, all integer variables are fixed, so this provides an upper bound for the optimum. The MILP is the linear outer approximation of the original MINLP, so it

provides a lower bound. The cycle of iterations is continued until this upper bound and the lower bound are within a specified tolerance.

The NLP subproblem is defined as:

$$x^k = \arg \min_x J(x, y^k) \quad \text{subject to} \quad G(x, y^k) \leq 0 \quad (\text{A.35})$$

The MILP master problem is defined as:

$$\{\tilde{x}^{k+1}, y^{k+1}, \alpha^{k+1}\} = \arg \min_{x, y, \alpha} \alpha \quad (\text{A.36})$$

subject to:

$$\begin{aligned} \alpha &\geq J(x^i, y^i) + \nabla J(x^i, y^i) \begin{bmatrix} x - x^i \\ y - y^i \end{bmatrix} \\ G(x^i, y^i) + \nabla G(x^i, y^i) \begin{bmatrix} x - x^i \\ y - y^i \end{bmatrix} &\leq 0 \\ \text{for} \quad i &= 1, \dots, k \end{aligned} \quad (\text{A.37})$$

The MILP master problem is usually solved using Branch and Bound.

The OA method generally requires relatively few cycles or major iterations. It is advantageous compared to BB when the NLP takes much computation time, because less iterations are needed.

A.6.4 Generalized Benders Decomposition

The Generalized Benders Decomposition method (GBD) [27] is similar to the Outer-Approximation method. The difference arises in the definition of the MILP master problem, because only inequality constraints that are active in the NLP subproblem are considered. They are regarded as equality constraints and substituted in the cost function using the Lagrange multipliers resulting from the NLP. Furthermore, the continuous variables x are fixed in the MILP. The NLP is the same as in the OA method.

The MILP master problem becomes:

$$\{\tilde{x}^{k+1}, y^{k+1}, \alpha^{k+1}\} = \arg \min_{y, \alpha} \alpha \quad (\text{A.38})$$

subject to:

$$\begin{aligned} \alpha &\geq J(x^i, y^i) + \nabla_y J(x^i, y^i) (y - y^i) + \\ &\quad (\mu^i)^T (G(x^i, y^i) + \nabla_y G(x^i, y^i) (y - y^i)) \\ \text{for} \quad i &= 1, \dots, k \end{aligned} \quad (\text{A.39})$$

where μ is a vector with the Lagrange multipliers of the constraints resulting from the NLP.

The MILP master problem has less constraints than when using the OA method, but usually more iterations are needed, because convergence is slower.

In [16], Branch and Bound, Outer Approximation and Generalized Benders Decomposition are applied to solve a MINLP representing the dual storage power net described in Chapter 5. It turned out that Branch and Bound outscored the other two methods in computation time.

A.6.5 Convert to nonlinear constraint

A variable y can be forced to take an integer value using the following nonlinear constraint:

$$\sin(\pi y) = 0 \tag{A.40}$$

This is a nonlinear non-convex constraint, so it depends on the solver whether the global optimum is found.

A variable y can be forced to take a binary value by introducing a variable z and using the following complementarity constraint:

$$yz = 0 \quad \text{and} \quad y + z = 1 \tag{A.41}$$

or, without an additional variable:

$$y(y - 1) = 0 \tag{A.42}$$

This way, dedicated solvers for problems with complementarity constraints can be used, as discussed in Section A.7.

A.6.6 Heuristic methods

Because the computation time increases exponentially with the number of discrete variables, in practice heuristic methods are often used, leading to a suboptimal solution. There are also heuristics that lead faster to the global optimum.

One possibility to obtain a suboptimal mixed integer solution is the following. First the problem is solved, with all integer variables y relaxed to continuous ones. This provides a lower bound to the mixed integer optimum. The resulting values of y are rounded off to integer values. The continuous optimization is repeated, with the variables y fixed at these integer values, to ensure that all constraints are satisfied, if possible. This provides an upper bound to the mixed integer optimum. By comparing this upper bound with the lower bound, it can be decided whether this solution is sufficient.

A.7 Complementarity Constraints

This section focusses on optimization problems with complementarity constraints on some of the decision variables:

$$\min_x f(x) \quad \text{subject to} \quad 0 \leq x_1 \perp x_2 \leq 0 \quad (\text{A.43})$$

where other constraints may also apply.

Operator \perp means that for each element i holds that either $x_1(i) = 0$ and/or $x_2(i) = 0$.

Complementarity constraints are a form of equilibrium constraints.

Several methods to handle complementarity constraints are presented.

A.7.1 Convert to Mixed Integer Programming problem

Complementarity constraints can be incorporated by introducing binary variables and adding linear constraints. The optimization problem becomes a Mixed Integer Programming problem, as discussed in Section A.6.

Suppose x is a vector with n elements and $0 \leq x \leq x_{max}$.

If only m elements of x may be nonzero, this can be accomplished by adding n binary variables β with the following linear constraints:

$$x \leq \beta x_{max} \quad \text{and} \quad \sum_{i=1}^n \beta_i \leq m \quad (\text{A.44})$$

Such a constraint is called a Special Ordered Set (SOS). The complementarity constraint can be regarded as a special case of a SOS.

Suppose x_1 and x_2 are subsets of x , each with length p , and with corresponding upper bounds x_{1max} and x_{2max} , where:

$$x_1^T x_2 = 0 \quad (\text{A.45})$$

This can be accomplished by introducing two vectors β_1 and β_2 each consisting of p binary variables, and adding the following constraints:

$$\begin{aligned} x_1(i) &\leq \beta_1(i) x_{1max}(i) \\ x_2(i) &\leq \beta_2(i) x_{2max}(i) \quad \text{for} \quad i = 1, \dots, p \\ \beta_1(i) + \beta_2(i) &\leq 1 \end{aligned} \quad (\text{A.46})$$

This can also be accomplished more efficiently, by adding only one vector β consisting of p binary variables, and the following constraints:

$$\begin{aligned} x_1(i) &\leq \beta(i) x_{1max}(i) \quad \text{for} \quad i = 1, \dots, p \\ x_2(i) &\leq (1 - \beta(i)) x_{2max}(i) \end{aligned} \quad (\text{A.47})$$

Note that $\beta(i) = 0$ yields $x_1(i) = 0$ and $\beta(i) = 1$ yields $x_2(i) = 0$

If x_1 and x_2 can be negative, the lower bounds $x_{1,min}$ and $x_{2,min}$ have to be incorporated:

$$\beta x_{1,min} \leq x_1 \leq \beta x_{1,max} \quad \text{and} \quad (1 - \beta) x_{2,min} \leq x_2 \leq (1 - \beta) x_{2,max} \quad (\text{A.48})$$

A.7.2 Substitute complementarity constraint in cost function

The complementarity constraint can be substituted in the cost function as a penalty.

The optimization problem:

$$\min_x J(x) \quad \text{subject to} \quad x_1^T x_2 = 0 \quad x_1 \geq 0 \quad x_2 \geq 0 \quad (\text{A.49})$$

then becomes:

$$\min_x J(x) + k x_1^T x_2 \quad (\text{A.50})$$

If the penalty factor $k \in R^+$ is chosen sufficiently high, the constraint will be satisfied with sufficient accuracy. However, the term $k x_1^T x_2$ is not convex and for a high value of k , this will result in a non-convex function.

If x_1 and x_2 are given by:

$$x_1 = A_1 x \quad \text{and} \quad x_2 = A_2 x \quad (\text{A.51})$$

then

$$x_1^T x_2 = x^T A_1^T A_2 x \quad (\text{A.52})$$

Define Q as:

$$Q = A_1^T A_2 \quad (\text{A.53})$$

and its symmetric equivalent \tilde{Q} as:

$$\tilde{Q} = \frac{1}{2}(Q^T + Q) \quad (\text{A.54})$$

Note that for every square matrix Q , the matrix \tilde{Q} is symmetric and the following holds for all x :

$$x^T Q x = x^T \tilde{Q} x \quad (\text{A.55})$$

This is a quadratic term, but \tilde{Q} usually has both positive and negative eigenvalues, so if it is added to an LP or QP, the problem becomes a non-convex QP. Most QP solvers that can handle non-convex QP's only find a local optimum.

A.7.3 Nonlinear Programming

Complementarity constraints can be incorporated in an NLP by adding a nonlinear inequality constraint as follows:

$$\min_x J(x) \quad \text{subject to} \quad x_1^T x_2 \leq 0 \quad x_1 \geq 0 \quad x_2 \geq 0 \quad (\text{A.56})$$

This is a set of nonlinear generally non-convex constraints, so it depends on the solver whether it can be solved. Both [24] and [49] report good results for specific problems using a Sequential Quadratic Programming (SQP) solver. Some modifications of the SQP solver may be needed.

A.8 Dynamic Programming

Dynamic Programming (DP), [8, 10] is a method to solve a discrete time dynamic optimization problem, *i.e.*, to find the optimal sequence of control variables:

$$[u(0), \dots, u(n-1)] \quad (\text{A.57})$$

that brings a system given by:

$$x(k+1) = f(x(k), u(k), k) \quad (\text{A.58})$$

from state $x(0) = x_0$ to $x(n) = x_n$, while minimizing the cost function:

$$J = \sum_{k=0}^n \gamma(x(k), u(k), k) \quad (\text{A.59})$$

To do so, the operating space (X, U) is discretized, making a grid, and all possible trajectories on this grid are evaluated. The number of computations is reduced by using Bellman's Principle of Optimality ([9] p. 15), which states that:

An optimal policy has the property that whatever the initial state and initial decisions are, the remaining decisions must constitute an optimal policy with regard to the state resulting from the first decision.

In other words: From any point on an optimal trajectory, the remaining trajectory is optimal for the corresponding problem initiated at that point.

Bounds on u and x are handled by the limited grid size. Other constraints can be incorporated by adding a large penalty to the cost if a constraint is violated.

Because the cost function is evaluated numerically, it makes no difference whether it is convex or not. Furthermore, integer variables take less computation time than continuous variables, that are usually discretized on a more dense grid. Nevertheless, the computation time increases rapidly with the number of states, inputs, and time steps, and their grid densities.

A.9 Evaluation

In this section, the optimization methods previously discussed are compared, with respect to their suitability for solving energy management problems.

The energy management problem is a dynamic optimization problem, for which Dynamic Programming seems the most suitable method. An advantage is that the cost function can be nonlinear and non-convex. A disadvantage is the large computation time, especially if there are multiple states.

The dynamic optimization problem can be rewritten as a static optimization problem. If the problem can be approximated accurately as a convex optimization problem, it can be solved using a convex NLP solver, or it can be further approximated to a QP or LP. LP's are faster to solve than QP's, but approximating a problem as an LP generally requires more constraints and additional variables, which increases computation time.

A mixed integer problem can be written as a continuous optimization problem with complementarity constraints and vice versa. Because both types of problems are NP-hard, they are both hard to solve. The computation time can be reduced by using a heuristic method, leading to a suboptimal solution.

Stability Analysis

B.1 Introduction

This chapter presents a stability analysis of two storage control strategies derived from global optimization as presented and implemented in Chapter 3. The method is also applicable to other systems with a storage unit.

This chapter considers the optimal storage control problem of systems consisting of one or more energy convertors and a storage device. The energy convertors are characterized by losses that depend on their time varying operating point. The problem is to control the energy storage such that usage of the primary energy source is minimal.

In Chapter 3, this idea is applied to the electric power supply in a conventional passenger vehicle, such that the fuel consumption is reduced. The storage control problem was formulated as an optimization problem and two practically implementable strategies were derived from it. The first strategy puts the optimization in a Model Predictive Control (MPC) framework using a limited prediction horizon. Secondly, a feedback strategy is derived doing without future knowledge. Their effectiveness was shown by simulations.

This chapter provides a more general description of this idea and analyzes the stability of these strategies.

This chapter is built up as follows: Section B.2 formulates the storage control problem as a quadratic knapsack problem. The Model Predictive Control strategy is presented in Section B.3. In Section B.4 the endpoint constraint, and thus the required prediction horizon, is replaced by state feedback. Conclusions are given in Section B.5.

B.2 Storage Control Problem

The storage control problem consists in controlling the storage power u , such that a cost Γ is minimized, subject to the demand that the stored energy x at the beginning and the end are equal. Using discrete time, this can be written as a dynamic optimization problem:

$$\min_u \Gamma(u) = \sum_{k=1}^N \gamma(u, k) \Delta t \quad (\text{B.1})$$

The state x is the discrete time integrated input u :

$$x(k+1) = x(k) + u(k) \Delta t \quad x(0) = x_0 \quad (\text{B.2})$$

or equivalently:

$$x(k) = x_0 + \sum_{j=1}^k u(j) \Delta t \quad (\text{B.3})$$

The endpoint constraint becomes:

$$x(n) = x(0) \quad \Rightarrow \quad \sum_{k=1}^N u(k) = 0 \quad (\text{B.4})$$

The cost rate γ is approximated by a quadratic function of u with time-varying coefficients:

$$\gamma(k) = \frac{1}{2} \varphi_2(k) u(k)^2 + \varphi_1(k) u(k) + \varphi_0(k) \quad (\text{B.5})$$

The term φ_0 can be omitted, because it does not influence the optimal solution for u . The optimization problem becomes a continuous quadratic knapsack problem:

$$\min_u \sum_{k=1}^N \frac{1}{2} \varphi_2(k) u(k)^2 + \varphi_1(k) u(k) \quad (\text{B.6})$$

$$\text{subject to} \quad \sum_{k=1}^N u(k) = 0 \quad (\text{B.7})$$

If no inequality constraints are present, this can be solved analytically by introducing the Lagrange function:

$$L(u, \lambda) = \sum_{k=1}^N \frac{1}{2} \varphi_2(k) u(k)^2 + \varphi_1(k) u(k) - \lambda u(k) \quad (\text{B.8})$$

where λ is the Lagrange multiplier. The optimal solution is given by:

$$\frac{\delta L(u(k), \lambda)}{\delta u(k)} = \varphi_2(k) u(k) + \varphi_1(k) - \lambda = 0 \quad (\text{B.9})$$

$$\frac{\delta L(u(k), \lambda)}{\delta \lambda} = \sum_{k=1}^n u(k) = 0 \quad (\text{B.10})$$

This results in:

$$u(k) = \frac{\lambda - \varphi_1(k)}{\varphi_2(k)} \quad (\text{B.11})$$

where:

$$\lambda = \sum_{k=1}^N \frac{\varphi_1(k)}{\varphi_2(k)} / \sum_{k=1}^N \frac{1}{\varphi_2(k)} \quad (\text{B.12})$$

The incremental costs are given by:

$$\frac{\partial \gamma(u(k))}{\partial u(k)} = \varphi_2(k) u(k) + \varphi_1(k) \quad (\text{B.13})$$

By substituting (B.11), it follows that the optimal solution is characterized by equal incremental cost at each time step, namely λ .

Note that, for given λ , computing $u(k)$ using (B.11) is equivalent to solving at each time instant k :

$$\min_{u(k)} \gamma(u, k) - \lambda u(k) \quad (\text{B.14})$$

B.3 Model Predictive Control

If only a limited prediction horizon is available, the optimization problem can be solved within a Model Predictive Control framework, using a receding horizon. At each time step k the optimization is carried out over the horizon $[k, \dots, k + N_p]$:

$$\min_u J(u, k) = \sum_{j=k}^{k+N_p} \gamma(j) \quad (\text{B.15})$$

The endpoint constraint incorporates feedback of the actual state $x(k)$:

$$x(k+n) = x_0 \quad \Rightarrow \quad \sum_{j=k}^{N_p+1} u(j) = \frac{x_0 - x(k)}{\Delta t} \quad (\text{B.16})$$

This results in an optimal sequence $[u(k), \dots, u(k + N_p)]$.

The input $u(k)$ is applied to the system, and then a new optimization is run using a shifted prediction horizon and updated state information.

The optimization can again be solved analytically using the Lagrange function, resulting in:

$$u(k) = \frac{\lambda(k) - \varphi_1(k)}{\varphi_2(k)} \quad (\text{B.17})$$

where:

$$\lambda(k) = \left(\frac{x_0 - x(k)}{\Delta t} + \sum_{j=k}^{k+N_p} \frac{\varphi_1(j)}{\varphi_2(j)} \right) / \sum_{j=k}^{k+N_p} \frac{1}{\varphi_2(j)} \quad (\text{B.18})$$

Although for the computation of $u(k)$ only current values $\varphi_1(k)$ and $\varphi_2(k)$ are needed, computation of the value of $\lambda(k)$ requires knowledge of φ_1 and φ_2 over the entire prediction horizon.

The expression for $u(k)$ can be separated in a time-varying feed forward and a linear time-varying state feedback:

$$u(k) = f(k) + g(k) x(k) \quad (\text{B.19})$$

where:

$$f(k) = -\frac{1}{\varphi_2(k)} \left\{ \varphi_1(k) - \left(\frac{x_0}{\Delta t} + \sum_{j=k}^{k+N_p} \frac{\varphi_1(j)}{\varphi_2(j)} \right) / \sum_{j=k}^{k+N_p} \frac{1}{\varphi_2(j)} \right\} \quad (\text{B.20})$$

and:

$$g(k) = -1 / \left(\Delta t \varphi_2(k) \sum_{j=0}^{N_p} \frac{1}{\varphi_2(k+j)} \right) \quad (\text{B.21})$$

The closed loop becomes a first order linear time-varying system:

$$x(k+1) = (1 + g(k) \Delta t) x(k) + f(k) \Delta t \quad (\text{B.22})$$

which has a pole at:

$$p = 1 + g(k) \Delta t = 1 - 1 / \left(\varphi_2(k) \sum_{j=k}^{k+N_p} \frac{1}{\varphi_2(j)} \right) \quad (\text{B.23})$$

For $\varphi_2 > 0$, the pole remains in the range $0 < p < 1$, which is a sufficient, although not necessary, condition for asymptotic stability.

B.4 MPC without Endpoint Constraint

When the available prediction horizon is very short, the variation in u will be small, and thus the performance will deteriorate from the global optimal solution. The hard endpoint constraint can be replaced by a soft one, by taking a different choice for the value of λ . It can be a guess of the optimal λ over a longer horizon. λ is constant over the horizon, but can be updated after each time step, *e.g.*, as function of the state. By using an estimated λ , only present values $\varphi_1(k)$ and $\varphi_2(k)$ need to be known.

The optimization problem becomes:

$$\min_u \sum_{j=k}^{k+N_p} \gamma(j) - \lambda(k) u(j) \quad (\text{B.24})$$

If no constraints are present, the solution does not depend on the horizon length, so a horizon of $N_p = 0$ is sufficient. The optimization problem then becomes:

$$\min_{u(k)} \gamma(k) - \lambda(k) u(k) \quad (\text{B.25})$$

This can be solved analytically, resulting in:

$$u(k) = \frac{\lambda(k) - \varphi_1(k)}{\varphi_2(k)} \quad (\text{B.26})$$

B.4.1 P-controller

To prevent drift of the state x , λ can be adapted using state feedback, *e.g.*, with a P-controller:

$$\lambda(k) = \lambda_0 + K_p (x_0 - x(k)) \quad (\text{B.27})$$

The state x is the discrete time integrated input u :

$$x(k+1) = x(k) + u(k) \Delta t \quad x(0) = x_0 \quad (\text{B.28})$$

The closed loop becomes a first order linear time-varying system:

$$x(k+1) = p(k) x(k) + v(k)$$

where:

$$p(k) = 1 - \frac{K_p \Delta t}{\varphi_2(k)} \quad v(k) = \frac{\lambda_0 + K_p x_0 - \varphi_1(k)}{\varphi_2(k)} \Delta t \quad (\text{B.29})$$

For $\varphi_2 > 0$ and $0 < K_p < \frac{2\varphi_2}{\Delta t}$, the eigenvalue p remains in the range $-1 < p < 1$, which is a sufficient, although not necessary, condition for asymptotic stability.

The eigenvalue can be kept at a constant desired value \tilde{p} , by making the gain K_p time-varying:

$$K_p(k) = -\frac{\varphi_2(k) (1 - \tilde{p})}{\Delta t} \quad (\text{B.30})$$

B.4.2 PI-controller

An integrating action can be added:

$$\lambda(k+1) = \lambda_0 + K_p (x_0 - x(k)) + K_i (y_0 - y(k)) \quad (\text{B.31})$$

where the additional state y is the discrete time integrated state x :

$$y(k+1) = y(k) + x(k) \Delta t \quad y(0) = y_0 \quad (\text{B.32})$$

The closed loop becomes a second order linear time-varying system:

$$\begin{bmatrix} x(k+1) \\ y(k+1) \end{bmatrix} = \begin{bmatrix} q(k) & r(k) \\ \Delta t & 1 \end{bmatrix} \begin{bmatrix} x(k) \\ y(k) \end{bmatrix} + \begin{bmatrix} w(k) \\ 0 \end{bmatrix} \quad (\text{B.33})$$

where:

$$q(k) = 1 - \frac{K_p \Delta t}{\varphi_2(k)} \quad r(k) = -\frac{K_i \Delta t}{\varphi_2(k)} \quad (\text{B.34})$$

and:

$$w(k) = \frac{\lambda_0 + K_p x_0 + K_i y_0 - \varphi_1(k)}{\varphi_2(k)} \Delta t \quad (\text{B.35})$$

The eigenvalues are given by:

$$e = \frac{1}{2} + \frac{1}{2} q \pm \sqrt{q^2 - 2q + 1 + 4 \Delta t r} \quad (\text{B.36})$$

For this system it is more difficult to prove stability.

Demanding that both poles have a desired constant value \tilde{e} , requires:

$$q^2 - 2q + 1 + 4 \Delta t r = 0 \quad \Rightarrow \quad r = \frac{(q-1)^2}{4 \Delta t} \quad (\text{B.37})$$

and:

$$q = 2 \tilde{e} - 1 \quad (\text{B.38})$$

so:

$$K_p(k) = -\frac{\varphi_2(k)(1-q)}{\Delta t} \quad K_i(k) = -\frac{\varphi_2(k)r}{\Delta t} \quad (\text{B.39})$$

B.5 Conclusions

The conventional MPC controller and the MPC-based controller with proportional feedback both result in discrete linear time varying first order closed loop system, for which stability is proven.

When using PI feedback, the closed a loop becomes a discrete second order linear time varying system, for which stability is not yet proven.

Bibliography

- [1] Z. M. Al-Hamouz and A. S. Al-Faraj. Transmission expansion planning using non-linear programming. In *Proc. of the IEEE/PES Transmission and Distribution Conf.*, volume 1, pages 50–55, Asia Pacific, October 6-10 2002.
- [2] N. Alguacil, A. L. Motto, and A. J. Conejo. Transmission expansion planning: A mixed-integer lp approach. *IEEE Trans. On Power Systems*, 18(3):1070–1077, August 2003.
- [3] I. Arsie, M. Graziosi, C. Pianese, G. Rizzo, and M. Sorrentino. Optimization of supervisory control strategy for parallel hybrid vehicle with provisional load estimate. In *Proc. of the 7th Int. Symp. on Advanced Vehicle Control (AVEC)*, Arnhem, The Netherlands, August 2004.
- [4] M. Back, M. Simons, F. Kirschaum, and V. Krebs. Predictive control of drivetrains. In *Proc. of the IFAC 15th Triennial World Congress*, Barcelona, Spain, 2002.
- [5] A. C. Baisden and A. Emadi. ADVISOR-based model of a battery and an ultra-capacitor energy source for hybrid electric vehicles. *IEEE Trans. on Vehicular Techn.*, 53(1):199–205, January 2004.
- [6] M. Balenovic. *Modeling and Model-Based Control of a Three-Way Catalytic Converter*. PhD thesis, Department of Electrical Engineering, Technische Universiteit Eindhoven, The Netherlands, 2002.
- [7] B. M. Baumann, G. Washington, B. C. Glenn, and G. Rizzoni. Mechatronic design and control of hybrid electric vehicles. *IEEE/ASME Trans. on Mechatronics*, 5(1):58–72, March 2000.
- [8] R. E. Bellman. *Dynamic Programming*. Princeton University Press, 1957.
- [9] R. E. Bellman and S. E. Dreyfus. *Applied Dynamic Programming*. Princeton University Press, 1962.
- [10] D. P. Bertsekas. *Dynamic Programming and Optimal Control*. Athena Scientific, Belmont, MA, 1995.
- [11] B. Bonsen, T. W. G. L. Klaassen, R. J. Pulles, S. W. H. Simons, and P. A. Veenhuizen M. Steinbuch. Performance optimization of the push-belt cvt by variator slip control. *International Journal of Vehicle Design*, 3(39):232–256, 2005.
- [12] C. C. Chan and K. T. Chau. *Modern Electric Vehicle Technology*. Oxford University Press, New York, 2001.

- [13] J.-S. Chen and M. Salman. Learning energy management strategy for hybrid electric vehicles. In *Proc. of the IEEE Vehicle Power and Propulsion Conference*, Chicago, IL, September 2005.
- [14] T. H. Cormen, C. E. Leiserson, R. L. Rivest, and C. Stein. *Introduction to Algorithms*. MIT Press and McGraw-Hill, 2nd edition, 2001.
- [15] B. de Jager. Predictive storage control for a class of power conversion systems. In *Proc. of the European Control Conf.*, Cambridge, UK, September 2003.
- [16] J. de Wit. Evaluation of mixed integer nonlinear programming routines. Technical report, Technische Universiteit Eindhoven, The Netherlands, 2005. Internal Traineeship report DCT 2005.42.
- [17] S. Delprat, J. Lauber, T. M. Guerra, and J. Rimaux. Control of a parallel hybrid powertrain: Optimal control. *IEEE Trans. on Vehicular Technology*, 53(3):872–881, May 2004.
- [18] M. Desbois-Renaudin, R. Trigui, and J. Scordia. Hybrid powertrain sizing and potential consumption gains. In *Proc. of the IEEE VTS Symposium on Vehicular Power And Propulsion*, Paris, France, October 2004.
- [19] K. Ehlers, H. D. Hartmann, and E. Meissner. 42V - An indication for changing requirements on the vehicle electrical system. *J. of Power Sources*, 95:43–57, 2001.
- [20] M. Ehsani, Y. Gao, S. E. Gay, and A. Emadi. *Modern Electric, Hybrid Electric, and Fuel Cell Vehicles : Fundamentals, Theory, and Design*. CRC Press, London, 2004.
- [21] A. Emadi, M. Ehsani, and J. M. Miller. *Vehicular Electric Power Systems: Land, Sea, Air, and Space Vehicles*. Marcel Dekker, New York, 2003.
- [22] European Council. New european driving cycle, 1970. Council Directive 70/220/EEC with amendments.
- [23] R. Fletcher. *Practical Methods of Optimization*. John Wiley & Sons, New York, 2nd edition, 2000.
- [24] R. Fletcher, S. Leyffer, D. Ralph, and S. Scholtes. Local convergence of SQP methods for mathematical programs with equilibrium constraints. Technical report, Dept. of Mathematics, University of Dundee, UK, 2002. Numerical Analysis Report NA/209 (available online at www.optimization-online.org/DB_HTML/2002/05/476.html).
- [25] C. A. Floudas. *Nonlinear and Mixed-Integer Optimization: Fundamentals and Applications*. Oxford University Press, 1995.
- [26] K. Fukuo, A. Fujimura, M. Saito, K. Tsunoda, and S. Takiguchi. Development of the ultra-low-fuel-consumption hybrid car - Insight. *JSAE Review*, 22(1):95–103, January 2001.
- [27] I. E. Grossmann. Review of nonlinear mixed-integer and disjunctive programming techniques. *Optimization and Engineering*, 3(3):227–252, 2002.

- [28] L. Guzzella and A. Sciarretta. *Vehicle Propulsion Systems - Introduction to Modeling and Optimization*. Springer-Verlag, Berlin Heidelberg, 2005.
- [29] D. Hermance and S. Sasaki. Hybrid electric vehicles take to the streets. *IEEE Spectrum*, 35(11):48–52, November 1998.
- [30] J. B. Heywood. *Internal Combustion Engine Fundamentals*. McGraw-Hill, 1988.
- [31] T. Hofman and R. van Druten. Energy analysis of hybrid vehicle powertrains. In *Proc. of the IEEE Int. Symp. on Vehicular Power and Propulsion*, Paris, France, October 2004.
- [32] V. H. Johnson, K. B. Wipke, and D. J. Rausen. HEV control strategy for real-time optimization of fuel economy and emissions. In *Proc. of the Future Car Congress*, Washington, DC, April 2000. SAE Paper 2000-01-1543.
- [33] A. Jokic and P. P. J. van den Bosch. Autonomous power networks based power system. In *Proc. of the IFAC Symp. on Power Plants and Power Systems Control*, Kananaskis, Canada, June 25-28 2006.
- [34] A. Jokic, E. H. M. Wittebol, and P. P. J. van den Bosch. Dynamic market behavior of autonomous network-based power systems. *Euro. Trans. Electr. Power*, 16:112, 2006.
- [35] J. G. Kassakian, J. M. Miller, and N. Traub. Automotive electronics power up. *IEEE Spectrum*, 37(5):34–39, May 2000.
- [36] J. T. B. A. Kessels. *Due to appear*. PhD thesis, Department of Electrical Engineering, Technische Universiteit Eindhoven, The Netherlands, 2007.
- [37] J. T. B. A. Kessels, W. H. A. Hendrix, and M. W. T. Koot. Vehicle modeling and validation. Final report 1/8, Technische Universiteit Eindhoven, The Netherlands, November 2005.
- [38] J. T. B. A. Kessels, M. Koot, B. de Jager, and P. J. J. van den Bosch. Energy management for vehicle power net with flexible electric load demand. In *Proc. of the 2005 IEEE Conf. on Control Applications*, pages 1504–1509, Toronto, Canada, August 2005.
- [39] D. B. Kok. *Design Optimisation of a Flywheel Hybrid Vehicle*. PhD thesis, Department of Mechanical Engineering, Technische Universiteit Eindhoven, The Netherlands, 1999.
- [40] I. Kolmanovsky, I. Siverguina, and B. Lygoe. Optimization of powertrain operating policy for feasibility assessment and calibration: Stochastic dynamic programming approach. In *Proc. of the American Control Conf.*, volume 2, pages 1425–1430, Anchorage, AK, May 2002.
- [41] M. Koot, J. Kessels, and B. de Jager. Energy management in a vehicle with a dual storage power net. In *Proc. of the 16th IFAC World Congress*, Prague, Czech Republic, July 2005.

- [42] M. Koot, J. Kessels, B. de Jager, M. Heemels, and P. van den Bosch. Energy management strategies for vehicle power nets. In *Proc. of the American Control Conf.*, pages 4072–4077, Boston, MI, June 2004.
- [43] M. Koot, J. Kessels, B. de Jager, and P. van den Bosch. Energy management for vehicle power nets. In *Proc. of the FISITA World Automotive Conf.*, Barcelona, Spain, May 2004.
- [44] M. Koot, J. Kessels, B. de Jager, and P. van den Bosch. Fuel reduction potential of energy management for vehicular electric power systems. *International Journal of Alternative Propulsion*, 1(1):112–131, 2006. Accepted.
- [45] M. Koot, J. T. B. A. Kessels, and B. de Jager. Fuel reduction of parallel hybrid electric vehicles. In *Proc. of the IEEE Vehicle Power and Propulsion Conference*, Chicago, IL, September 2005.
- [46] M. Koot, J. T. B. A. Kessels, B. de Jager, W. P. M. H. Heemels, P. P. J. van den Bosch, and M. Steinbuch. Energy management strategies for vehicular electric power systems. *IEEE Trans. on Vehicular Technology*, 54(3):771–782, May 2005.
- [47] C.-C. Lin, H. Peng, and J. W. Grizzle. A stochastic control strategy for hybrid electric vehicles. In *Proc. of the American Control Conf.*, pages 4710–4715, Boston, MI, June 2004.
- [48] C.-C. Lin, H. Peng, J. W. Grizzle, and J. M. Kang. Power management strategy for a parallel hybrid electric truck. *IEEE Trans. on Control Systems Technology*, 11(6):839–849, November 2003.
- [49] X. Liu, G. Perakis, and J. Sun. A robust SQP method for mathematical programs with linear complementarity constraints. 2004. (available online at www.optimization-online.org/DB_HTML/2003/09/737.html).
- [50] J. M. Maciejowski. *Predictive Control with Constraints*. Prentice Hall, 2001.
- [51] J. M. Miller. *Propulsion Systems For Hybrid Vehicles*. IEE, London, 2004.
- [52] K. G. Murty. *Linear Programming*. John Wiley & Sons, New York, 1983.
- [53] P. Nicastrì and H. Huang. 42V PowerNet: Providing the vehicle electrical power for the 21st century. In *Proc. of the SAE Future Transportation Technology Conf.*, Costa Mesa, CA, August 2000. SAE Paper 2000-01-3050.
- [54] E. Nuijten, M. Koot, J. Kessels, B. de Jager, M. Heemels, W. Hendrix, and P. van den Bosch. Advanced energy management strategies for vehicle power nets. In *Proc. of the EAEC 9th Int. Congress: European Automotive Industry Driving Global Changes*, Paris, France, June 2003.
- [55] E. H. J. A. Nuijten. The development of an optimal energy management system for vehicle electric power nets. Master’s thesis, Dept. of Electrical Engineering, Technische Universiteit Eindhoven, The Netherlands, 2002.

- [56] T. H. Ortmeyer and P. Pillay. Trends in transportation sector technology energy use and greenhouse gas emissions. *Proceedings of the IEEE*, 89(12):1837–1847, December 2001.
- [57] G. Paganelli, G. Ercole, A. Brahma, Y. Guezennec, and G. Rizzoni. General supervisory control policy for the energy optimization of charge-sustaining hybrid electric vehicles. *JSAE Review*, 22(4):511–518, April 2001.
- [58] N. J. Schouten, M. A. Salman, and N. A. Kheir. Fuzzy logic control for parallel hybrid vehicles. *IEEE Trans. on Control Systems Technology*, 10(3):460–468, May 2002.
- [59] F. C. Schweppe, M. C. Caramanis, R. D. Tabors, and R. E. Bohn. *Spot Pricing Of Electricity*. Kluwer Academic, Dordrecht, 1988.
- [60] A. Sciarretta, M. Back, and L. Guzzella. Optimal control of parallel hybrid electric vehicles. *IEEE Trans. on Control Systems Technology*, 12(3):352–362, May 2004.
- [61] A. Sciarretta, L. Guzzella, and M. Back. A real-time optimal control strategy for parallel hybrid vehicles with on-board estimation of the control parameters. In *Proc. of the IFAC Symp. on Advances In Automotive Control*, Salerno, Italy, April 19-23 2004.
- [62] J. Scordia, M. Desbois-Renaudin, R. Trigui, B. Jeanneret, and F. Badin. Global optimization of energy management laws in hybrid vehicles using dynamic programming. *International Journal of Vehicle Design*, 39(4), 2005.
- [63] D. Seville. Electrical energy management: 42V perspective. In *MIT 42V meeting*, Dearborn, MI, March 2003.
- [64] A. F. A. Serrarens. *Coordinated Control of The Zero Inertia Powertrain*. PhD thesis, Department of Mechanical Engineering, Technische Universiteit Eindhoven, The Netherlands, 2001.
- [65] J. Sijs. On-line estimation of fuel consumption for producing electrical power in a vehicle. Master’s thesis, Dept. of Electrical Engineering, Technische Universiteit Eindhoven, The Netherlands, 2006.
- [66] E. Spijker. *Steering and Control of a CVT based Hybrid Transmission for a Passenger Car*. PhD thesis, Department of Mechanical Engineering, Technische Universiteit Eindhoven, The Netherlands, 1994.
- [67] R. Stone. *Introduction to Internal Combustion Engines*. MacMillan Press LTD, 3rd edition, 1999.
- [68] E. D. Tate and S. P. Boyd. Finding ultimate limits of performance for hybrid electric vehicles. In *Proc. of the SAE Future Transportation Technology Conf.*, Costa Mesa, CA, August 2000. SAE Paper 2000-01-3099.
- [69] P. P. J. van den Bosch and F. A. Lootsma. Scheduling of power generation via large-scale nonlinear optimization. *J. of Optimization Theory and Appl.*, 55:313–326, 1987.

- [70] R. M. van Druten. *Transmission Design of The Zero Inertia Powertrain*. PhD thesis, Department of Mechanical Engineering, Technische Universiteit Eindhoven, The Netherlands, 2001.
- [71] B. G. Vroemen. *Component Control for The Zero Inertia Powertrain*. PhD thesis, Department of Mechanical Engineering, Technische Universiteit Eindhoven, The Netherlands, 2001.
- [72] M. J. West, C. M. Bingham, and N. Schofield. Predictive control for energy management in all/more electric vehicles with multiple energy storage units. In *Proc. of the IEEE Int. Electric Machines and Drives Conf.*, volume 1, pages 222–228, June 2003.
- [73] M. H. Westbrook. *The electric car : development and future of battery, hybrid and fuel-cell cars*. IEE, London, 2001.
- [74] J. S. Won and R. Langari. Intelligent energy management agent for a parallel hybrid vehicle. In *Proc. of the American Control Conf.*, Denver, CO, June 2003.
- [75] J. S. Won, R. Langari, and M. Ehsani. An energy management and charge sustaining strategy for a parallel hybrid vehicle with cvt. *IEEE Trans. on Control Systems Technology*, 13(2):313–320, March 2005.
- [76] H. Y. Yamin. Review on methods of generation scheduling in electric power systems. *Electric Power Systems Research*, 69:227248, 2004.

Nomenclature

<i>Symbol</i>	<i>Quantity</i>	<i>Unit</i>
v	vehicle speed	m/s
ω	engine speed	rad/s
τ_d	drive train torque	Nm
τ_m	engine torque	Nm
\dot{m}	fuel rate	g/s
P_f	fuel rate	kW
P_m	mechanical engine power	kW
P_d	mechanical drive train power	kW
P_g	mechanical alternator power	kW
P_e	electrical alternator power	kW
P_l	electrical load power	kW
P_b	battery power	kW
P_s	stored battery power	kW
P_{bs}	stored battery power	kW
P_c	ultracap power	kW
P_{cs}	stored ultracap power	kW
E_s	energy stored in battery	kJ
E_{bs}	energy stored in battery	kJ
E_{cs}	energy stored in ultracap	kJ
SOE	state of energy	%
SOC	state of charge	%
λ	incremental cost	-
M	mass	kg
A_d	frontal area	m ²
C_d	air drag coefficient	-
C_r	rolling resistance coefficient	-
w_r	wheel radius	m
f_r	final drive ratio	-
g_r	gear ratio	-
ω_i	idle speed	rad/s
ρ	air density	kg/m ³

Nomenclature

g	gravity	m/s^2
β_{ice}	brake specific fuel consumption	g/kWh
η_{ice}	engine efficiency	-

Summary

The electric energy consumption in passenger vehicles is rapidly increasing. To limit the associated increase in fuel consumption, an energy management system has been developed. This system exploits the fact that the losses in the internal combustion engine vary with the operating point, and uses the possibility to temporarily store electric energy in a battery, such that electric energy is only produced at moments when it is cheap to generate.

To come to a practically applicable solution, a vehicle model is derived, containing only the component characteristics relevant for this application.

The energy management problem is formulated as an optimization problem. The fuel consumption over a driving cycle is minimized, while respecting physical limitations of the components and maintaining an acceptable energy level of the battery.

Several optimization methods are studied to come to a solution. The dynamic optimization problem is solved using Dynamic Programming. After rewriting it as a static optimization problem and approximating the cost function by a quadratic function, the problem is solved using Quadratic Programming, which requires less computation time.

A real-time implementable strategy has been derived from the Quadratic Programming problem, that does not require a prediction of the future driving cycle. This strategy compares the current cost of producing electric energy with the estimated average cost. By adapting the average cost based on the energy level of the battery, it is ensured that the battery energy level will remain around the desired value.

Simulations show that a fuel reduction up till 2% can be obtained on a conventional vehicle without major hardware changes. Higher reductions are possible on the exhaust emissions.

To predict and explain the amount of fuel reduction that can be obtained with a given vehicle configuration, a set of engineering rules is derived based on typical component characteristics. Their results correspond reasonably well with the simulations.

An advanced power net topology is studied which contains both a battery and an ultracapacitor that are connected by a DC-DC converter and a switch. Because of the increased complexity, this system is modeled using linear and piecewise linear approximations of the component characteristics, such that the energy management problem can be casted as a Linear Programming problem. The discrete switch makes it a Mixed Integer Linear Programming Problem. A realtime strategy, similar to the strategy for the conventional power net, has been derived. The additional fuel reduction that is obtained with the dual storage power net is small, because the maximum profit that can be obtained with an ideal lossless battery is not much higher than with a normal battery.

Subsequently, hybrid electric vehicles are studied that use an Integrated Starter Generator which can be used for generating electric power and for vehicle propulsion. Several con-

figurations are studied with respect to their potential fuel reduction. Configurations that enable start-stop operation of the engine obtain a much higher fuel reduction, up to 40%.

The controllers are tested in real-time on a Hardware-in-the-Loop environment, where a vehicle simulation model is combined with existing electric components. It is shown that the electric power setpoints provided by an energy management strategy can be realized in practice.

Samenvatting

In moderne auto's wordt steeds meer elektrische energie verbruikt. Om het hiermee gepaard gaande brandstofverbruik te verminderen, is een geavanceerd energie management systeem ontwikkeld. Dit systeem maakt gebruik van het feit dat de verliezen in de verbrandingsmotor variëren met het werkpunt (koppel en toerental) en benut de mogelijkheid om elektrische energie tijdelijk op te slaan. Zodoende wordt alleen op de meest gunstige momenten elektriciteit gegenereerd.

Om tot een praktisch bruikbare strategie te komen, is een voertuigmodel opgesteld, waarbij alleen de voor deze toepassing relevante componenten zijn meegenomen.

Het energie management probleem is geformuleerd als een optimalisatieprobleem. Hierbij wordt het brandstofgebruik over een gegeven route geminimaliseerd, waarbij rekening wordt gehouden met de fysische beperkingen van de componenten en het toegestane energieniveau in de batterij.

Verschillende optimalisatiemethoden zijn bestudeerd om tot een oplossing te komen. Het dynamisch optimalisatie probleem is opgelost met Dynamisch Programmeren. Door het probleem om te schrijven naar een statisch optimalisatie probleem, en de kostfunctie te benaderen met een kwadratische functie, is het opgelost met Kwadratisch Programmeren, wat minder rekentijd vergt.

Vervolgens is het Kwadratisch Programmeer probleem vertaald naar een realtime implementeerbare regelstrategie die geen informatie over de toekomstige route vereist. Deze strategie vergelijkt de huidige kosten voor het produceren van elektrische energie met de geschatte gemiddelde kosten. Door de geschatte gemiddelde kosten aan te passen aan de hand van het momentane energieniveau in de batterij, wordt gezorgd dat het energieniveau in de buurt van de gewenste waarde blijft.

Simulaties laten een brandstofbesparing van ca. 2% zien, zonder dat er hardware-matige aanpassingen aan het voertuig nodig zijn. Op de uitlaatgas emissies worden hogere besparingen behaald.

Om te voorspellen en te verklaren hoeveel brandstof besparing mogelijk is voor een bepaalde voertuigconfiguratie, is een set vuistregels opgesteld, gebaseerd op typische component karakteristieken. De resultaten blijken redelijk overeen te komen met de simulaties.

Vervolgens is er een meer geavanceerde elektrische topologie bestudeerd, waarbij zowel een accu als een supercondensator gebruikt worden, die onderling verbonden zijn middels een DC-DC converter en een schakelaar. Vanwege de hogere complexiteit is dit systeem gemodelleerd met lineaire en stuksgewijs lineaire benaderingen van de component karakteristieken. Hiermee kan het energie management-probleem geformuleerd worden als een Lineair Programmeer-probleem. Vanwege het discrete gedrag van de aanwezige schakelaar is dit een Mixed Integer Lineair Programmeer-probleem. Net als voor het con-

ventionele elektriciteitsnet is er een realtime strategie ontworpen. Simulaties laten slechts een kleine toename in brandstofreductie zien, omdat zelfs met een ideale verliesloze batterij de mogelijke brandstofbesparing beperkt is.

Tevens is er gekeken naar hybride elektrische voertuigen die gebruik maken van een geïntegreerde startmotor/generator die zowel voor elektriciteit genereren als voor aandrijven van het voertuig gebruikt kan worden. Voor verschillende configuraties is de haalbare brandstofbesparing onderzocht. Met name door gebruik te maken van start-stop operatie van de verbrandingsmotor kan een hoge brandstofbesparing bereikt worden.

De strategieën zijn geïmplementeerd op een Hardware-in-the-Loop opstelling, waarbij een simulatie model van het voertuig gecombineerd wordt met bestaande elektrische componenten. Hiermee is aangetoond dat de door de strategieën voorgeschreven elektrische vermogens in praktijk gerealiseerd kunnen worden.

Dankwoord

Dit proefschrift is tot stand gekomen met de hulp van velen om mij heen.

Als eerste wil ik John bedanken voor de aangename en stimulerende samenwerking. Je was een grote steun gedurende dit project. Gaandeweg heb ik steeds meer bewondering gekregen voor je niet aflatende optimisme.

Will Hendrix wil ik bedanken voor zijn geweldige inzet bij het operationeel maken van de experimentele opstelling, het verzamelen van modellen, het organiseren en leiden van alle projectvergaderingen, het schrijven van notulen en rapporten en talloze andere dingen waarmee je John en mij een hoop werk uit handen genomen hebt.

Bram en Maarten wil ik bedanken voor het ieder op eigen wijze zorgen voor mijn dagelijkse begeleiding en Paul voor het leiden van het project.

Van de vele studenten en medewerkers die tijdelijk meegewerkt hebben aan dit project, wil ik met name Emiel Nuijten, Michiel Pesgens, Rogier Ellenbroek, Jeroen de Wit, Maurice Heemels en Frans Veldpaus bedanken voor hun inhoudelijke bijdragen aan mijn werk en de prettige samenwerking.

Van Ford in Aken wil ik Daniel Kok, Engbert Spijker en Edo Aneke bedanken voor hun bijdragen tijdens de projectvergaderingen.

Okko Bosgra, Michel Verhaegen, Henk Nijmeijer en Daniel Kok wil ik bedanken voor het nakijken van mijn proefschrift.

Mijn collega's, zowel bij werktuigbouwkunde als bij elektrotechniek, worden bedankt voor alle gelegenheden tot werkontwikkend gedrag.

Mijn vrienden en oud-huisgenoten ben ik dankbaar voor de nodige afleiding buiten werktijd.

Tenslotte wil ik mijn broer, zus, vader en bovenal mijn moeder bedanken voor de mentale steun die ik vooral in het laatste jaar hard nodig had.

Curriculum Vitae

- 13-01-1977 Born in Sittard, The Netherlands
- 1989-1995 Secondary school: VWO at Stella Maris College in Meerssen
- 1995-2001 MSc study: Mechanical Engineering at Technische Universiteit Eindhoven
External traineeship carried out at Philips Center for Applied Technology
Internal master's project: "Identification and control of the RRR-robot"
- 2002-2006 PhD student at the Department of Mechanical Engineering at Technische Universiteit Eindhoven
Project: "The Development of an Energy and Power Management System for Conventional and Future Vehicle Power Nets"

